
Politecnico di Torino

Dipartimento di Ingegneria Meccanica e Aerospaziale

Corso di Laurea Magistrale in Ingegneria Aerospaziale

# Conceptual Design of a Powered-Lift eVTOL Aircraft with a Fuel Cell–Battery Hybrid System for Urban Air Mobility

**Relatore**
Prof. Davide Ferretto

**Candidato**
Matteo Ingrosso

**Correlatrice**
Prof.ssa Nicole Viola

ANNO ACCADEMICO 2024/2025

# Contents

# List of Figures

# List of Tables

# Abstract

This thesis presents the conceptual design process of a Powered-Lift electric Vertical Take-off and Landing (eVTOL) Aircraft with a Fuel Cell–Battery Hybrid System for Urban Air Mobility (UAM) applications. The primary objective is to evaluate the feasibility and benefits of such aircraft as a promising solution to the growing traffic congestion in ever more urbanized cities, with the additional advantages of reducing air pollution from traditional road transport systems. The study focuses on the potential of hybrid powerplant configurations that combine the high power density of batteries for power-demanding flight phases such as take-off, with the high energy density of fuel cells for energy-demanding flight phases such as climb and cruise. Following the initial sizing process, a design space exploration is conducted to evaluate how various design parameters influence aircraft performance and to identify the operational ranges where hybrid solutions become competitive with battery-only configurations. Multiple powerplant architectures are explored, including battery-only, fuel cell-only, and hybrid systems. Ultimately, several configurations are proposed and evaluated using different figures of merit for various urban operational scenarios.

# Acknowledgements

I wish to express my sincere gratitude to my academic advisors for their continuous, invaluable and essential guidance throughout the development of this thesis, from the initial definition of the objectives to the interpretation of the key findings. Their expertise and constructive feedback were fundamental to the quality and direction of this work. I am also thankful for the lectures and academic instruction that provided the theoretical foundation and methodological tools necessary to undertake this research. Finally, I would like to thank all those who supported me along this journey, whose encouragement and thoughtful discussions were a source of inspiration and growth.

# Introduction

United Nations projections show that by 2050, more than 68.3% of the worldwide population will live in urban areas. This accelerated shift towards urban settlements will cause serious traffic congestion problems, with the risk of worsening air pollution without effective improvement in current transportation systems. Urban Air Mobility (UAM), with its gradual and phased integration into the urban transportation system, represents a promising solution to the aforementioned problems, enabling the capability of moving people and goods by air. A deep understanding of the emerging concept of UAM is reviewed in the first chapter of this work, followed by an analysis of the existing technologies supporting electric propulsion, which is particularly focused on the use of fuel cells exploiting the high energy content of hydrogen, and batteries, a leading technology in many electrification processes involving transportation systems. UAM for moving people by air could indeed be possible using powered-lift eVTOL (electric Vertical Take-off and Landing) aircraft, which are capable of behaving similarly to rotorcraft and helicopters in the very first mission phases, while morphing in fixed-wing aircraft during cruise, leading to much improved flight performance. The necessity of this dual behaviour lies in the infeasibility of long runways within the urban scenarios, where these vehicles are required to perform vertical flight in order to leave their suitable airports, which in the context of UAM, are known as “vertiports”. All the existing eVTOL aircraft concepts make use of batteries, which are fundamental for the initial power-demanding flight phases. However, these technologies are not the best performing ones when it comes to energy-demanding flight phases, given their low energy density. Therefore, the conceptual design carried out in this work focuses on designing an eVTOL aircraft, using both conventional and innovative approaches, implementing battery-only, fuel cell only and hybrid powerplant solutions with defined power sharing strategies. The conceptual design is then supported by a comprehensive design space exploration, where the effect of

individual parameters is discussed in order to understand their impact on the final aircraft. This study aims to assess the feasibility and potential benefits of hybrid fuel cell - battery architectures for eVTOL applications, under realistic mission constraints and technology assumptions. Practically, an iterative sizing process has been conducted, including both conventional and recent formulations for the various subsystems and aircraft elements, also implementing existing models for the various figures of merit used to assess the output results. Among the several scenarios that may concern the concepts of UAM and the broader one of IAM (Innovative Air Mobility), the main applications on which this thesis focuses are: airport transit, intercity and point-to-point routes, and tourism and island connectivity—consequently involving longer ranges and different or additional environmental constraints compared to intracity solutions. Finally, it is worth underlining how this study relies on the European project "eVTOLUTION", focused on the multi-fidelity hybrid design of eVTOLs, for certain aspects related to the mission profile and the methodology adopted to conduct the sizing process, with innovative inspiration for the trade-offs introduced in the powerplant architecture for longer ranges. [1]

[1]This project has received funding from the European Union's Horizon Research and Innovation Programme under grant agreement No 101138209

# 1. Urban Air Mobility

## 1.1 New trends in urban settlements

In 2023, 4.61 billion people, more than half of the world's population, lived in urban areas; in high-income countries such as Western Europe, United States and Japan, the percentage rises to 81%, while it drops to 35% for low-income countries. Even though it is not possible to universally define urban areas, since each country has its own definition along with metrics to assess this phenomenon and consequently to share data, United Nations projections show how by 2050 more than 68.3% of the worldwide population and 83.6% of the European one, will live in urban areas.[1]

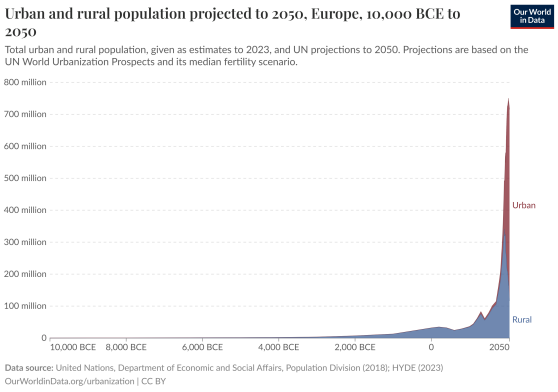


Figure 1.1: Urban and Rural population projections, Europe

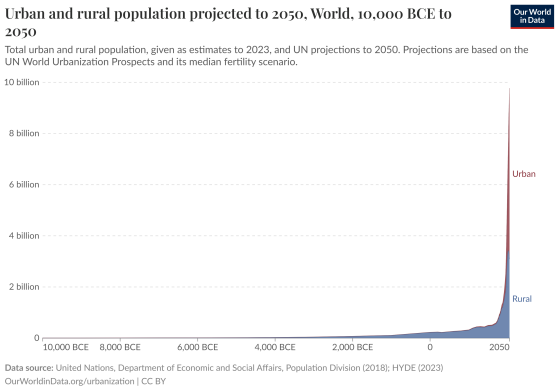


Figure 1.2: Urban and Rural population projections, World

The foreseen accelerated increase in population density in cities, will undoubtedly cause serious traffic congestion problems, affecting the average commuting time of people travelling to work. Furthermore, without effective upgrades in energy use, air pollution will increase accordingly. Poor air quality directly affects

[1] Hannah Ritchie, Veronika Samborska, and Max Roser. "Urbanization". In: *Our World in Data* (2024). https://ourworldindata.org/urbanization.

the health of people living in neighbourhoods near to trafficked areas. Urbanization is a complex phenomenon, that has its roots in very ancient times, with both advantages and drawbacks, assessing this phenomenon lies beyond the scope of this document, this thesis, however, focuses on the opportunities, for highly crowded urban settlements, to address some of the aforementioned problems of traffic congestions, through the use of alternative transport systems. In metropolis, phenomena of super-commuting, workers that need to travel very long distances, are on the rise. The following plot, depicts the average commuting time of people living in the European Union, as can be seen, about 35% of workers, spend between 30 and 60 minutes, to reach their workplace.[2]

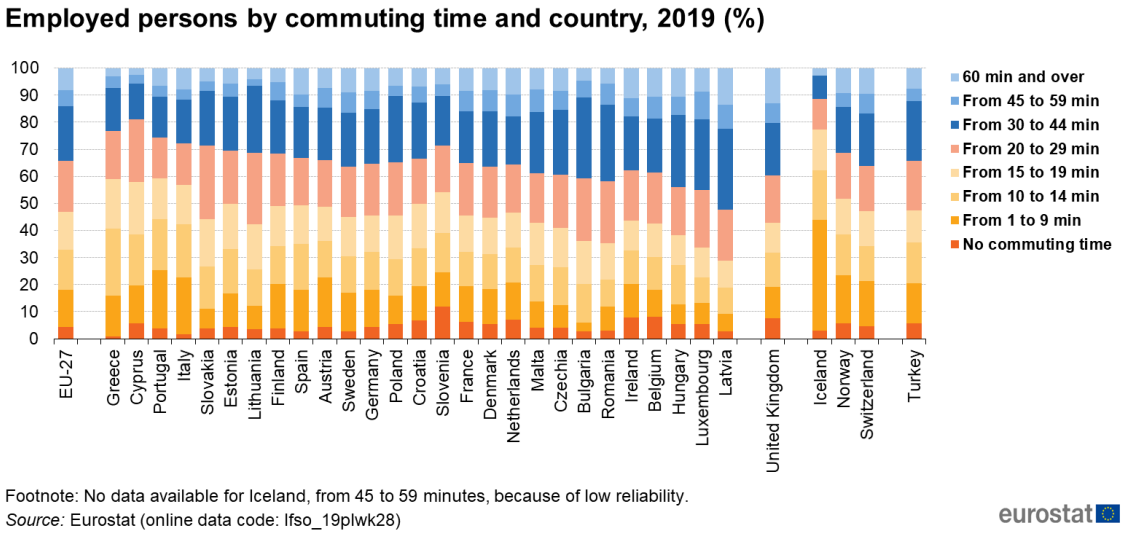


Figure 1.3: Employed persons by commuting time and country in European Union

The average commuting time, is sometimes referred to as the Marchetti constant, named after the Italian physicist who first studied the phenomenon, according to Marchetti, people tend to adjust their living conditions in such a way that their average travel time to workplace stays constant. Several studies show the

[2]Eurostat. *Main place of work and commuting time - statistics*. Accessed: 2025-04. 2020. URL: https://ec.europa.eu/eurostat/statistics-explained/index.php?title=Main_place_of_work_and_commuting_time_-_statistics.

negative impacts caused by long commuting times on the physical and mental health of workers, along with lower satisfaction with work and increased stress and sleep quality [3]. Though the adoption of Electric Vehicles (EVs), has the potential to improve the local air quality of urban areas, it would have no significant impact on traffic congestion and average communing times.

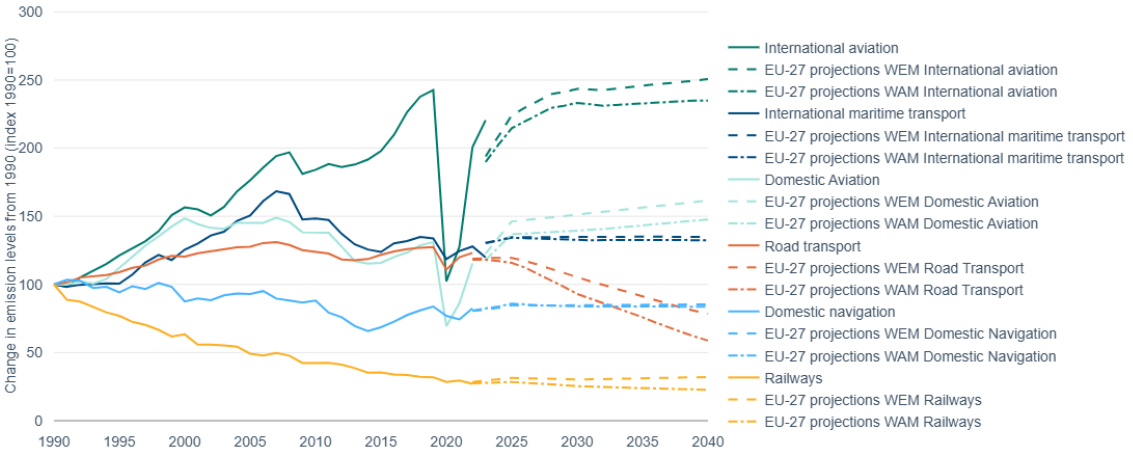


Figure 1.4: Greenhouse gas emissions from transport in Europe [4]

The plot above shows the change in emissions levels from 1990 by transport mode in European Union countries. As seen, road transport is the only transport system whose emission have not decreased since 1990, unlike other domestic transport modes such as aviation, navigation and railways. It is also possible to observe how Covid-19 pandemic extremely affected emissions caused by international and domestic aviation, in particular, international aviation emissions in 2020 were 58% lower than in 2019. Additionally, for each transport mode, it is also possible to observe two future scenarios: with existing measures to lower emissions (WEA), including already adopted measures, and with additional measures (WEA), including planned policies and national targets.[3] The impact of aviation

[3]European Environment Agency. *Greenhouse gas emissions from transport in Europe*. Accessed: 2025-04. 2024. URL: https://www.eea.europa.eu/en/analysis/indicators/greenhouse-gas-emissions-from-transport?activeAccordion=ecdb3bcf-bbe9-4978-b5cf-0b136399d9f8.

on climate change, along with efforts to research new sustainable fuels and disruptive technologies to lower noxious and $CO_2$ emissions and, consequently, meet EU decarbonization goals, is a complex topic that lies beyond the scope of this thesis.

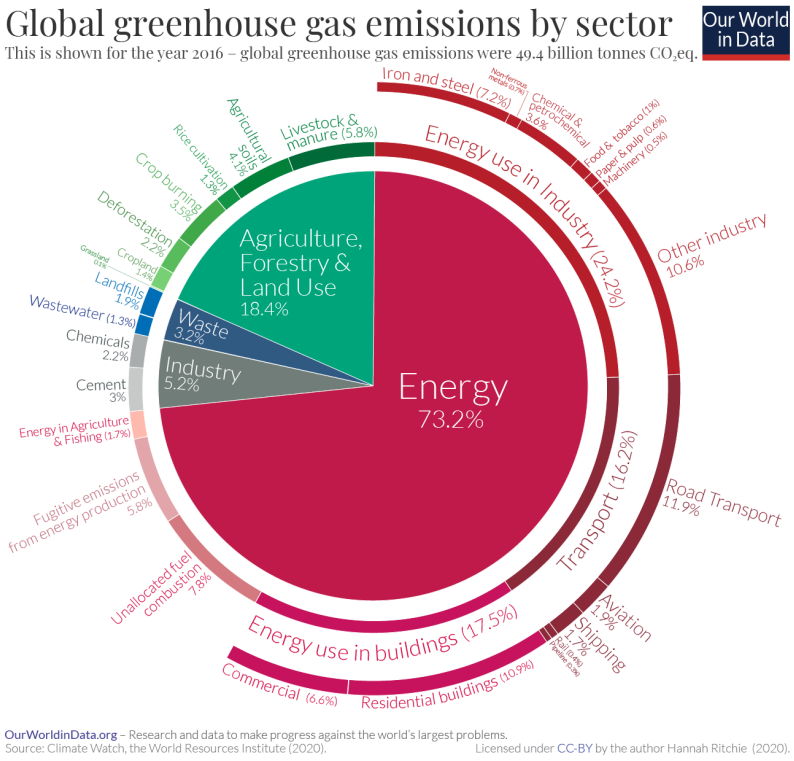


Figure 1.5: Global greenhouse gas emissions by sector

As it can been seen in the above pie chart, transport system accounts for 16.2% of the worldwide greenhouse gas emissions, and within it, road transport has the major impact, accounting for 73.5%, followed by aviation, responsible for the 11.7% of the GHG emissions of the transport sector and 1.9% of the global emissions.[4] Undoubtedly, most part of the $CO_2$ emitted by aviation is due to international flights rather than domestic and regional solutions, a deeper analysis of the environmental impact of aviation, would in fact demonstrate how regional aircraft and commuters, only account for 4% of the total emissions due to Aviation. The new concepts developed for UAM, which will be discussed in more details in

[4]Hannah Ritchie. "Sector by sector: where do global greenhouse gas emissions come from?" In: *Our World in Data* (2020). https://ourworldindata.org/ghg-emissions-by-sector.

the following sections, are mainly designed to be powered by electrical energy, thanks to distributed electric propulsion (DEP), this would enable for these concepts to have a zero environmental impact on both the air quality of urban areas and the overall GHGs emitted by aviation. As it will be detailed subsequently, DEP is a fundamental ingredient, even for certification bodies, to enable VTOL classification.

UAM (Urban Air Mobility) could represent a promising solution to the increasing congestion of ever more urbanized cities, with the potential to reduce both the average commuting time of people working in urban areas and air pollution caused by road transport systems powered by fossil fuels.

## 1.2 Urban Air Mobility

To clearly identify some key aspects of Urban Air Mobility, it is important to explain the definitions of some acronyms often associated with this emerging mobility concept. First, **Air Mobility**, regards the capability of moving people and goods by air, encompassing activities often done by airlines, helicopters and business jet. **Advanced Air Mobility (AAM)** regards instead the aforementioned capability, through the use of next-generation concepts such as eVTOL aircrafts or drones, in a safe, quick and sustainable way. **Innovative Air Mobility (IAM)** could be defined as a synonym of AAM, coined by EASA (European Aviation Safety Agency). Urban Air Mobility (UAM) is classified under the broader category of IAM. UAM represents an innovative way of moving passengers and goods in urban and metropolitan areas (within a city) by air in response to traffic congestions, using emerging electric aerial vehicles such as those able to perform vertical take-off and landing (eVTOL). UAM, has the objective to improve urban mobility, allowing quick, safe and sustainable additional transport modes to connect people and places. When aiming to connect more distant areas, such as suburbs, villages, rural regions, industrial sites, while still utilizing new innovative technologies and infrastructure, we refer to this concept as Regional Air Mobility (RAM). The range

of new and improved services and operations enabled by IAM, such transportation of passengers and goods, mapping, inspections and photogrammetry, is referred to by EASA as **Innovative Aerial Services (IAS)**. [6]

- **Innovative Aerial Services (IAS)**: the set of operations and/or services that are of benefit to the citizens and to the aviation market, and that are enabled by new airborne technologies; the operations and/or services include both the transportation of passengers and/or cargo and aerial operations (e.g. surveillance, inspections, mapping, telecommunications networking, etc.);
- **Innovative Air Mobility** (IAM): the safe, secure and sustainable air mobility of passengers and cargo enabled by new-generation technologies integrated into a multimodal transportation system;

An eVTOL (electric Vertical take-off and landing) aircraft is an aircraft able to take-off and land vertically, similarly to helicopter and rotorcraft, using electric power. eVTOLs, play a fundamental role in UAM, where taking off and landing vertically is the only way to facilitate flights in highly crowded urban areas, due to the impracticability of runways. The need for electric propulsion arises from the goal of avoiding further air pollution in urban areas. To properly work in urban scenarios, eVTOLs must be supported by robust infrastructures like **vertiports**, analogous to heliports for helicopters, sites where eVTOLs can take-off and land, they are likely to be located in strategic points within urban areas, with waiting areas for passengers and basic maintenance staff. **Vertihubs**, will be the most robust facilities associated with eVTOLs, providing aircraft parking and full maintenance services. Due to their significant sizes, they will be likely to be located along peripheries of urban areas.

### 1.2.1 Types of eVTOL aircraft

According to EASA Special Conditions for small-category VTOL aircrafts (SC-VTOL), eVTOLs are characterized by two fundamental characteristics: vertical take-off and landing capability (VTOL) and distributed electric propulsion (DEP),

through the use of lift/thrust units, LTUs. The large number of engines that characterizes DEP, allows to relax the one-engine-inoperative (OEI) failure event found in fixed-wing aircraft, which requires to generate a restoring yawing moment through the rudder. This condition is usually the most demanding condition for the vertical tail plane (VTP) sizing. In the EASA classification, subsequently widely adopted, eVTOL aircrafts split into two categories: wingless and powered lift. In Wingless solutions, vertical lift is achieved through electric propulsion units while forward thrust generation is enabled trough collective differential actuation, multicopters, for example, belong to this category. Similarly to helicopters, multicopters require a massive amount of power to generate enough thrust to counteract the aircraft weight in each instant of the mission. On the other hand, several authors agree on the better manoeuvrability enabled by these vehicles, representing the closest architecture to pure helicopters. In powered lift architectures, the thrust, generated in various ways, needs only to compensate for aerodynamic drag, while the aircraft's weight is balanced by the lift produced by the wing. Differently from wingless solutions, powered lift enables extended range missions at higher altitudes. Powered lift architectures come in several configurations, among them, it is possible to include independent thrust, vectored thrust and combined thrust. The better performance of powered-lift configuration, is accompanied by the supplementary complexity of the system, driven by the presence of a wing, propulsion units for forward flight and potentially systems for thrust vectoring. In independent thrust configuration, LTUs design for producing vertical lift are different from the ones employed in forward flight, the reduced complexity achieved comes at the cost of additional inoperative weight during the cruise phase. These additional units, represent also a source of additional drag. In the vectored thrust solution, thrust vectoring is achieved using specifically designed systems able to rotate the propulsion units, in order to have all the LTUs providing both vertical lift and thrust in forward flight. Finally, the combined thrust solutions, represents a hybrid configuration of the previous two ones described, in fact, among the several LTUs, some of them are fixed and provide only vertical lift (as in the independent

thrust case), while others rotate providing both vertical lift and forward thrust (as in the vectorized thrust case), along with the advantaged of both solutions, this configuration is accompanied by the related issue regarding the vectorization system and the additional weight and consequent drag in the cruise phase.[5]

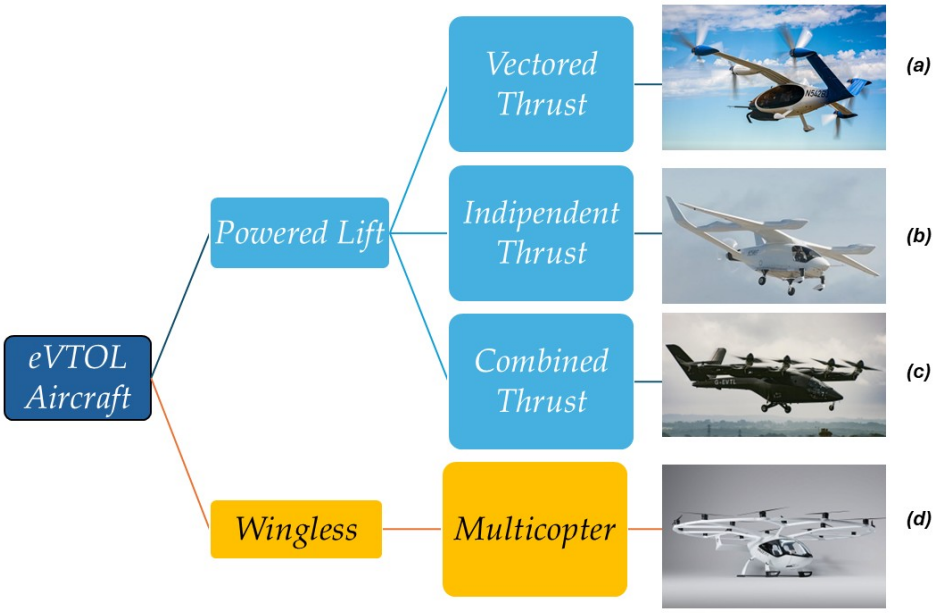


Figure 1.6: eVTOL aircraft architecture classification. 1a. Joby S4 1b. Beta-Alia 250 1c. Vertical Aerospace VX4 1d. Volocopter Volocity

### 1.2.2 Mission Types

It is important to understand feasible and practical applications, eVTOLs could be suitable for. Even though this type of vehicles shares some features with helicopters, as the one regarding take-off and landing, the more efficient behaviour during the cruise phase along with reduced acoustic emissions, could enable a wider presence in urban areas at lower service costs, provided economies of scale are achieved. Among possible use cases, it is possible to find interesting scenarios:

- **Airport Transit**, high frequency trips between airports and city centres or

[5] Osita Ugwueze et al. "An Efficient and Robust Sizing Method for eVTOL Aircraft Configurations in Conceptual Design". In: *Aerospace* 10 (Mar. 2023), p. 311. DOI: 10.3390/aerospace10030311.

airports and regional centres. The typical journey distance should be between 10 and 50 miles.

- **Intercity and point-to-point routes**, including journeys covering longer distances up to 100 miles.
- **Tourism and island connectivity**, aiming to fulfil premium travellers demand.

Though UAM will enable connectivity in urban areas by air, airspace restrictions and existing helicopter routes, will affect journeys distances, lengthening them. Direct journeys will likely to occur for inter-city and tourisms applications, provided the airspace is less congested. In conducting sizing procedures, additional distances with respect to the intended journey must be taken into account, beyond the mandatory diversion sizing.

eVTOL aircrafts have the potential to impact and improve other strategic sectors, enabling law enforcement, search and rescue operations along with national security applications. Deploying helicopters for emergencies is usually very expensive, eVTOLs can contribute to enlarge fleets for urban emergency operations, while reserving helicopters for more complex environments at higher altitudes.

### 1.2.3 Regulatory framework

To fully operate, eVTOL aircraft need to demonstrate to certification authorities (EASA for Europe, FAA for United States), adequate safety level aimed to preserving human life, avoiding injuries to passengers and the crew and damages to objects. Certification authority is a third-party institution between manufacturers and customers, with no other missions beyond safety. The certification process is conducted by the certification body together with the manufacturer, in deference to existing aeronautical regulations and laws. In order to ensure safety and quality of the product, the certification authority establishes a certification basis, requiring a series of numerical, analytical, practical simulations and documentation to be produced, intended to demonstrate compliance of the product with aviation

standards in force. All the information related to the requirements necessary for aircraft to be compliant with regulations in force, are contained within CS (Certification Specifications), once that an aircraft prototype has demonstrated compliant safety levels, the certification body issues a type certificate to the manufacturer, synthesizing the full process underwent by the product with a positive outcome in demonstrating safety. At this point, the manufacturer accompanies each unit sold with a copy of this type certificate, named as certificate of airworthiness. To initiate the certification process, it is important to address the class of aircraft, for example, small rotorcrafts (up to 9 pax and MTOW less than 7000 lb, 3175 kg), are certificated through CS-27. For eVTOL powered-lift aircrafts, since their hybrid nature (rotors + wing), it is not possible to address them neither in the CS-25 (small airplanes) nor to CS-27 (small rotorcrafts), therefore EASA, with the initial concepts, used to defined Special Conditions for each. At a certain point, the need to provide consistency among all projects, led them to the definition of SC-VTOL (Special Condition for VTOLs)[6], "with the objective to provide certification basis for different types of aircraft, regardless the type of architecture or technology on board, aiming to have level playing field with adequate safety objectives, especially for passengers and 3rd parties, inside congested environments." EASA takes care in specifying how SC is applicable for concepts having more than 2 LTUs, due to its particular interest in increasing safety through redundancy. Even though SC is a unique concept, it incorporates elements from CS-23 and CS-27, for example, the first definition of small VTOL used to coincide with the one of small rotorcraft, therefore with a maximum take off weight less than 3175 kg, up to 9 passengers. The latest SC version has modified it to 5700 kg.

As mentioned before, Safety is the primary objective, that must be addressed along with every aspect able to impact it, regarding aircraft intrinsic safety features demonstrated through AMC (Acceptable Means of Compliance) but is also

[6]European Union Aviation Safety Agency. *Special Condition for VTOL and Means of Compliance*. Accessed: 2025-04. 2024. URL: https://www.easa.europa.eu/en/document-library/product-certification-consultations/special-condition-vtol.

important not to forget contribution to Safety due to Operations and Licensing, Maintenance and Air Traffic Management.

SC-VTOL identifies two main categories and their related performance requirements:

- **Basic**, reserved to VTOLs flying outside congested areas and typically outside the urban environment. This category applies either for private flights or commercial flights different from commercial air transport of passengers. The associated performance requirement regards the ability to perform a controlled emergency landing in the case a failure during flight occurs.

- **Enhanced**, associated to congested areas (typical of urban environments) or to commercial air transport of passengers. In this case, if a failure event occurs during flight, it is necessary to demonstrate ability in having enough performance to either continue the flight to the final destination or to divert to an alternative vertiport.

Specifically regarding to Safety Levels, they differ depending on the specific addressed category.

- **Basic**, safety objectives are analogous to CS-23, even though slightly augmented since the more complex flight controls, distributed electric propulsion (DEP) requires. As mentioned before, this category requires controlled emergency landing.

- **Enhanced**, safety objectives are analogous to Category CS-27 (Category A) for helicopters and CS-23 Level 4, which numerically corresponds one another. Continued safe flight and landing required for this category must be accomplished with the identification in advance of appropriate landing sites

In SC-VTOL, EASA mandates the use of recorders, which have been recently introduced also in general aviation airplanes. EASA also addresses cases of bird-strike events, while single failure catastrophic events are not addressed due to the

advantages of DEP. Crashworthiness and Crash-resistant fuel systems are also deeply discussed by EASA regarding the Safety of VTOL aircrafts for passengers and people acting in the interested congested areas. Finally, limited damages are accepted as long as integrity of occupants is assured.

### 1.2.4 Social acceptance of Urban Air Mobility

A study on the social acceptance of the UAM within European cities has been conducted by EASA, with interesting and unexpected findings[7]. The survey involved seven cities in the European Union: Barcelona (Spain), Budapest (Hungary), Hamburg (Germany), Milan (Italy), Öresund (Slovenia), Paris (France), with more than 3600 people interviewed. The total number of participants distribution was balanced per age (15% per each age group 18-24, 25-34, 35-44, 45-54, 55-64, 65-75), employment status (full-time, part-time, not working), education (up to higher schooling, finished college, post-graduate), gross household incomes (low, medium, high) and gender.

[7] European Union Aviation Safety Agency. *Study on the Societal Acceptance of Urban Air Mobility in Europe*. Tech. rep. Accessed: 2025-04. European Union Aviation Safety Agency, 2021. URL: https://www.easa.europa.eu/en/full-report-study-societal-acceptance-urban-air-mobility-europe.

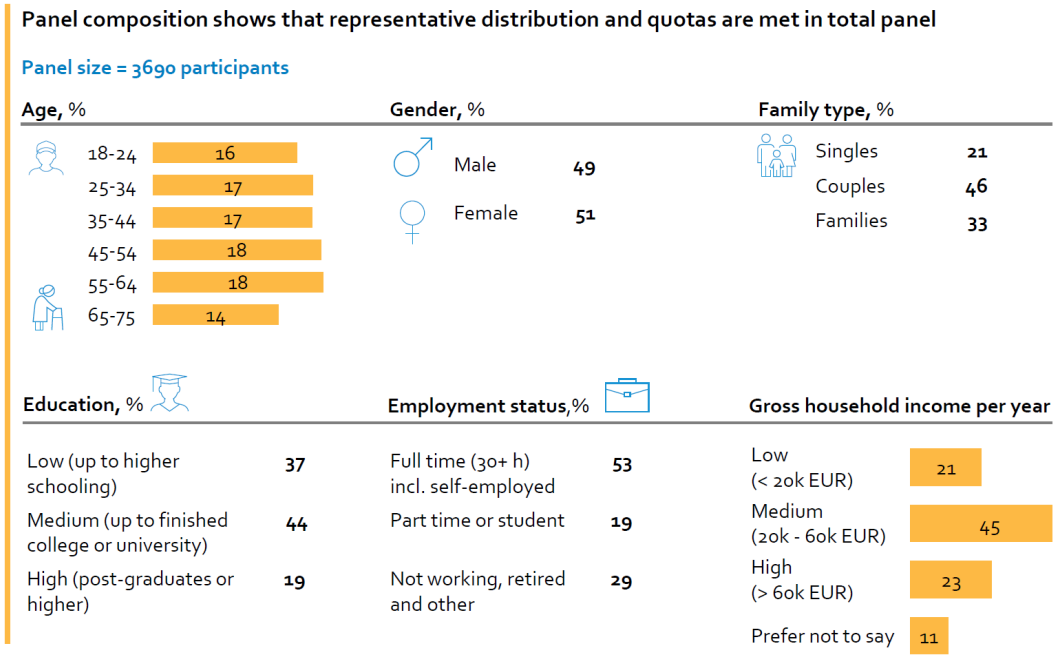


Figure 1.7: EASA survey on UAM social acceptance: participants composition

The study regarded the participants perception towards noise, safety and visual impact of drones and eVTOLs (air-taxis) on the urban environment, studied through the administration of qualitative and quantitative questionnaires, along with practical demonstrations. It is fundamental to say that the study conducted regarded UAM in general, therefore referring to both eVTOL aircraft for transporting people and drones for good delivery and other applications aforementioned. The surprising key findings were summarized by EASA itself and hereafter discussed.

Though participants to the survey belonged to different subgroups, specifically created in order to have a sample as heterogeneous as possible, the major part of them showed a positive attitude towards the possibilities enabled by UAM, with only 3% having a negative perception of UAM. A large part of the people interviewed, would be interested in using services brought by UAM, both air-taxis and drones, and in particular:

- 64% interested in using drone

- 49% interested in using air-taxis services
- 43% interested in using both drones and air taxis
- 71% likely to use at least one service

The major part of the sample interviewed, also felt safe as pedestrians with drones and eVTOLs flying above them, they would feel even safer with manned configurations rather than unmanned ones. A higher percentage of people would be likely to use manned air taxi rather than unmanned. Several use-cases of UAM were showed to participants, who were then asked to rank the relative usefulness, among 14 use-cases proposed, those related to medical services and emergency transport, received the highest scores, together with those of public interest related to health and safety while use-cases associated to single benefit, received the lowest scores. As it usually happens for helicopters, higher noise emissions generated by these vehicles for limited emergency operations would be more likely to be accepted by the public. Improved response times in case of emergencies, reduction of traffic jams and reduction of local emissions, were among the most important benefits associated with UAM, according to the participants response. Qualitative interviews confirmed that better attitude toward services of public interest. For air-taxis, the main concerns perceived by participants regarded environmental impact (38%), safety (37%) and security (29%). It is also important to add how participants were educated on the difference between safety and security, even though in some languages the two words receive the same translation.

**Figure 39:** Noise produced by air taxis is expected to be much higher than that produced by drones

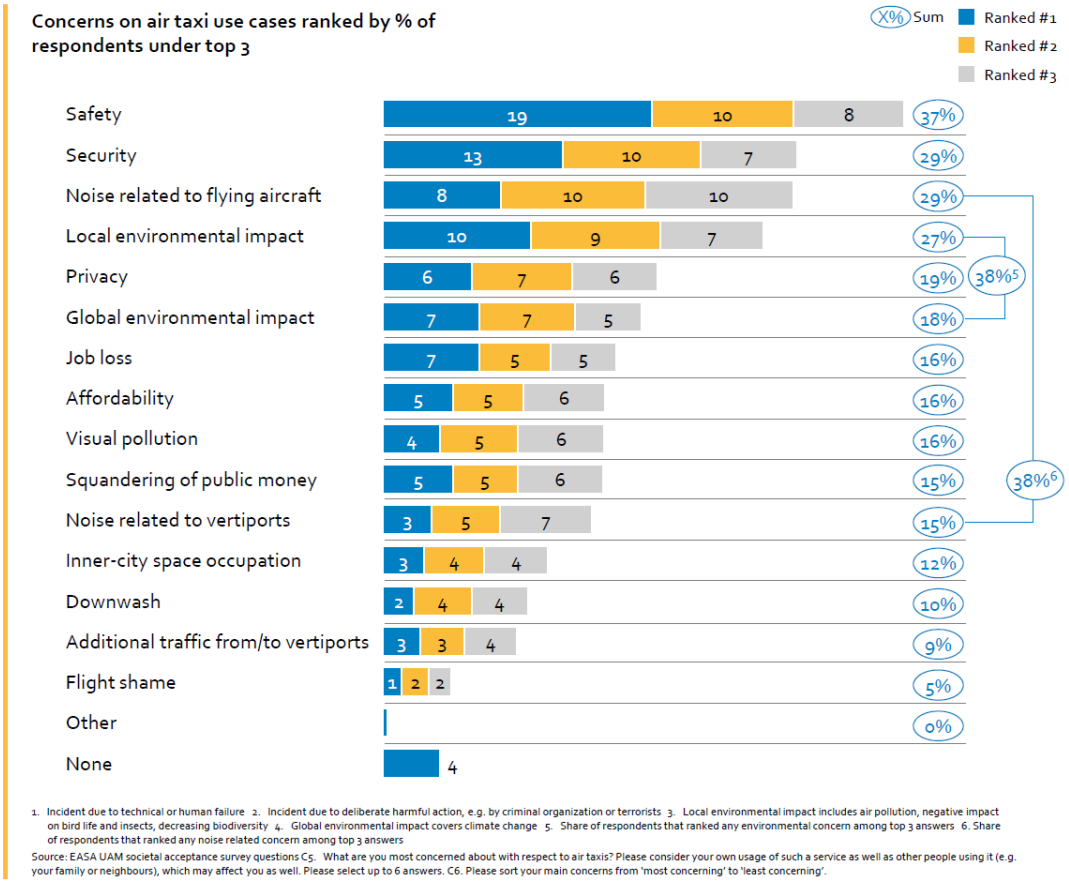


Figure 1.8: EASA survey on UAM social acceptance: concerns on air taxi use cases.

Response of participants living in different cities resulted in being aligned regarding environmental concerns, in particular a potential negative impact on wildlife was the most important environmental concern, along with noise pollution and environmental impact from disposal. Environmental impact related to climate change was more important to younger people, who instead showed a calmer attitude towards noise emissions. Regarding noise emissions, participants were asked to listen to different sounds (at the same sound level, in dBA). Sounds due to air taxis and drones, resulted in being more annoying than sounds that people were more familiar to. In fact, even helicopters, usually considered an undesirable source of noise, received better scores than UAM vehicles.

**Figure 46:** Result overview of noise perception study

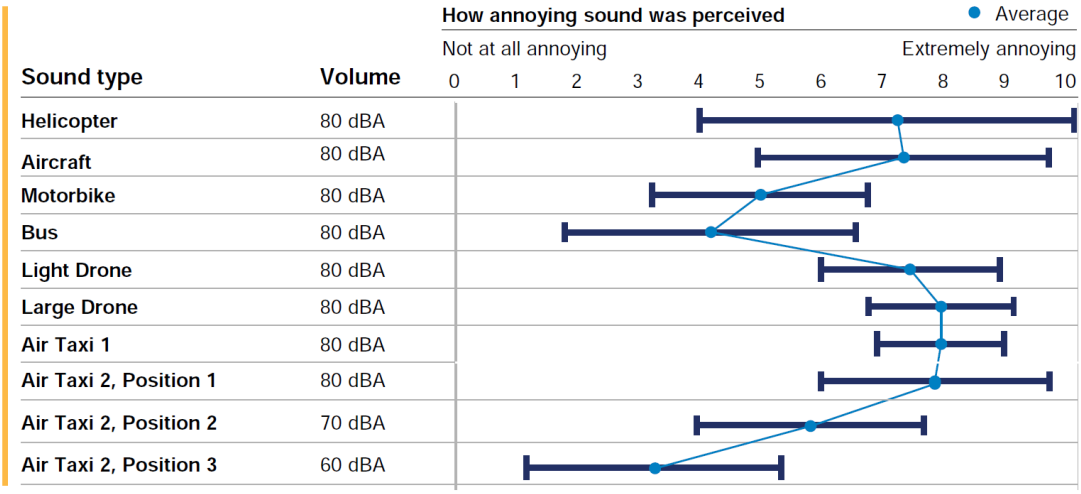


Figure 1.9: EASA survey on UAM social acceptance: noise perception assessment

It also interesting to see how concerns related to vertiports, are mostly like the ones related to air taxis, ranging from safety to noise pollution, up to visual pollution. Visual pollution represents a particular concern for the cultural heritage of European cities landscapes; therefore, their visual impact should be limited. Trust levels on air-taxis security and cybersecurity are just above 50%, with similar values occurring for drones. Among that conclusion that the conducted study allows to draw, together with the ones already drawn by EASA, it is possible to find how even though European citizens would show an initial positive attitude towards UAM and some of the enablable applications, there is no shortage of concerns regarding safety, security and environmental impact of eVTOLs. It is fundamental to highlight, as it often happens for aerospace applications, public acceptance plays a fundamental role in determining the success of advanced air mobility. Among the challenges for UAM, it is possible to highlight:

1. **Safety**, ensuring that UAM achieves safety levels similar to the ones characterizing civil aviation, widely trusted by the public.

2. **Environmental impact**, in terms of noise emission, pollution and effects on wildlife.

3. **Establishment of standards and dedicated regulatory frameworks**, aimed to demonstrate safety levels and product quality.

4. **Integration of** these **new concepts** within the existing airspace along with continuous coordination between all authority levels

5. **Integration of infrastructures** within the existing urban environment, avoiding negative and unacceptable visual impacts, particularly considering the cultural heritage of landscapes in European cities.

6. **Establishment of standard to demonstrate robustness towards possible cyber-attacks**, guaranteeing the security of the involved vehicles

# 2. Energy Sources for Electric VTOL aircraft

In order for the next generation of VTOL aircraft to be full electric, an investigation on possible sources of electrical energy must be conducted. Aviation's impact on global pollution has already been discussed in the previous chapter and further assessment could demonstrate how aircraft of interest for this thesis have the lowest impact. However, the goal is to introduce these new concepts in urban scenarios without worsening air quality of cities, but instead improving it by diminishing traffic congestion and emission arising themfrom. Electrical energy to feed electric motors could be produced on-board in a sustainable way through batteries or fuel cells, ignoring the use of internal combustion engines (ICE). Internal combustion engines, even those fed by sustainable fuels such as hydrogen, would still have NOx as pollutants, contributing to worsening air quality. On the other hand, hydrogen for internal combustion engines would still be an opportunity for large aircraft to zero carbon dioxide emissions as fuel cells couldn't provide these aircraft with enough power densities, in this regard, it is possible to find in literature some studies regarding hybrid solutions of fuel cells and combustion engines for large aircraft. Batteries represent compact solutions with high power-to-weight ratios, which are their strengths. On the other hand, these technologies are characterized by low energy-to-weight ratios, meaning that they could provide high power only for very short periods of time. The conceptual design conducted in the following chapters, will assess feasibility of hybrid solutions involving batteries and fuel cells, according to the different mission phases.

## 2.1 Fuel Cells Technology

### 2.1.1 Hydrogen

Hydrogen is the lightest chemical element of the periodic table and the most abundant in the universe. Composed of 1 proton and 1 electron, at standard conditions, (STP-IUPAC T = 298.15 K, p = 0.9869 atm) it is a gas in the form of $H_2$ [10]. Hydrogen is an energy carrier and not an energy source, therefore it is able to store important amount of energy and can be produced in several ways, among which, it is possible to find: thermochemical conversion of fossil fuels involving processes of steam reformation or coal gasification and methods which exploit electrolysis using energy from nuclear or renewable sources.

#### Production

**Steam methane reforming** (**SMR**) [11] is a process conducted at high temperatures (between 800°C and 900°C), where steam is used to produce hydrogen from methane. In the reaction process, methane reacts with steam, at very high values of pressure (up to 30 bar) producing hydrogen and carbon monoxide. The presence of a catalyst (usually Nickel-Alumina) accelerates the reaction process. In turn, reaction between carbon monoxide and steam, involves carbon dioxide and hydrogen as reaction products, this second process is known as water-gas shift reaction (WGSR). Eventually, in a final process of Pressure Swing Adsorption (PSA), pure hydrogen is purified from carbon dioxide. An eventual pre-reforming process, enables decomposition of complex hydrocarbons into methane.

$$CH_4 + H_2O \rightleftharpoons CO + 3H_2 \quad \text{(Steam Reforming, reaction, SR)}$$

$$CO + H_2O \rightleftharpoons CO_2 + H_2 \text{ (Water-Gas Shift reaction, WGSR)}$$

$$CH_4 + 2H_2O \rightleftharpoons CO_2 + 4H_2 \text{ (Direct Steam Reforming, DSR)}$$

**Partial oxidation of methane (POM)** or other hydrocarbons, is considered an alternative to SMR. In this process, methane reacts with a limited amount of

oxygen, producing hydrogen ($H_2$) and carbon monoxide (CO). Carbon monoxide, is then interested in a WGSR, involving carbon dioxide ($CO_2$ ) and additional hydrogen as reaction products.

$$CH_4 + \frac{1}{2}O_2 \rightleftharpoons CO \ + \ 2H_2 + \text{ heat}$$

Hydrogen produced by **electrolysis** is often referred to as green hydrogen or even purple hydrogen, if electricity is produced through nuclear power. Electrolysis is a process involving a direct decomposition of water into gaseous $H_2$ at the cathode and $O_2$ at the anode. Even though the process is characterized by very high efficiencies, it is not cost-effective as the previous discussed thermo-chemical processes. Even though electrolysis is the cleanest way to produce hydrogen, it is also the most expensive. Nowadays a very low amount of hydrogen is produced through renewable ways, while steam reformation processes, which also involve carbon dioxide production, are the most popular ones.

| % Production | Process |
|---|---|
| 49 | SMR |
| 29 | Oil Reforming |
| 18 | Coal Gasification |
| 3.9 | Water Electrolysis |
| 0.1 | Others |

Table 2.1: Global Hydrogen Production by method (Dincer & Acar, 2015)

Several industries make abundant usage of hydrogen; production of ammonia is undoubtedly the most demanding one, followed by oil refining and methanol production. Transportation is included in a tiny fraction of the worldwide demand, accounting for less than 10 % .

## Storage

Hydrogen density depends on temperature and pressure conditions. Depending on the application, hydrogen may be required in a liquid or in a gaseous

| % Use | Industry |
|---|---|
| 25 | Petroleum Refining |
| 55 | Ammonia Production |
| 10 | Methanol Production |
| 10 | Others (including Transportation, production of HCl) |

Table 2.2: Hydrogen use in industry

form, which drastically impacts storage. Moreover, production processes produce hydrogen in a gaseous form and the potential liquefaction process requires an important amount of energy. In the aerospace industry, the powerful combination of liquid hydrogen and liquid oxygen as propellants, allows to reach very high values of specific impulse for the first stages of rockets. Furthermore, the space sector makes important endeavours to deal with hydrogen low density and critical phenomena like boil-off, with important impacts on the logistics of the propellants themselves. Hydrogen can even be stored at higher densities in **reversible metal hydrides**, which offer the advantage of low-pressure storage, comfortable shape and reasonable volumetric store efficiency. It is a very safe form of storage in case of any accidental breakdown of storage, the gas remains in the hydride and does not escape.

Hydrogen can store significant amount of energy and it is in fact characterized by high specific energy, however the low densities lead to large tanks, due to the structural and thermal design required. To enable higher densities, high pressure and low temperatures conditions must be guaranteed. An important parameter, which represents the ratio of the $H_2$ hydrogen stored and to the total storage mass (hydrogen + tank), is the **gravimetric index (GMI)**:

$$GMI = \frac{m_{H2}}{m_{H2} + m_{TANK}}$$

### Safety and delivery

Delivery of hydrogen is fundamental in the overall energy infrastructure. It can be transported through pipelines or through trucks, in this case road transport implies liquefaction processes, which are usually very expensive. As all fuels, several risks may be caused by hydrogen if it is not properly handled. Hydrogen has in fact a low ignition point, its flame is nearly visible and can cause cold burns. Hydrogen storage is a well-established reality in electric cars with fuel cells, where the hydrogen refuelled in the vehicles is typically characterized by very high pressures (70 MPa for cars, 35 MPa for heavy trucks), cars often require no more than 5 kg, while buses and trucks could require up to 20 kg of gaseous hydrogen. Existing protocols for hydrogen refuelling in the United States for electric cars with fuel cells on board (SAE J2601 and J-2601-2), define different refuelling rates, ranging from 30 g/s up to 120 g/s. Even though refuelled hydrogen is characterized by very high pressures, as it will be discussed in the following sections, fuel stacks typically have operating pressures no more higher than few atmospheres, therefore tanks need on-tank valves for delivering hydrogen at the expected pressure for the fuel cell.

| **Pressure (bar)** | **T (°C)** | $\rho_{h2}\ kg/m^3$ |
|---|---|---|
| 350 | 15 | 23.99 |
| 350 | 0 | 25.10 |
| 700 | 15 | 40.17 |
| 700 | 0 | 41.69 |
| 0.987liq | -253 | 70.99 |

Table 2.3: Hydrogen density at high pressures

## 2.1.2 Thermodynamics of Fuel Cells

A fuel cell is an electrochemical device which converts the chemical energy of a fuel and oxidant directly into electricity. While fuel cells might be classified

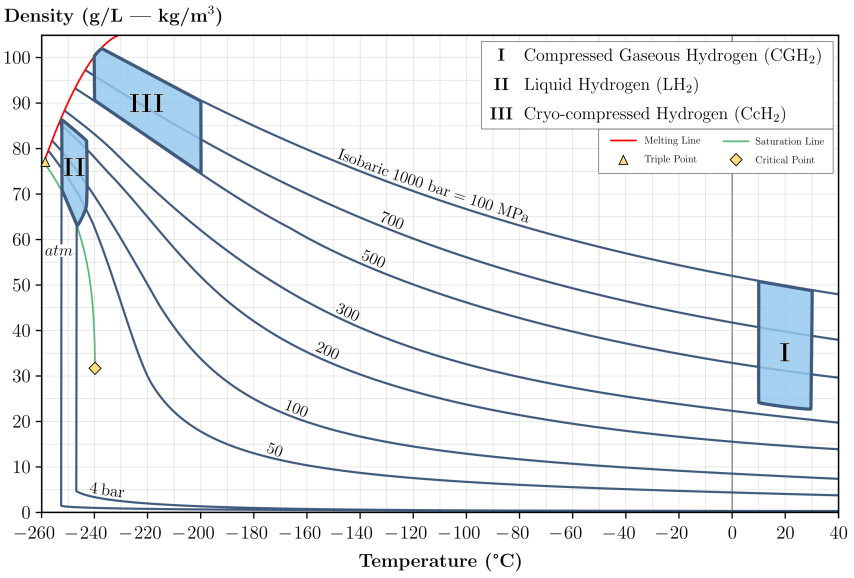


Figure 2.1: Hydrogen density with respect to pressure and temperature. Image from [12]

in several ways, they all consist of an anode, a cathode and an electrolyte [13]. In hydrogen-based **PEM (Proton Exchange Membrane)** fuel cells, positive ions (protons) generated by the oxidation reaction at the anode, pass through the electrolyte, while electrons flow through an external circuit producing electricity. At the cathode, electrons and protons combine with the oxidant (oxygen) in the presence of a catalyst, to form water as the reaction product.

$$\begin{aligned} &\text{Anode reaction:} && H_2 \rightarrow 2H^+ + 2e^- \\ &\text{Cathode reaction:} && \tfrac{1}{2}O_2 + 2H^+ + 2e^- \rightarrow H_2O \\ &\text{Global reaction:} && H_2 + \tfrac{1}{2}O_2 \rightarrow H_2O \end{aligned}$$

Fuel cells are very attractive for power generation, since they are characterized by high efficiencies and low emissions. Furthermore, they are modular, therefore they can be combined in stacks to deliver a specific voltage and power required, for a given application. Fuel cells applications range from portable electronics to stationary power generation and transportation.

First law of thermodynamics allows to assess the behaviour of the fuel cell, defining a balance among the heat transferred to the steady flow stream, the work done by the flow and the change in entalphy of the flow stream from the

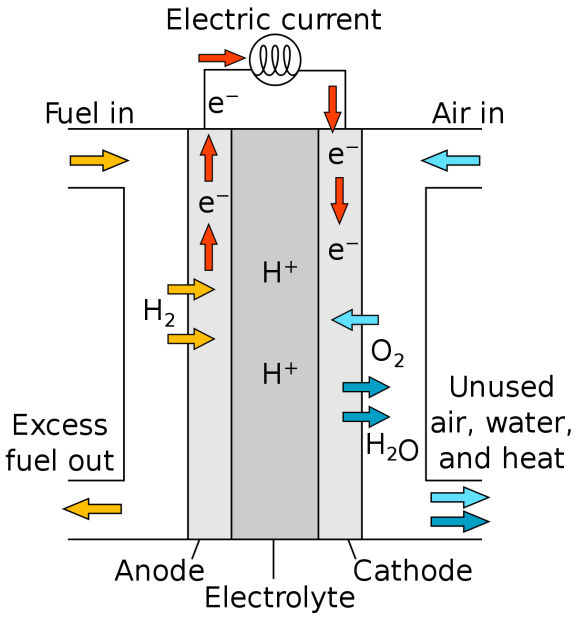


Figure 2.2: Fuel Cell Scheme. Image from [14]

entrance to exit. The second law of thermodynamics, instead, allows to define an expression for the heat transferred for reversible process.

$$\Delta Q - \Delta W = \Delta H \qquad \text{(First law)}$$
$$\Delta Q = T\Delta S \qquad \text{(Second law)}$$
$$\Delta G = \Delta H - T\Delta S \qquad \text{(Gibbs free energy)}$$
$$\Delta W_{\text{max}} = -\Delta G$$

In order to assess the ideal reversible cell voltage, it is possible to equate the magnitude of $\Delta H$ to the electrical energy, as it follows:

$$-\Delta H = q \cdot E_h$$
$$q = N \cdot N_A \cdot q_e$$

where:

$N$ , number of electrons involved in the reaction

$N_A$ , Avogadro's number

$q_e$ , elementary charge of an electron

The product $N_A \cdot q_e$ is also referred to as Faraday's constant. Depending whether or not, the water produced is in liquid or vapour form, it is possible to assess the ideal reversible cell voltage:

| water product | conditions | $\Delta H$ [kJ/mole] | $E_h$ [$V$] | $E_v$ [$V$] | $\eta$ |
|---|---|---|---|---|---|
| liquid | STP | -286 | 1.48 | 1.229 | 0.829 |
| vapour | STP | -242 | 1.25 | 0.979 | 0.784 |

Table 2.4: Efficiency of the fuel cell. $E_h$, is the ideal cell reversible voltage, $E_v$, is the Nerst's voltage

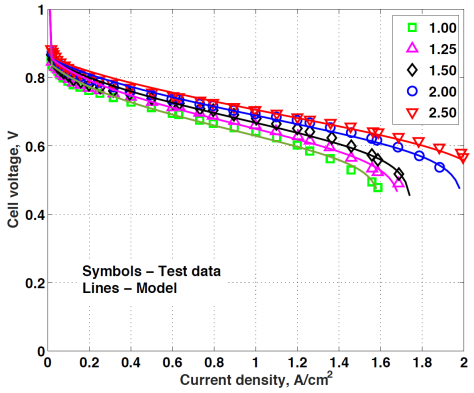


Figure 2.3: Current density-voltage (i-v) characteristics of a modern PEMFC at various stack pressures. Curve from [15]

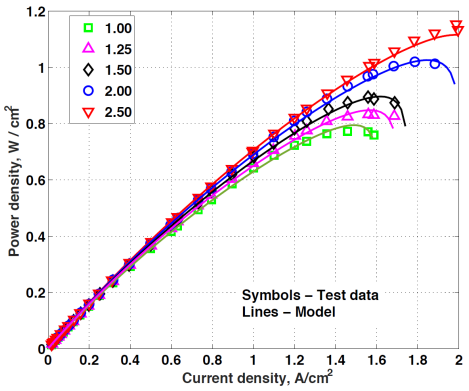


Figure 2.4: Current density-power (i-p) characteristics of a modern PEMFC at various stack pressures. Curve from [15]

### 2.1.3 PEMFC System

Multiple cells assembled together form a stack, a modular element capable of delivering the desired voltage and current when properly configured. Several additional subsystems including compressors and heat exchangers are necessary in order for the overall system to operate; these systems, together with the fuel stack, are usually referred to as the PEMFC stack system. When also accounting also for the hydrogen and its tank, the system is usually referred to as the PEMFC System. As discussed in chapter 3.6, this definition enables a fair comparison between fuel cells and batteries. All these additional subsystems contribute additional weight to the system and consume power generated by the fuel cells – this extra load is usually referred to as the Balance of Plant (BoP), and it reduces

the original efficiency of the fuel cells.

## 2.2 Hydrogen Infrastructure in Europe

In order for eVTOL aircraft with a hybrid fuel cell - battery system to operate within Europe and in the rest of the world, it is important to assess the presence of an existing dedicated infrastructure for hydrogen production and delivery. Hydrogen is produced across Europe in many different locations, following the previously mentioned production processes (e.g. SMR, Partial Oxidation, etc..). However, it is fundamental to understand whether it is feasible to deliver hydrogen to eVTOL operational infrastructures (e.g. Vertiports) for refuelling purposes. Technologies for long term ground storage are not necessarily applicable to the aviation sector. For instance, while hydrogen is often stored in liquid form in industrial and space applications to prevent boil-off, fuel-cell powered aviation systems require gaseous hydrogen. Even in the space sector, where hydrogen is used as a propellant for liquid rocket engines (LRE), extensive technologies are needed to prevent boil-off. Ground vehicles powered by fuel cells, offer a relevant reference point for assessing the current hydrogen landscape in Europe. In fact, in 2024, the total FCEV (Fuel Cell Electric Vehicles) fleet, was composed of more than 6500 vehicles and particularly concentrated in Germany, France and the Netherlands. The highest percentage of these EVs consists of cars, followed by buses, trucks and vans, depending on the country. In Italy, the total fleet is split roughly equally between cars and buses, although, as will be shown later, there is only one operating hydrogen refuelling station. In Europe, there are currently 186 hydrogen refuelling stations, including both standard for cars (700 bar) and for cars and heavy-duty vehicles (350 bar), although not all stations provide both refuelling standards.


Figure 2.5: H2 refuelling stations for FCEV within Europe. [16]

In the following map is possible to analyse several aspects related to the European hydrogen production capacity, covering both conventional fossil-based methods and electrolysis. As it is possible to observe, Germany contributes to the highest share of hydrogen production, followed by the Netherlands, Poland and France. As expected, conventional methods using fossil fuels are the most exploited ones, while electrolysis (a low-emission option), remains limited. Hydrogen is often produced as a by-product, in petrochemical processes aimed at primarily produce ethylene and styrene. As it is possible to observe, in the Netherlands, a small portion of production includes carbon capture techniques. While many current production sites do not focus on low-emission hydrogen or direct aviation applications, the increasing number of hydrogen plants across Europe and the EU's plans for a dedicated hydrogen pipeline network suggest strong potential for future aviation integration. These developments align with the EU's decarbonization targets for 2050.

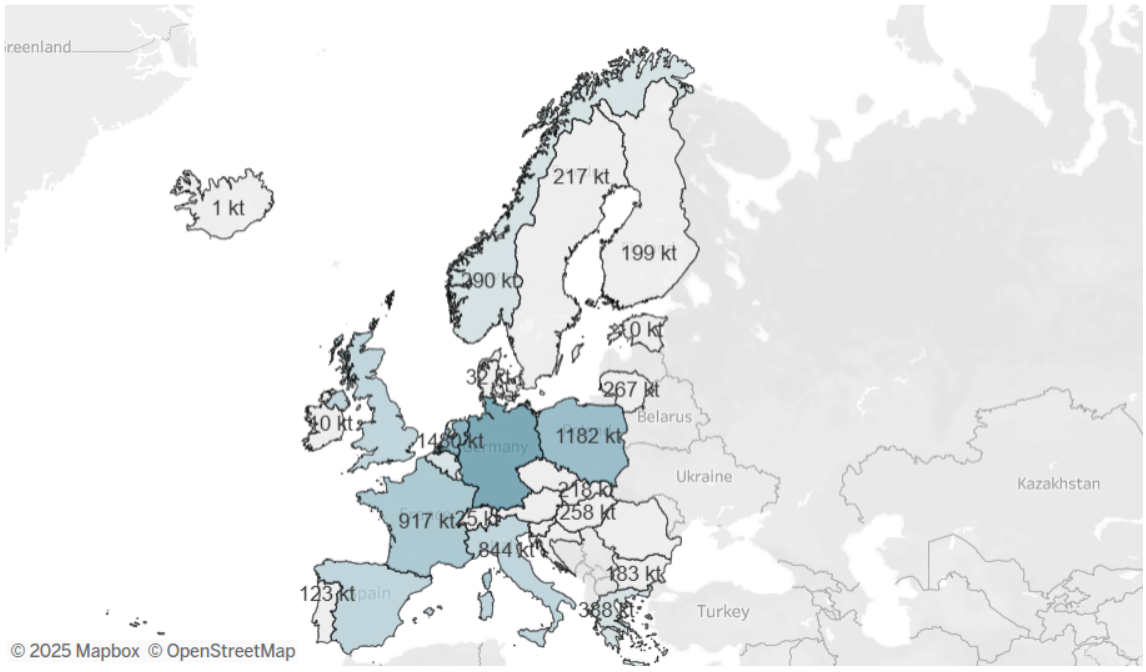


Figure 2.6: European Hydrogen Production capacity per country [17]

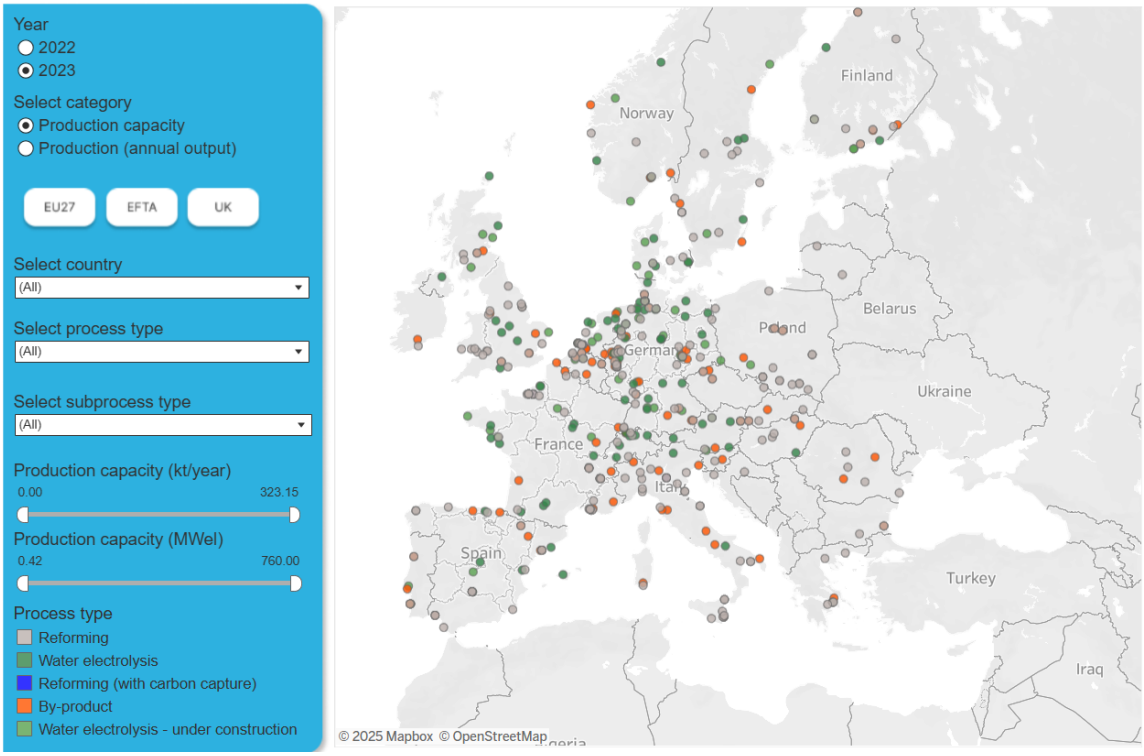


Figure 2.7: European Hydrogen Production sites per country [17]

Establishing a dense hydrogen distribution infrastructure across Europe is

crucial not only for eVTOL operations but also for a broader energy transition. The EU's long-term vision includes large-scale, long-distance hydrogen transport by 2050, using 75% retrofitted natural gas pipelines and 25% newly constructed hydrogen specific ones. Although hydrogen and methane are both transported in gaseous form, hydrogen's distinct chemical properties (notably its embrittlement effect on metals) complicate infrastructure conversion. With the support from national infrastructure operators, the EU has outlined the phased development of a hydrogen transmission grid. This network will resemble the existing natural gas grid in layout – comprising pipelines, compression stations, valves, metering and gate stations – including additional measures that will be necessary to prevent material degradation.

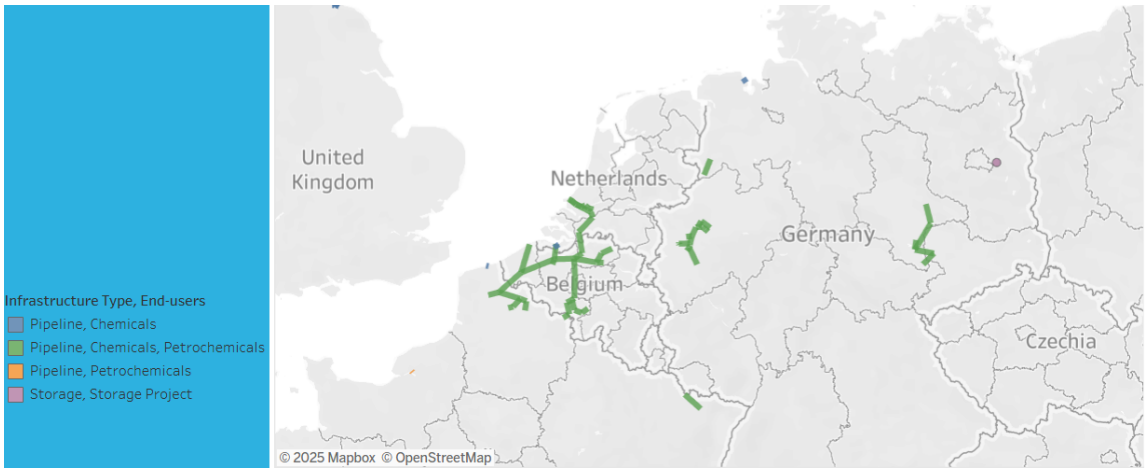


Figure 2.8: Current Hydrogen distribution infrastructure in Europe

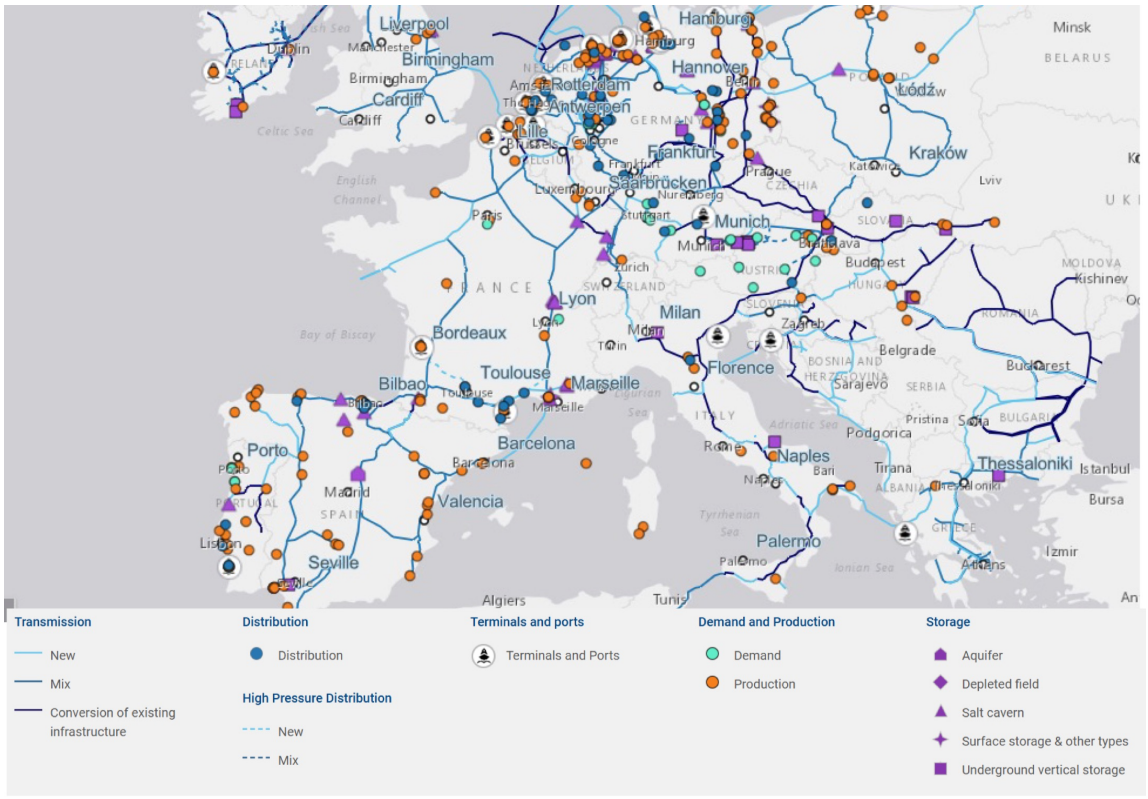


Figure 2.9: Outlined Hydrogen infrastructure by 2050 [18]

As it can be seen, the current infrastructure is limited and present only in a few European countries (notably Germany and the Netherlands). However, the upcoming widespread hydrogen network will facilitate eVTOL refuelling operations, allowing vertiports to support both hydrogen refuelling and battery recharging in hybrid-electric platforms. The presented map highlights key hydrogen production sites and pipeline routes that align well with the proposed city-pairs discussed in Chapter 5. For example, the FCO–NAP route could be particularly advantageous due to the presence of two nearby production points.

## 2.3 Battery Technology

Batteries are devices able to store electrical energy; they are made of electrochemical cells, assembled in such a way to deliver the desired voltage and current. The fundamental electrochemical mechanisms governing them, even though very

similar to those of fuel cells, lie beyond the scope of this thesis and therefore are not discussed. However, some of the most important concepts associated to battery technology are presented below. **State-of-Charge (SoC)**, is typically used to indicate the energy level of a battery at a given time. Batteries can support a maximum number of charge-discharge cycles, which deeply depend on:

- **Battery chemistry**
- **Rate of charging and discharging**, higher the rate, the more the battery may deteriorate.
- **Operating temperature**, batteries do not perform well above and below certain temperature range.
- **Depth of discharge**, to avoid battery deterioration, the *SoC* is always kept between 20% and 80%.

When referring to the remaining capacity of a battery, it is typically referred to as **State-of-Health (SoH)**. When this value reaches a threshold where the battery is no longer useful, it is usually referred to as **EoL (End of Life)**. The EoL is typically set at 80% of the initial capacity. Battery life increases when charged slowly, while it decreases if charged quickly. As for fuel cells, **battery efficiency**, defines the energy conversion efficiency from chemical to electrical energy. Furthermore, batteries are characterized by:

- **BED (Battery Energy Density)**, given by the ratio of the maximum deliverable energy to the battery mass.
- **BPD (Battery Power Density)**, given by the ratio between the maximum power deliverable and the battery mass, indicating how quickly the energy stored can be delivered.

Finally, as with fuel cells, which need several additional subsystems to operate, batteries usually need a dedicated thermal management system to prevent overheating.

# 3. Conceptual design of a powered-lift eVTOL

The conceptual design of a hybrid electric powered-lift VTOL aircraft, poses interesting challenges, which differ from those encountered when sizing conventional concepts. First, it is not possible to apply established methodologies to guide the design process from the high-level requirements to expected qualitative and quantitative estimates. Nevertheless, it is still possible to find in literature some guidelines inspired by classical approaches. Though the exponential growth of the eVTOL market in the recent years, the establishment of statistical base useful to identify trends among physical quantities, remains difficult. The intrinsic hybrid nature of this type of aircraft, equipped with a fixed wing and several propellers, requires a deep understanding of the aerodynamics governing these two different components as well as their reciprocal interactions. While batteries are gradually more integrated in aircrafts, particularly in modern concepts (MEA, More Electric Aircraft), PEM Fuel Cells, although their promising potential, are still under development, leading to some important uncertainties in their quantitative characterization in terms of power and energy density, which can also vary with operating conditions. Beyond these challenges, it is worth discussing the potential benefits of designing this type of aircraft. The vertical take-off and landing capabilities, would enable operations in very dense urban areas, where long runways are unfeasible. The significant amount of power required to lift the aircraft, could be delivered by batteries, characterized by high power density. After a brief transition, where propellers rotate by 90 degrees to compensate for the aerodynamic drag, the wing generates lift in forward flight, enabling more efficient operations. Eventually, fuel cells could play a primary role in supplying energy during cruise phases, exploiting hydrogen's high energy density. In the conceptual design conducted in the following sections, different cases for the powerplant have been considered.

## 3.1 Top Level Aircraft Requirements (TLARs)

The conceptual design is a multidisciplinary process, involving several disciplines of the aeronautical engineering, including aerodynamics, structures, systems, propulsion, flight mechanics and many other. It is often referred to as a very iterative and recursive process, as the initial estimates are powerful feedback to assess whether the defined requirements are realistic or overly demanding. The definition of the top-level requirements, which will be hereafter presented, is driven by the identification of some opportunities or needs to be addressed by the design. It is also very interesting to point out how changes in these early phases severely impact the final configuration, while incurring relatively low cost. The introduction of modifications in advanced phases of the process, including preliminary and detail design phases, is generally more costly and results in smaller impact on the final product. While system requirements are interested in the iterative nature of the design process, it is important to highlight that the mission objectives, are established at the start of the conceptual design phase and therefore do not iterate. The conceptual design should explore feasible solutions able to meet the agreed mission objectives. Finally, it is important to underline how, in the following sections, "weights" and "masses" might be used as synonyms to indicate quantities expressed in $Kg$ or in $lb$.

| TLRs | Value |
|---|---|
| Passengers | 4 |
| Range | 150 km |
| Pilot(s) | 1 |
| Cruise Speeed | 250 km/h |
| Mach | 0.21 |
| Cruise Altitude | 610 m |
| Propulsion | Full Electric |
| Configuration | Combined-Thurst |
| Entry into service | 2035 |

Table 3.1: Top Level Aircraft Requirements

## 3.2 eVTOL Aircraft reference dataset

Even though eVTOL are innovative and unique concepts, for which it is difficult to define solid statistical base, it can be still useful to gather some general characteristics of eVTOLs with similar architecture to the one intended. It is useful to examine some existing powered-lift eVTOL concepts in order to identify common design choices as well as unique features that distinguish each aircraft. General characteristics such as maximum range and cruise speed are reported for all the aircraft in the table below.

### 3.2.1 Wisk Aero 6th gen.


Figure 3.1: Wisk Cora 6th gen. [19]

The unique feature of this aircraft is undoubtedly the absence of a pilot; it is, in fact, designed to fly autonomously. Twelve propellers enable vertical lift, while only six of them are also tilt-propellers useful for forward flight. The aircraft, as all the other concepts hereafter discussed, makes use of batteries, which take about 15 minutes to recharge. The aircraft has a fixed skid landing gear, which is also a very common design choice for helicopters. The tail plane incorporates classical configurations with vertical and horizontal stabilizers. The presence of multiple propellers, a feature shared by many existing eVTOL concepts, represents a key feature, providing safety through redundancy.

### 3.2.2 Archer Aviation Midnight

Figure 3.2: Archer Aviation Midnight [20]

Similarly to the previous design, it is still possible to find twelve propellers for vertical lift, among which six of them are able to tilt for forward flight. Furthermore,

it is possible to find a V-tail, which can function either as a horizontal tail or a vertical one, according to the deflection of the control surfaces. It also has a fixed tricycle wheeled landing gear, which facilitates ground handling. The cruise phase is performed at an altitude of 610 m (2000 ft).

### 3.2.3 Lilium Jet

Figure 3.3: Lilium Jet [21]

Lilium Jet can carry up to 7 passengers and 1 pilot. Its unique feature is the presence of thirty-six electric vectored thrust fans, each powered by its own electric motor, enhancing the concept of safety through redundancy. The aircraft also benefits from a lightweight fuselage, made with carbon fiber composite materials.

### 3.2.4 Joby S4

Figure 3.4: Joby S4 [22]

The Joby S4 aircraft has in total six tilting propellers, two of which are located on the V-tail, while the remaining four are on the fixed wing. The aircraft features a tricycle wheeled landing gear, able to retract in flight. Once again, the fuselage benefits from carbon fiber composite materials. Finally, this aircraft has a wingspan of 10.7 m and a fuselage length of 7.3 m.

### 3.2.5 Vertical Aerospace VX4

Figure 3.5: Vertical Aerospace VX-4 [23]

Dimensions are among the unique features of the VX4: 13-meters long with a wingspan of 15 meters. Its landing gear is similar to the one previously introduced: retractable and wheeled. Its wing features several control surfaces, including ailerons and flaps, to enhance manoeuvrability. It has in total 8 propellers, each powered by its own electric motor, while only 4 of them have tilting features. Once again, the vertical and horizontal tail merge together in a V-tail configuration.

### 3.2.6 Beta Technologies ALIA-250

Figure 3.6: Beta Technologies ALIA-250 [24]

Beta Alia's aircraft is characterized by 5 propellers, four of them dedicated to vertical flight while the fifth one is necessary to perform forward flight capabilities. The wingspan reaches 15 meters, while the landing gear incorporates a unique configuration: fixed skid with quadricycle wheels. Similarly to the previous design discussed, the control and stability functions are achieved through the use of a V-tail.

| | Wisk Aero 6th gen. | Archer Midnight | Lilium Jet |
|---|---|---|---|
| **Passengers (pax)** | 4 | 4 | 6 |
| **Cruise Speed (km/h)** | 220 | 241 | 250 |
| **Maximum Range (km)** | 145 | 80 | 175 |
| **Vehicle Configuration** | Lift+Cruise | Vectored Thrust | Vectored Thrust |
| **MTOW (kg)** | 3175 | 3175 | 3175 |
| **Pilot** | Autonomous | 1 | 1 |

| | Joby S4 | Vertical Aerospace VX4 | Beta Technologies ALIA-250 |
|---|---|---|---|
| **Passengers (pax)** | 4 | 4 | 4 |
| **Cruise Speed (km/h)** | 322 | 241 | 250 |
| **Maximum Range (km)** | 241 | 161 | 500 |
| **Vehicle Configuration** | Vectored Thrust | Vectored Thrust | Lift+Cruise |
| **MTOW (kg)** | 1815 | 3150 | 3175 |
| **Pilot** | 1 | 1 | 1 |

Table 3.2: eVTOL aircraft reference dataset

## 3.3 Aerodynamics

### 3.3.1 Hover Aerodynamics

Lift generation and propulsion in eVTOLs are enabled by the presence of rotors, which play a key role in helicopters; therefore a deep understanding of helicopter aerodynamics is crucial when studying eVTOL design. Similarly to wing loading for fixed-wing aircraft, an important parameter for helicopters is the disk loading $\frac{T}{A}$, the ratio between the thrust generated and the total disk area of rotors. On the other side, for eVTOL aircraft it still possible to identify a wing-loading value in forward flight, with similar considerations of fixed-wing conventional aircraft. It is possible to demonstrate that high disk loading, reduce hover efficiency, characterized by the ratio of helicopter maximum take off weight and the required power to lift-off. Though helicopters are usually characterized by very low lift-to-drag ratios compared to fixed-wing aircraft, since the several power losses, eVTOL are expected to reach higher ratios, setting around 10, similarly to tilt-rotors helicopters, such as the XV-15.

Helicopters aerodynamics are usually described by two fundamental theories: momentum theory and blade element theory (BET). The former allows for the estimation of the induced power required to lift the rotorcraft, while neglecting the blade geometry; it defines the primary relationship between induced power and thrust. The latter, increases the estimated power value by introducing profile power contributions due to circulation variations along the blade span. Hereafter, the fundamental results of these two theories are presented for the simple case of hover, which is one of the most important flight conditions for eVTOL aerodynamics. [25]

$$P_i = T \cdot u \quad u, \text{inflow velovity} \qquad \text{(Momentum Theory)}$$
$$P = P_i + P_p = T \cdot u + \frac{3}{4} T \frac{V_{tip}}{E} \quad \text{(Blade Element Theory)}$$

Another fundamental parameter is the Figure of Merit (FM), defined as the ratio between the ideal (induced) power and the actual required power. Although it

might seem desirable to achieve a value of FM = 1, for the same power loading, higher figures of merit, lead to higher disk loading, which affect rotor performance and lead to stronger downwashes. Helicopters typically reach values around 0.75-0.80.

$$FM = \frac{P_{id}}{P_{eff}} \approx \frac{P_i}{P_i + P_p} \rightarrow P_{eff} = \frac{(T_{VTOL})^{\frac{3}{2}}}{\sqrt{2 \cdot \rho \cdot A_{disk}}} \cdot \frac{1}{FM}$$

In vertical flight, it is important to highlight that the aforementioned aerodynamic theories (Momentum Theory and Blade Element Theory), provide reliable estimates for ascending flight and hover, but lead to misleading conclusion in descending flight, particularly when the descent rate (which is negative) module is comparable to the inflow velocity through the disk. In this case, the flow no longer follows the canonical slipstream model described by momentum theory; a recirculating flow region forms slightly below the rotor and begins to be ingested by the rotor itself, entering the well-known vortex ring state. At higher descent rates, the flow reorganizes into a more structured regime, transitioning into the autorotation state.

The assessment of Vortex Ring State (VRS) for eVTOL aircraft lies beyond the scope of this thesis; however it is fundamental to be aware how hazardous this phenomenon can be for eVTOL aircraft. VRS is a complex aerodynamic phenomenon influenced by parameters such as disk loading and even by descent trajectory models, which are closely linked to vertiport regulations. Other complex aerodynamic phenomena eVTOL should deal with, regard the effects of downwash and outwash, and how vertiports can be designed to mitigate their consequences.

### 3.3.2 Cruise Aerodynamics

After a brief transition, the eVTOL begins to behave as a fixed-wing aircraft, whose aerodynamics differs from the one of helicopters. Hereafter, only the relevant elements for the conceptual design phase are presented and discussed. First, as stated in the TLRs, the Mach number does not exceed 0.21, therefore, the aircraft is characterized by subsonic flow regime, similar to regional aircraft. The

subsonic flow allows to neglect complex phenomena which usually occur at higher velocities and are generally related to the transonic effects and the generation of shock waves.

Even though streamlines accelerate along the wing profile, the flow might reach higher subsonic conditions but cannot become supersonic, hence the introduction of sweep angles, should not be necessary. However, it still important to note that sweep angles deeply impact aeroelastic phenomena, which are very difficult to assess in the conceptual design phase, as they are also influenced by materials and aerodynamic coupling.

## 3.4 Mission Analysis

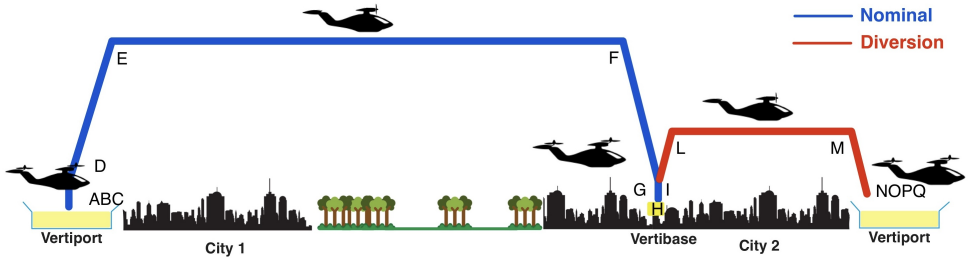


Figure 3.7: Mission profile for an inter-city application

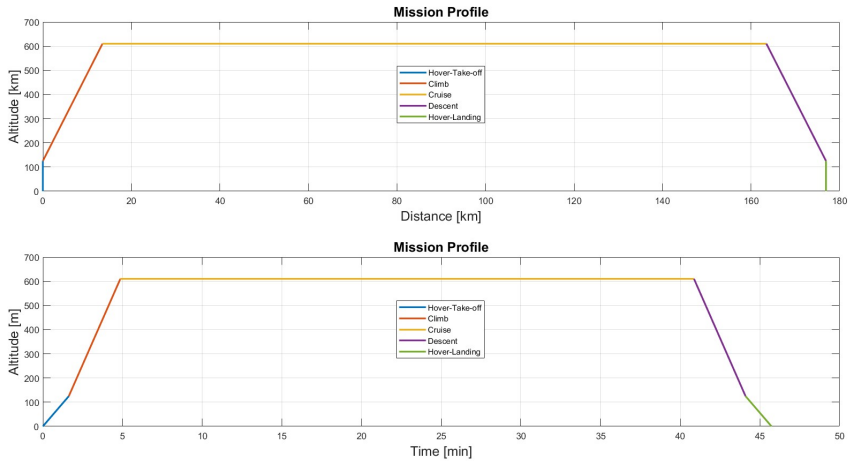


Figure 3.8: Nominal mission profile on MATLAB

| Mission Profile | | | | | | |
|---|---|---|---|---|---|---|
| Mission Phase | Phase | Duration (min) | Horizonral Speed (km/h) | Vertical Speed (m/s) | Starting Altitude (m) | Ending Altitude (m) |
| Take-off | A - B | 0.5 | 0 | - | 0 | 15 |
| Hovering | B-C | 1.13 | 0 | - | 15 | 100 |
| Transition | C-D | 0.17 | - | 2.5 | 100 | 125 |
| Climb | D-E | 3.23 | Note | 2.5 | 125 | 610 |
| Cruise | E-F | 36 | 250 | 0 | 610 | 610 |
| Descent | F-G | 3.23 | Note | -2.5 | 610 | 125 |
| Transition | G-H | 0.17 | - | -2.5 | 125 | 100 |
| Transition and Climb | G-I-L | 1 | 170 | 2.5 | 100 | 250 |
| Cruise | L-M | 10 | 170 | 0 | 250 | 250 |
| Descent and Transition | M-N-O | 1 | 170 | -2.5 | 250 | 100 |
| Hover and Landing | O-P-Q | 1.33 | 0 | -2.5 | 100 | 0 |

Table 3.3: eVTOL aircraft mission profile

A fundamental assumption when analysing the mission, regards the fact that for the conditions of interest (altitudes and corresponding air densities), CAS, IAS and TAS can be approximately considered equivalent.

### 3.4.1 Phases Analysis

#### Take-off

In the take-off phase, the rotors start rotating at maximum power. The aircraft reaches altitude of 15 m in vertical flight, leaving the vertiport.

### Hover

The aircraft reaches an altitude of 100 m and a RoC (Rate of Climb) of 2.5 m/s. Therefore it is possible to establish the required time and acceleration as it follows:

$$\begin{cases} V = V_0 + a \cdot \Delta t \quad V = RoC \\ \Delta S = \frac{1}{2} \cdot a \cdot \Delta t^2 \quad \Delta S = h_f - h_i \end{cases}$$

### Transition

In the transition phase, the aircraft keeps following a constant Rate-of-Climb, the propellers rotate and the aircraft accelerates until the climb speed.

### Climb

In the climb phase, the aircraft aims at maximizing the Rate-of-Climb, hence it should satisfy the following conditions:

$$V \ t.c. \ (RoC)_{max} \rightarrow \left(E \cdot \sqrt{CL}\right)_{Max} \text{ Minimum Power}$$

$$C_L = \sqrt{\frac{3 \cdot C_{D0}}{k}}, \ C_D = 4 \cdot C_{D0}, \ V = \sqrt{\frac{2 \cdot \frac{W}{S}}{\rho C_L}}$$

### Cruise

In the cruise phase, the aircraft has a constant velocity of 250 km/h in level flight at an altitude of 610 m, as defined in the top level requirements

### Descent

In the descent phase, the aircraft reaches an altitude of 125 m, with a constant RoD (Rate of Descent) of -2.5 m/s. In this condition, to maximize the range, the aircraft should satisfy the following conditions:

$$V \ t.c. \ (\Delta s)_{max} \rightarrow (E)_{max} \text{ Maximum Efficiency}$$

$$C_L = \sqrt{\frac{C_{D0}}{k}}, \ C_D = 2 \cdot C_{DO}, \ V = \sqrt{\frac{2 \cdot \frac{W}{S}}{\rho C_L}}$$

#### Diversion

The aircraft should be able to perform a diversion, as described in the table, in the case the intended destination's vertiport should not be available.

#### Transition, Hover and Landing

The eVTOL should perform a transition from forward flight to vertical flight, rotating its propellers and decelerating from the descent horizontal speed to 0 m/s. In these phases the eVTOL maintains a constant RoD. In the mission definition, it is very important to ensure the eVTOL has a RoD $<< u_h$, which is the induced hover velocity through the rotor disk, to avoid any possible Vortex Ring State ouset.

## 3.5 Matching Chart

The matching chart is a fundamental two-dimensional graphical tool in the conceptual design phase, in which performance requirements are expressed through mathematical relationships. For the most power-demanding phases, it is possible to establish a mathematical relationship between the ratio (P/W) and the wing-loading. An eVTOL has two input parameters: wing-loading and disk-loading, therefore the matching can be constructed fixing one of the two parameters. This tool allows therefore to analyse the design space in terms of power requirements, identifying the point, for a given wing-loading, at which all the requirements are met, thus determining the necessary power. The mathematical expressions for the most power-demanding flight phases are derived from the flight mechanics equations. [26]

The flight phases identified are take-off, cruise, climb and stall. The last one, in accordance with the aircraft desired characteristics, allows to define the maximum wing-loading.

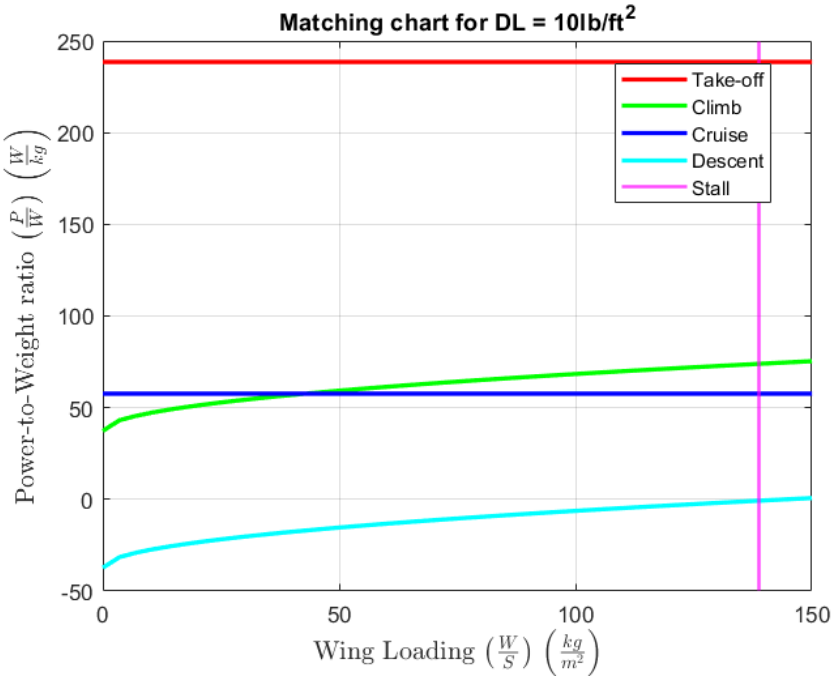


Figure 3.9: A possible matching chart output for eVTOL sizing. 10 $lb/ft^2$, corresponds to 48.8 $kg/m^2$.

### Take-off

The mathematical expression for the take-off power requirement has been derived using the Momentum Theory, as explained in the aerodynamic section.

$$\left(\frac{P}{W}\right)_{TO} = g \cdot \sqrt{\frac{W \cdot g}{2 \cdot \rho \cdot A}} \cdot \frac{k_t}{FM} \quad \text{[W/kg] Take-off}$$

For the following phases, all the power requirements are derived in the same way, with the following hypothesis:

$$\begin{cases} \sin\gamma \approx \gamma \\ \cos\gamma \approx 1 \end{cases}$$

The flight mechanics equations used are hereafter reported:

$$\begin{cases} L = W \cdot \cos(\gamma) \cdot g & \text{Lift-direction} \\ T = D + W \cdot g \cdot \sin(\gamma) & \text{Drag-direction} \end{cases}$$

Furthermore, for the cruise phase $\gamma = 0\,\text{deg}$, while for the Climb and Descent phase, $RoC/RoD = V \sin\gamma$.

**Climb**

$$\left(\frac{P}{W}\right)_{Cl} = g\cdot\left[\frac{1}{E_{cl}}\cdot\sqrt{\frac{2\frac{W}{S}g}{C_{L_{cl}}\rho}} + RoC\right] \text{ [W/kg] Climb}$$

**Cruise**

$$\left(\frac{P}{W}\right)_{cr} = g\cdot\left[\frac{1}{E_{cr}}\cdot\sqrt{\frac{2\frac{W}{S}g}{C_{L_{cr}}\rho}}\right] \text{ [W/kg] Cruise}$$

**Descent**

$$\left(\frac{P}{W}\right)_{de} = g\cdot\left[\frac{1}{E_{de}}\cdot\sqrt{\frac{2\frac{W}{S}g}{C_{L_{de}}\rho}} - |RoD|\right] \text{ [W/kg] Descent}$$

**Stall**

$$\left(\frac{W}{S}\right)_{MAX} = \frac{\frac{1}{2}\rho V_{stall}^2 C_{L,max}}{g} \text{ [kg/m}^2\text{] Stall}$$

Hereafter, the several coefficients introduced in the previous formulations, are explained.

| Parameter | Note |
|---|---|
| $k_T \approx 1.16$ | Power excess to lift the aircraft |
| FM | See 3.3 |
| $\gamma$ | Flight-path angle |
| RoC/RoD | Rate of Climb/Descent See 3.4 |

## 3.6 Weight estimation

It is essential to recognize the importance of weight distribution along the aircraft, in order to ensure its static stability in every flight condition. However, before discussing systems' integration within the aircraft, it is fundamental to estimate

the weight of each subsystem, relying on expressions deriving from classical approaches. The weight definition for each subsystem and/or structural element, has been obtained through semi-empirical and statistical models (based on regression methods). In the case of our interest, Roskam Class II method[1] has been used. Since weight distribution highly depends on aircraft mission and performance, it is necessary to address the eVTOL in the right aircraft classification, among those available in the reference source. It is therefore necessary to highlight how eVTOL represent a newborn unique concept, diffent from those concepts on which the applied methods had been built on.
Class II method, distinguishes among 4 different aircraft categories:

- General Aviation Airplanes
- Commercial Transport Airplanes
- Military Patrol
- Fighter and attack airplanes

For the case of our interest, an eVTOL can be addressed through the first category.
In order to address General Aviation airplanes, the method suggests several options based on the perfomance of the aircraft itself, in particular:

- CESSNA, applicable to "small, relatively low performance type airplanes with maximum speeds below 200 kts"
- USAF, applicable to "light and utility type airplanes with performance up to about 300 kts"
- Torenbeek, "applicable to light transport airplanes with take off weights below 12500 lb"

[1] Jan Roskam. *Airplane design / Jan Roskam*. eng. Lawrence: The University of Kansas, 1985. ISBN: 9781884885112.

In the following aircraft weight distribution assessment, given the general characteristics of the eVTOL of our interest, weight assessment will be performed using CESSNA and Torenbeek methods. For each weight formula, it will be clearly specified which method has been used.
In addition to classical formulas presented in the reference, additional formulation for the PEMFC system will be introduced and discussed.
In the end, it is fundamental to remind how the formulations are not built in the SI system therefore parameters such as wing surfaces and weight need first to be converted in Imperial units.

**Wing**

$$W_{wing} = 0.04671 \cdot \left(MTOW^{0.397}\right) \cdot \left(S^{0.36}\right) \cdot \left(n_{ult}^{0.397}\right) \cdot \left(A^{1.712}\right) \quad \text{Cessna}$$

**Fuselage**

$$W_{fus} = 14.86 \cdot \left(MTOW^{0.144}\right) \cdot \left(\frac{l_{fus}}{\phi_{fus}}\right)^{0.778} \cdot \left(l_{fus}^{0.383}\right) \cdot \left(n_{pax}^{0.455}\right) \text{ Cessna}$$

**Landing gear**

$$W_{lg} = 0.054 \cdot \left(L_{lg}^{0.501}\right) \cdot (MTOW \cdot \eta_{lg})^{0.684} \quad \text{USAF}$$

Since the CESSNA and Torenbeek methods, for the landing gear mass estimation, require parameters unavailable at this stage of the sizing process, in this case the USAF method has been used instead.

**Empennage**

For the empennage, including both the horizontal and vertical tail, the following formulation has been adopted:

$$W_{EMP} = 0.04 \cdot \left(n_{ult} \cdot (S_v + S_h)^2\right)^{0.75} \quad \text{Torenbeek}$$

### PEMFC System

The weight of the PEMFC system includes both the fuel cell stack and the Balance of Plant components, which comprise all the elements necessary for the operations of the fuel cell, such as compressors, heat exchangers and air supply system. The hydrogen tank and the hydrogen itself are also included in the formulation, in order to make the whole system comparable with batteries. The formulation for the PEMFC system, derives from[2] and hereafter presented. In order to exploit the following formula to estimate the system's weight, it is important to identify the operating point on the cell's current voltage (i-v) curve. Two points of interest can be identified:

- **Maximum Power**, the point where the product of current and voltage, is maximized.
- **Maximum Efficiency**, the point at which the fuel cell reaches the highest conversion efficiency.

In this conceptual design phase, it has been decided to operate the fuel cell at point of maximum power.

$$W_{PEMFC,\ Stack} = \frac{k_A \rho_c}{1-\eta_{OW}} \cdot \frac{P}{pc_{max}}$$
$$W_{PEMFC,\ Stack\ System} = W_{PEMFC,\ Stack} \cdot (1+f_{BOP})$$

$$\dot{W_{H_2}} = \frac{\lambda_h \cdot m_h}{N_e \cdot F} \cdot \frac{P \cdot (1+f_{BOP})}{v_{c,\ max}} \text{ [kg/s]}$$
$$W_{H_2,\ tank} = \frac{1}{\eta_{BO} \cdot w_{frac}} \cdot W_{H2}$$

$$W_{PEMFC,\ System} = W_{PEMFC,\ Stack\ System} + W_{H_2} + W_{H_2,\ tank}$$

[2] Wanyi Ng and Anubhav Datta. "Hydrogen Fuel Cells and Batteries for Electric-Vertical Takeoff and Landing Aircraft". In: *Journal of Aircraft* 56.5 (2019), pp. 1765–1782. DOI: 10.2514/1.C035218. eprint: https://doi.org/10.2514/1.C035218. URL: https://doi.org/10.2514/1.C035218.

| Parameter | Value | Notes |
|---|---|---|
| $k_A$ | 4 | Ratio between cross-sectional and active area |
| $\rho_c$ | 1.57 | Fuel cell material density |
| $\eta_{OW}$ | 0.3 | Additional weight fraction accounting for seals, connectors etc.. |
| $f_{BOP}$ | 0.2 | Balance of Plant |
| $pc_{max}$ | 1.16 | Operating Point |
| $vc_{max}$ | 0.564 | Operating Point |
| $\lambda_h$ | 1 | Effective Stoichiometry |
| $m_h$ | 2.016 | $[kg/mol]$ |
| $N_e$ | 2 | Number of electrons involved per molecule |
| $F$ | 96485 | Faraday's constant |
| $\eta_{BO}$ | 1.02 | To account for Boil-off |
| $w_{frac}$ | 0.05-0.15 | Structural weight fraction H2 tank |

Table 3.4: PEMFC System Parameters

### Battery

In the conceptual design of a powered-lift eVTOL, batteries play a fundamental role in satisfying the power demands during highly demanding phases, such as take-off; due to their high BPD (Battery Power Density), higher than fuel cells, they can deliver the required power with a relative low weight. The energy the battery is required to deliver, is obtained by the product of power and the duration of the phase in which battery is employed. Thus, according to the operational strategy (Battery and Fuel Cell Hybridization), it is fundamental to assess whether power or energy delivery represents the most demanding condition. When assessing power and energy requirements, it is important to account for some parameters such as the system's State-of-Charge (SoC) limits, which are conventionally set between 20% and 80%, in order to battery deterioration over time. An efficiency factor for Lithium-Ion batteries is also introduced, in order to account for energy conversion losses.

| Parameter | Value | Note |
|---|---|---|
| BED | 250-350 | [Wh/kg] |
| BPD | 750-1050 | [W/kg] |
| C-rate | 3 | [1/hr] |
| EOL | 85 % | |
| $\eta_b$ | 0.9 | Battery Efficiency |

Table 3.5: Battery Parameters

$$W_b = \max\left( \frac{1}{BED} \cdot \frac{E_{req} \cdot (1 + SoC_{min})}{\eta_{bat} \cdot EOL}, \frac{1}{BPD} \frac{P_{req} \cdot (1 + SoC_{min})}{\eta_{bat} \cdot EOL} \right)$$

**Flight Control System**

$$W_{FCS} = 0.0168 \cdot MTOW \quad \text{Cessna}$$

**Motors and propellers**

$$W_{prop} = 0.144 \cdot \left(2 \cdot R_{prop} \cdot P_{max} \cdot \sqrt{n_{blades}}\right)^{0.782} \text{ Cessna}$$

$$W_{Motors} = 0.4106 \cdot \left(P_{nec}^{0.89}\right) \text{ Ng-Datta}$$

**Electrical System**

$$W_{EPS} = 0.0268 \cdot MTOW \text{ Cessna}$$

**Avionics**

$$W_{AVIONICS} = 0.008 \cdot MTOW + 40 \text{ Torenbeek}$$

**Furnishings**

$$W_{FURN} = 0.412 \cdot \left(n_{pax}^{1.145}\right) \cdot \left(MTOW^{0.489}\right) \quad \text{Cessna}$$

## 3.7 Power Source Hybridization Strategy

For the powerplant system, five different possible architectures have been considered:

1. Batteries **(B)** supply energy during the whole mission
2. Fuel Cell **(FC)** supply energy during the whole mission
3. First Hybridization Strategy: **(BFCH-1)**, batteries supply energy during the hovering phases, while the fuel cells provide power for the remainder of the mission. This strategy has been the first one hypothesized and the most intuitive one.
4. Second Hybridization Strategy: **(BFCH-2)**, the required energy in the hovering phases is provided in equal form 50%-50% by batteries and fuel cells. The energy required for the remainder of the mission is provided by fuel cells.
5. Third Hybridization Strategy: **(BFCH-3)**, fuel cells deliver constant power with batteries compensating for additional power required during hover. Specifically, fuel cells provide constant power at a value given by the maximum between the power demanded by the cruise and climb phases.

The diversion phase has been evaluated as accounting for an additional 30% of the total energy consumed. In order not to oversize the battery, in hybrid configurations, it is always performed using fuel cells. The presented strategies significantly affect the eVTOL sizing in several ways. In order to conduct an accurate assessment and identify the best strategy for delivering power, other requirements characterizing the eVTOL, such as range and disk loading, must be included in the discussion. As shown in several academic studies, the convenience of hybrid solutions specifically depend on the range and on the features of batteries and fuel cells.

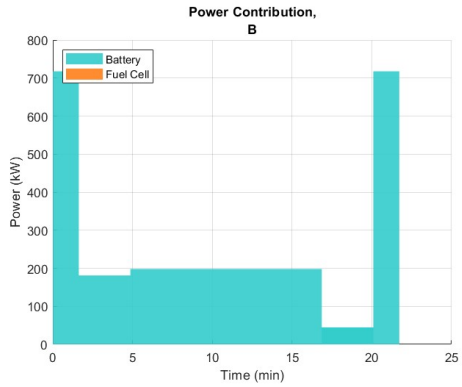


(a) Battery only

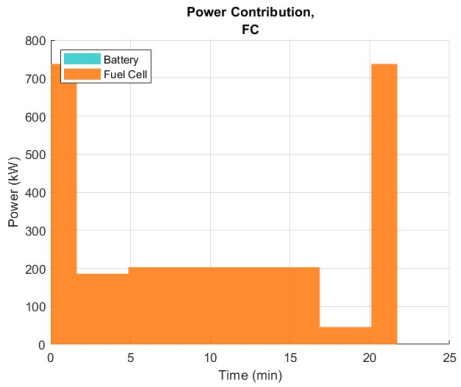


(b) Fuel Cell Only

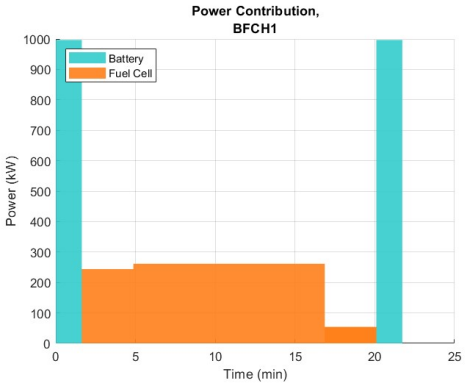


(c) BFCH-1

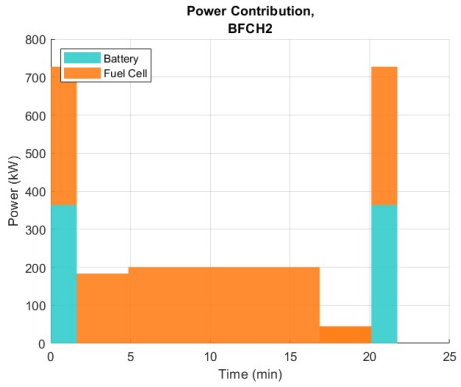


(d) BFCH-2

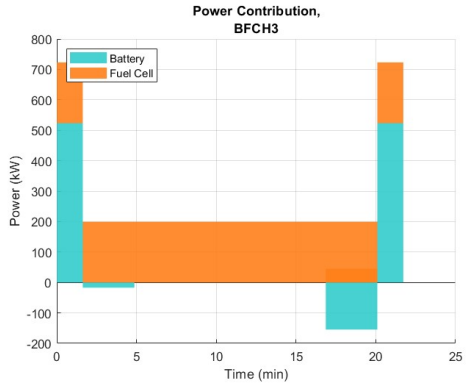


(e) BFCH-3

Figure 3.10: Overview of the five configurations/scenarios.

The examples have to be considered purely representative of the sharing architectures and are intended for demonstration purpose only. They refer to a 50 km range mission for representation purpose. More detailed performance anal-

ysis are presented and discussed in the following chapter. In the BFCH3 configuration, the negative value reached by batteries, represent an opportunity for them to be recharged by the additional power delivered by the PEMFC system. During their operational life, eVTOLs will need to recharge batteries, increasing ground time. In hybrid solutions, fuel cells might also be used to deliver power to recharge batteries, increasing operational efficiency. In the following sections, aircraft configurations equipped with a hybrid fuel cell - battery powerplant may, in some cases, be referred to directly by their specific powerplant designation (e.g., BFCH3, indicating a configuration featuring a hybrid powerplant with the corresponding power-sharing strategy).

### 3.7.1 Hybrid Fuel Cell - Battery Powerplant system

In the below scheme, a possible architecture for the hybrid fuel cell - battery powerplant system is presented. As it is possible to observe, the PEMFC system includes the stack, which is the core of the system where the oxidation–reduction reactions occur. It is characterized by a number of cells defined in order to ensure a 250 V output voltage. Air is supplied from the outside, although an air compression unit (such as blowers) would be necessary to compress it to higher pressure values to improve fuel cell performance. This would actually require a further trade-off analysis, since the improved performance must be assessed against the additional weight introduced by the compression system. Along with the necessary power, fuel cells produce water, which could be partially stored and partially used by the humidification unit. This justifies the presence of a water tank. Fuel cells also produce a significant amount of heat; therefore, in order to keep them cooled, a heat exchanger is necessary. In fact, since PEMFCs involve a polymeric membrane, and this membrane deteriorates at high temperatures, a proper cooling strategy is required. Hydrogen is supplied in gaseous form from a structurally reinforced tank, and a pressure regulation valve is necessary to deliver it at the correct pressure for the required reactions to occur. The heat produced by the fuel cell can be recovered using an additional recovery system (recuperators). The

output power produced by the PEMFC system is sent through a DC/DC unidirectional converter to reach the 270 V DC main bus. On the other hand, for the battery, a bidirectional converter is more appropriate, since the proposed architecture allows the battery to be recharged by the PEMFC system. In this case, a DC/DC converter is still necessary to compensate for battery output voltage fluctuations caused by various parameters (battery state-of-health and others). Power management allows the output power to be delivered to the propellers in order to generate thrust. Assuming the electric motors require AC, a DC/AC converter is employed to deliver 115 V AC at variable frequency. Although further discussion is necessary, a gearbox system—used to convert torque and angular speed—has been included to further deliver power to the propellers. In addition to the propellers, for which the sizing process has been defined, the scheme includes additional elements requiring power. In particular, avionics, lighting, and flight control systems could be powered with 28 V DC, requiring a DC/DC converter, while ECS and similar systems could be powered with 115 V AC. Sensors and transducers allow feedback information, regarding electric motors and flight conditions, to be sent to the power management unit, in order to control the output power. The system could include an additional battery to power essential units in case of emergency or incorporate redundancy strategies to exclude non-essential systems under such conditions.

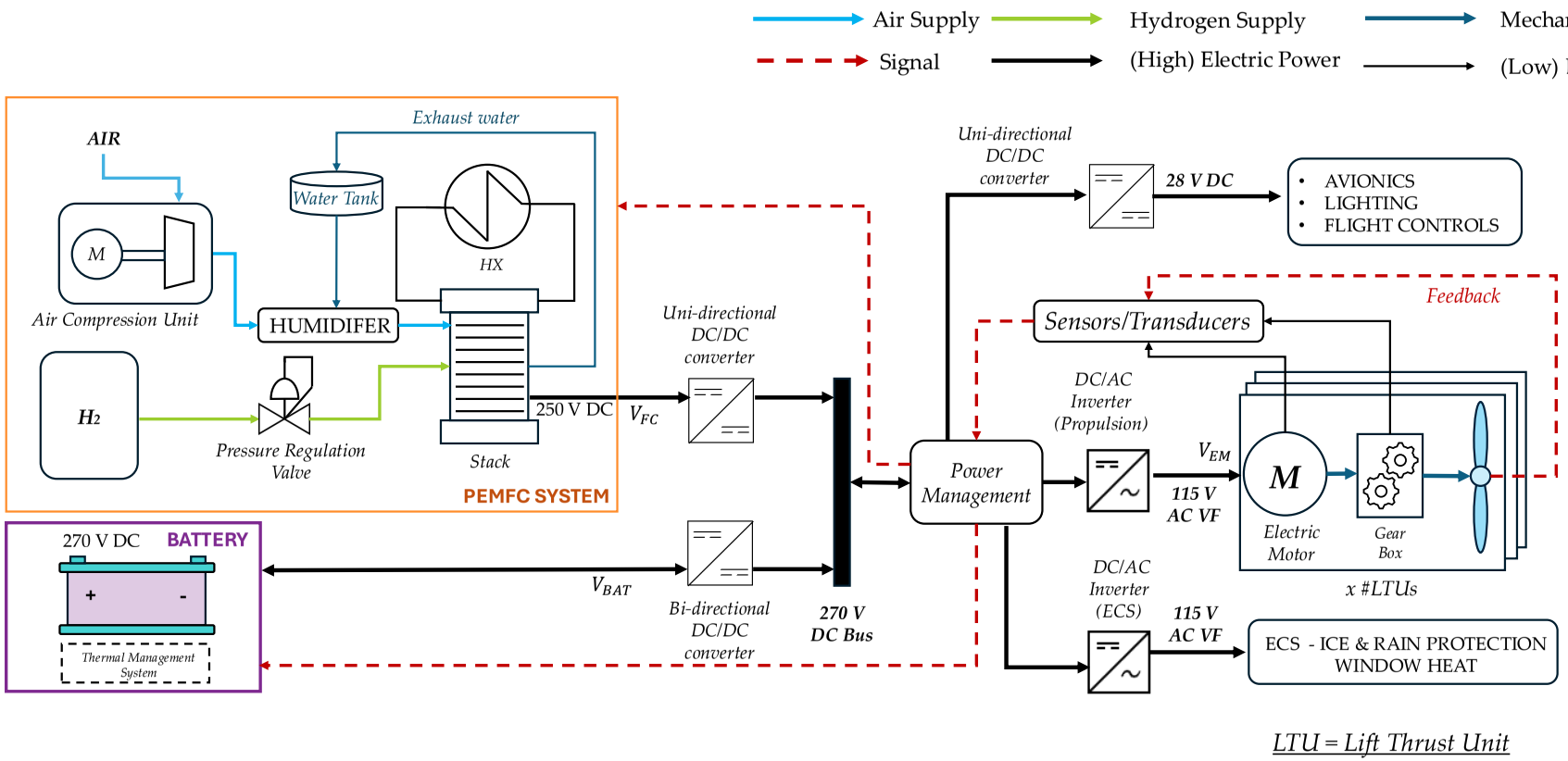
Air Supply
Hydrogen Supply
Mechanical Connection
Signal
(High) Electric Power
(Low) Electric Power
AIR
Exhaust water
Water Tank
HX
M
Air Compression Unit
HUMIDIFER
H2
Pressure Regulation Valve
Stack
250 V DC
PEMFC SYSTEM
Uni-directional DC/DC converter
VFC
270 V DC
BATTERY
+
-
Thermal Management System
VBAT
Bi-directional DC/DC converter
270 V DC Bus
Power Management
Uni-directional DC/DC converter
28 V DC
AVIONICS
LIGHTING
FLIGHT CONTROLS
Feedback
Sensors/Transducers
DC/AC Inverter (Propulsion)
VEM
115 V AC VF
M
Electric Motor
Gear Box
x #LTUs
DC/AC Inverter (ECS)
115 V AC VF
ECS - ICE & RAIN PROTECTION WINDOW HEAT
LTU = Lift Thrust Unit

## 3.8 Numerical sizing methodology

Up to this point, the conceptual design methodology has been described, and all the necessary tools and theories required to perform the aircraft sizing have been presented and discussed. Starting from them, an iterative MATLAB code has been built, using a fixed point method. Although this thesis aims to discuss a possible eVTOL configuration in accordance with the project "eVTOLUTION", a decision was made to conduct the conceptual design by analyzing further aircraft configurations, in order to analyze trends in key design parameters. Starting from a value for the maximum take-off weight (MTOW) and an input wing-loading (WS), it is possible to determine the wing area. In a similar way, the input disk loading parameter leads to a value for the rotors area. The Roskam Class II method formulations, which enable the overall aircraft weight estimation, highly depend on several parameters, among which the wing area and the rotors' area. Even the necessary power, which leads to size subsystems like PEMFC and batteries, depends on the MTOW, through the matching chart; therefore, after an accurate assessment of the structural weight and the contribution of subsystems, the final weight of the aircraft will differ from the original one. The resulting maximum take off weight can then be used as input to repeat the sizing cycle. For certain configurations, it is possible to observe slight changes between consecutive iterations; therefore, by establishing a certain tolerance value, it is possible to identify a stable configuration that can be saved for use in the final results discussion. After reaching a maximum number of iterations, the sizing cycle automatically stops. All the elements presented in this chapter have been included in the MATLAB code, among which there are: the mission profile, to establish power demand and energy consumption throughout the mission, weight estimation formulations and powerplant strategies. The modular nature of the sizing process allows for changes in input parameters. For example, it is possible to improve the battery energy density (BED), define a specific operating range, or adjust disk and wing loading values. However, some parameters can only be varied within specific

limits. For instance, increasing the aircraft's velocity beyond a certain threshold would push it into the high-subsonic or transonic flow regime—conditions that are not currently modeled. Additionally, the wing structure has not been characterized for such regimes, as features like sweep angle have not been incorporated.

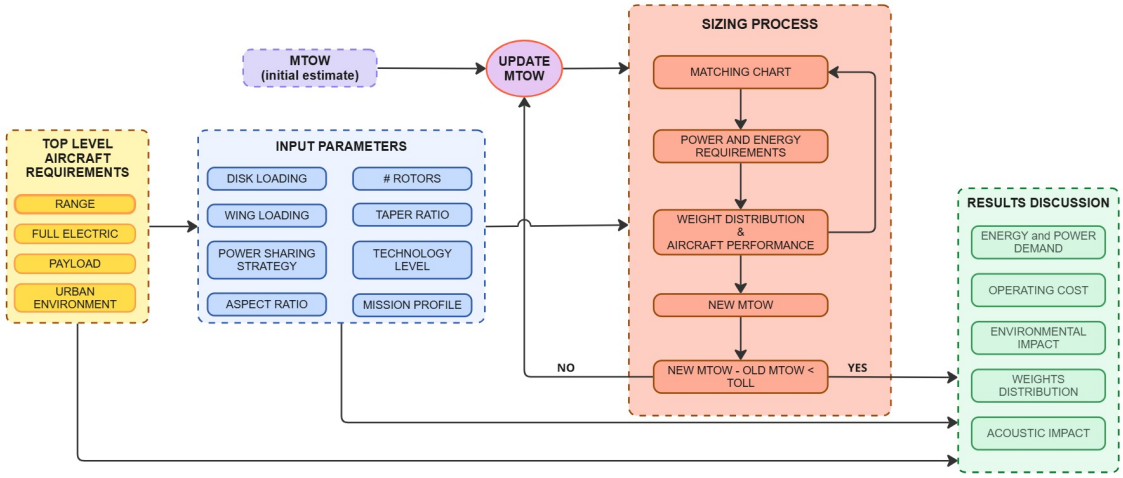


Figure 3.11: Numerical sizing process

# 4. Performance Analysis and Design Space Exploration

## 4.1 Lift-to-drag ratio estimation

Lift-to-drag ratio is an important parameter useful to assess the aircraft performance. Fixed-wing aircraft, such as gliders, can reach really high values. However the presence of additional elements such as engine nacelles and tails, increase drag component and lowers the overall ratio. Helicopters, on the other hand, are usually characterized by very low values, due to the many contributions to the aerodynamic friction. eVTOL aircraft have L/D ratios ranging between values common to both aircraft and helicopters, depending on flight condition. In conducting the aircraft sizing process, the cruise condition was considered.

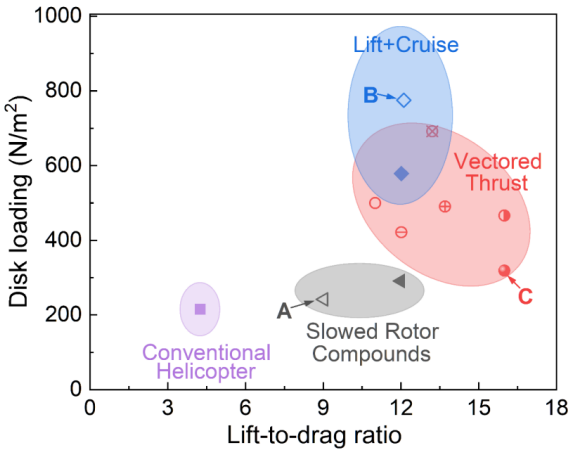


Figure 4.1: eVTOL L/D ratio for different configurations. Credits: [29]

In forward flight, the power required by the aircraft consists of three main contributions: induced power, necessary to generate thrust; profile power, to account for additional aspects introduced by Blade Element Theory and parasite power, which accounts for fuselage friction contributions, increasing the overall

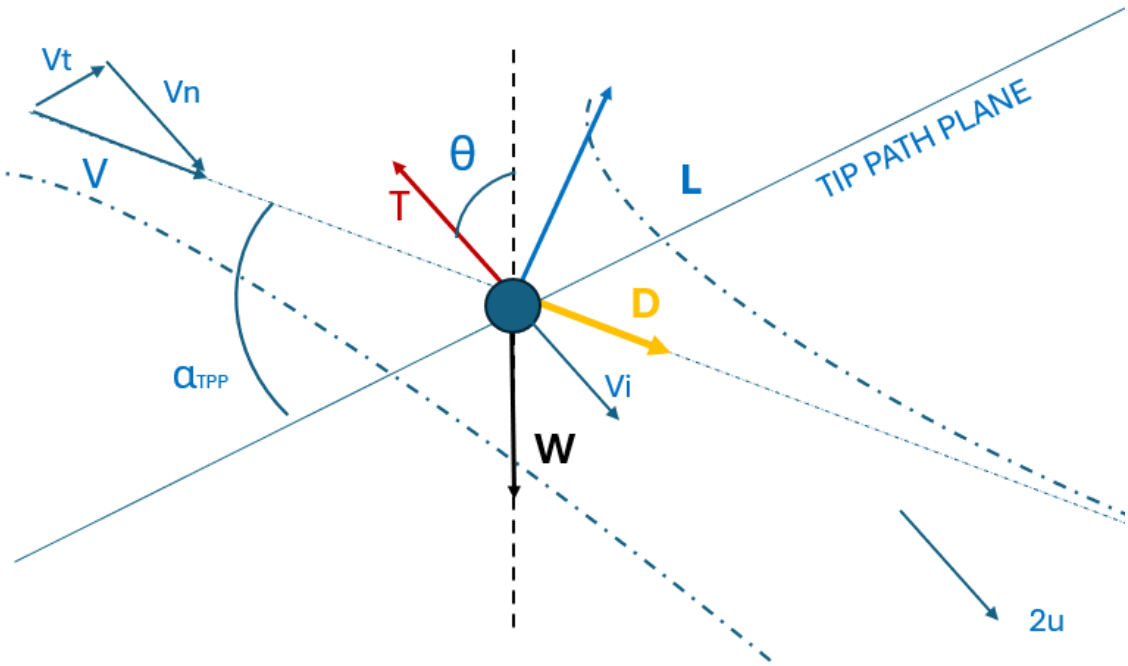


Figure 4.2: Forces acting on the eVTOL as a point mass

power demand. In forward flight, rotors always counteract the aerodynamic drag. However, if the aircraft has a pitch angle greater than 0°, the rotors also contribute to counteract the aircraft weight too, reducing the necessary lift required from the wings. The increased power necessary to sustain flight, leads to lower values for the L/D ratio. To evaluate the aforementioned parameter, the following equations have been introduced in the sizing process.

$$\begin{aligned} v_n &= V \sin \alpha_{TPP} \\ v_t &= V \cos \alpha_{TPP} \\ T &= 2A\rho v_i \sqrt{(v_n + v_i)^2 + v_t^2} \end{aligned}$$

Although the aerodynamic flow in forward flight strongly differs from the hover condition, both for helicopters and eVTOL aircraft, to assess the induced velocity through the disk area, some hypothesis are then introduced to extend the results of the Momentum Theory.

$$\begin{aligned} T &= 2A\rho v_i \sqrt{(V \sin \alpha_{TPP} + v_i)^2 + (V \cos \alpha_{TPP})^2} \\ &= 2A\rho v_i \sqrt{V^2 + 2V v_i \sin \alpha_{TPP} + v_i^2} \\ &\approx 2A\rho v_i V \text{ if V} >> v_i \end{aligned}$$

Therefore, is possible to introduce the follwing adimensional expressions for the velocities of interest and evaluating the induced inflow paramter $\lambda_i$:

$$\mu_n = \frac{v_n}{\Omega R};\ \mu_t = \frac{v_t}{\Omega R};\ \lambda_i = \frac{v_i}{\Omega R};\ \mu = \frac{V}{\Omega R}$$

$$\begin{aligned}\lambda &= \mu_n + \lambda_i \\ &= \frac{v_n}{\Omega R} + \frac{v_i}{\Omega R} \\ &= \frac{v_n}{\Omega R} + \frac{T}{2\rho\,(\Omega R)^2\sqrt{\frac{(V\sin\alpha_{TPP}+v_i)^2+(V\cos\alpha_{TPP})^2}{(\Omega R)^2}}} \\ \lambda &= \mu_n + \frac{C_T}{2\sqrt{\mu_t^2+\lambda^2}}\end{aligned}$$

Where $C_T$, is defined in the following way:

$$C_T = \frac{T}{\rho(\Omega R)^2 A}$$

The presented formulations are fundamental to evaluate the induced velocity in forward flight, which is then used to evaluate the induced power contribution. Also, it is important to observe how the last equation presented, needs to be solved iteratively. Eventually, is it possible to assess the induced power in forward flight:

$$P_i = kTv_i \text{ Induced Power}$$

The other two power contributions are presented again below and discussed.

$$P_0 = \frac{1}{8}\rho S(\Omega R)^3\sigma\left(1+K\mu^2\right)C_{d0} \text{ Profile Power}$$

Profile power is introduced to account for phenomena related to rotors' blades geometry that cannot be considered in the induced power contribution with K = $[4.5 \div 5]$. Further formulations accounting for reverse flow effects do exist.

$$P_p = \frac{1}{2}\rho V^3 f + \frac{1}{2}\rho V^3 S_w C_{Dw} = \frac{1}{2}\rho V^3\left[f + S_w\left(C_{D0w} + \frac{C_{Lw}^2}{\pi ARe}\right)\right] \text{ Parasite Power}$$

The Parasite power is due to viscous effect of the aerodynamic flow and phenomena of flow separation. $f$, is usually known as 'equivalent wetted area' in helicopters' performance analysis. In addition, the wing drag contribution is introduced. Is it also possible to express the total power in an adimensional form as it follows:

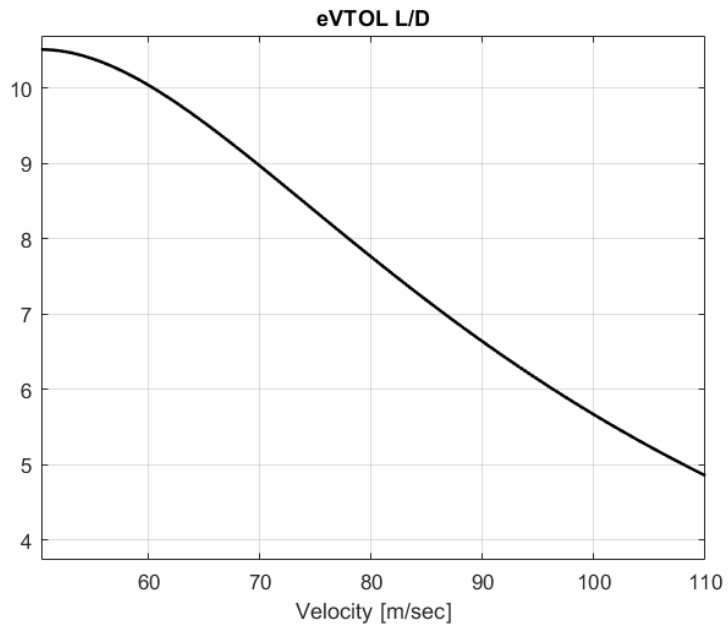


Figure 4.3: L/D for a general eVTOL configuration.

$$\begin{aligned} C_P &= C_{Pi} + C_{P0} + C_{Pp} \\ &= \frac{kC_T^2}{2\sqrt{\mu_t^2 + \lambda^2}} + \frac{1}{8}\sigma C_{D0}\left(1 + k\mu^2\right) + \frac{1}{2}\mu^3\left[\frac{f}{A} + \frac{S_W}{A}\left(C_{D0_w} + \frac{C_{LW}^2}{\pi ARe}\right)\right] \end{aligned}$$

To estimate the L/D ratio, it is important to establish the aircraft velocity and to solve the flight mechanics equations to properly identify lift contributions, in this way is then possible to finely assess thrust component and therefore power. Finally, the L/D ratio is estimated using the following equation:

$$\frac{L}{D} = \frac{W \cdot V}{P} = \frac{W \cdot V}{P_o + P_p + P_i}$$

## 4.2 Weight over range analysis

In accordance with the objectives of this thesis, the maximum take-off weight (MTOW) over range analysis is crucial. In fact, to support the use of hybrid powerplant configurations, it is fundamental to carefully consider all potential advantages and disadvantages. To address this objective, the evolution of MTOW

with respect to range has been explored for several cases. Some of the most significant cases are presented below, it is important to note, how in each case, **disk loading (T/A)**, **wing loading (W/S)** and **powerplant characteristics** have been kept constant. As it can be seen, a higher disk loading leads to an increase in the aircraft weight, higher disk loading, in fact, lead to greater induced power and consequently, heavier powerplant. It is also possible to identify several **Break Even Points (BEP)**, where, depending on the range, some powerplant configurations result in lighter aircraft configurations. BEPs are influenced by the above parameters kept constant. In particular, higher disk loading tends to shift BEPs to the right (toward longer ranges), while on the other hand, improved characteristics of the propulsion system, shift them on the left. In the following charts, the expression *Tech Level*, refers to the characteristics of the battery and the fuel cells:

| Tech Level | Battery Energy Density (Wh/kg) | Hydrogen Tank wt% |
|---|---|---|
| 1 | 250 | 5.5 |
| 2 | 300 | 7.5 |
| 3 | 350 | 15 |

Table 4.1: Technology Levels

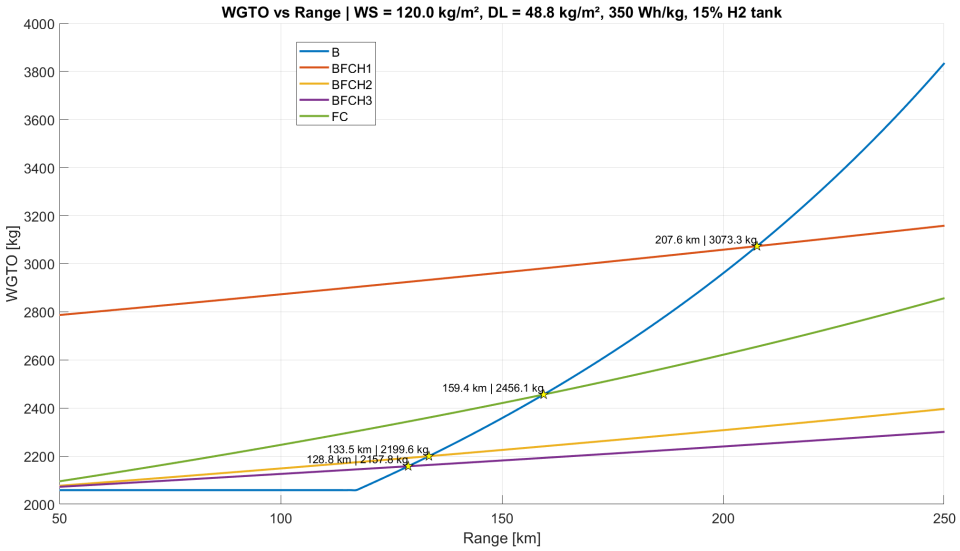


Figure 4.4: WGTO over Range. WS = 120 $kg/m^2$, DL = 48.8 $kg/m^2$, Tech Level = 3

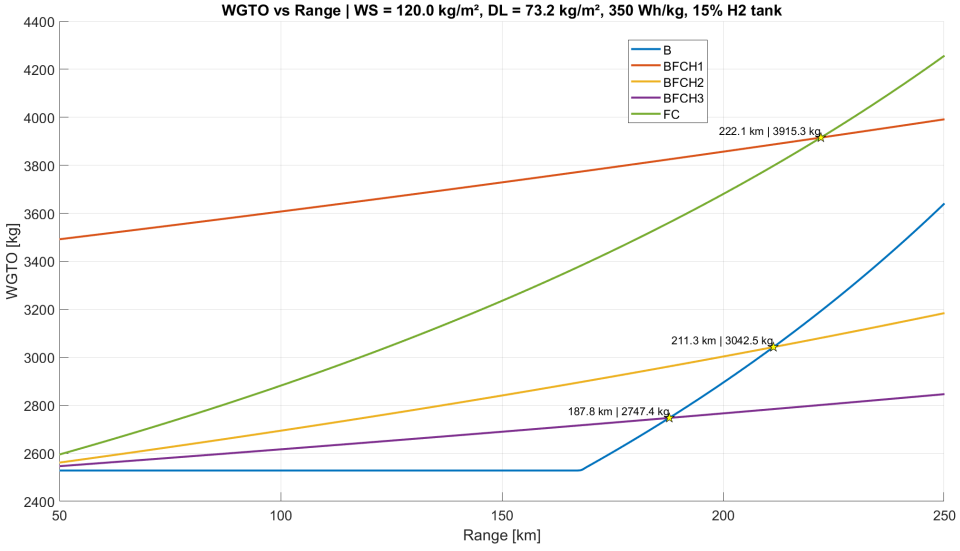


Figure 4.5: WGTO over Range. WS = 120 $kg/m^2$, DL = 73.2 $kg/m^2$, Tech Level = 3

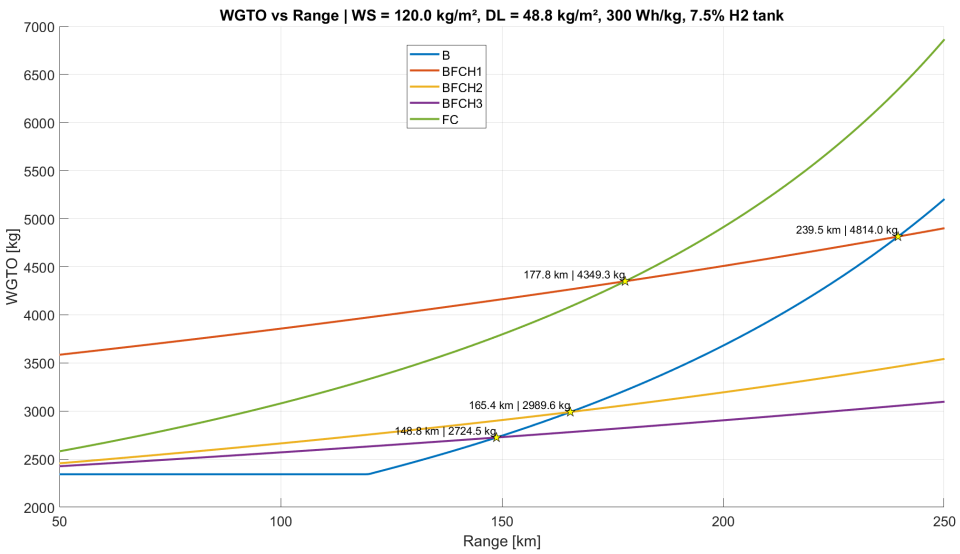


Figure 4.6: WGTO over Range. WS = 120 $kg/m^2$, DL = 48.8 $kg/m^2$, Tech Level = 2

Increased ranges, lead FC only configurations to rapidly gain weight: this effect is primarily due to the limited structural efficiency of the hydrogen tank, which is particularly constrained by the hydrogen density and the storage conditions discussed in Chapter 2. Battery-only configurations, similarly to Fuel Cell, tend to gain weight at higher ranges, since the limited energy density compared to conventional fossil fuels. The horizontal trait that characterizes the battery-only configuration curve, is due to the way battery is sized: in fact, until battery is power-sized rather than energy-sized, its weight and therefore the overall aircraft weights, depends only on the necessary power, which if the above parameters are kept constant, is consequently constant.

Wing loading, depending on the range, have a minimal impact on the curves, which instead strongly depend on the disk loading, therefore in the following table is kept constant at a high reasonable value of 120 $kg/m^2$.

| $DL\ lb/ft^2$ | $WS\ kg/m^2$ | Tech Level | BEP Range | BEP Weight |
|---|---|---|---|---|
| 10 | 120 | 1 | 155.4 | 3622 |
| 15 | 120 | 1 | 246.7 | 7419 |
| 20 | 120 | 1 | – | – |
| 10 | 120 | 2 | 148.8 | 2725 |
| 15 | 120 | 2 | 222.1 | 4035 |
| 20 | 120 | 2 | – | – |
| 10 | 120 | 3 | 128.8 | 2158 |
| 15 | 120 | 3 | 187.8 | 2747 |
| 20 | 120 | 3 | 242.9 | 3529 |

Table 4.2: Summary of the Brek-Even-Point between Battery-only configurations and BFCH3 Powerplant configurations. Double dash (–) potentially refers to intersections beyond 250 km.

In reference to the above table, the conversion between $lb/ft^2$ to $kg/m^2$, leads to: $10lb/ft^2 \rightarrow 48.8kg/m^2$, $15lb/ft^2 \rightarrow 73.2kg/m^2$ and $20lb/ft^2 \rightarrow 97.6kg/m^2$.

The previous charts confirm that, as anticipated, the third hybrid configuration (BFCH3) is the best-performing among the three options, consistently resulting in lighter aircraft configurations. The second hybrid configuration (BFCH2) leads to slightly heavier aircraft weights across all cases. Finally, the first hybrid configuration (BFCH1) consistently results in the heaviest aircraft among those equipped with hybrid powerplants.

## 4.3 Disk loading and Wing loading effects on aircraft weight

High wing loading values, as for conventional aircraft, result in smaller wing surface areas. However, excessively high wing loading introduces important structural stress at the wing root, requiring reinforcement and consequently, additional

weight. Disk Loading, although typically considered similar to wing loading in helicopters, have significant and unique impacts. First of all, low disk loading results in greater rotor disk areas, increasing the space required for the eVTOL, rotors are therefore greater and heavier, increasing the eVTOL overall weight. In contrast, high disk loading, reduce the spatial distribution of the vehicle and leads to smaller rotors, but the resulting increased induced power, leads anyway to heavier powerplant. In an Urban Air Mobility (UAM) scenario, high disk loading can induce important downwash effects that might impact pedestrians and people living near vertiports, however, these are not the only environmental effects eVTOL might have and need to be carefully discussed and analysed in vertiports design. Moreover, higher disk loading, similarly to helicopters, reduces hover efficiency: this is the primary reason why eVTOL aircraft converge toward similar values. Finally, it is possible to observe how, Disk Loading has a crucial effect on the aircraft's Maximum Take-Off Weight (MTOW) of the aircraft, while on the other hand, Wing Loading has a smaller impact. Specifically, higher disk loading leads to an increase in the eVTOL aircraft's maximum take-off weight. In contrast, higher wing loading results in lighter aircraft configurations. In the following images, iso-contour plots for different ranges and technology levels for the powerplant, are presented:

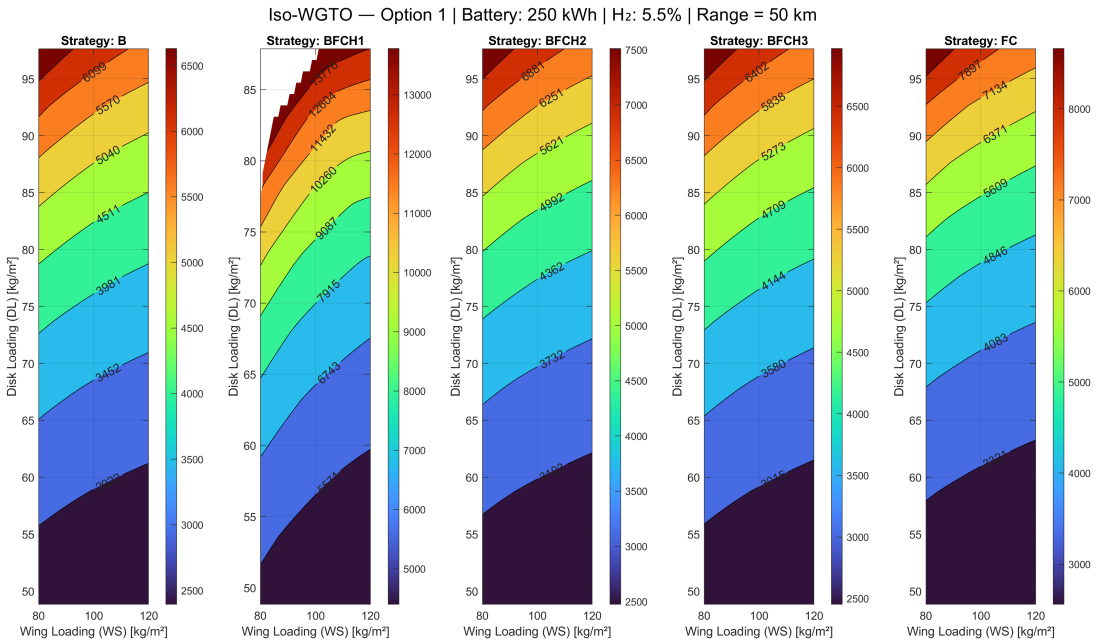


Figure 4.7: Disk and Wing loading effect on MTOW. Range = 50 km, Tech Level = 1

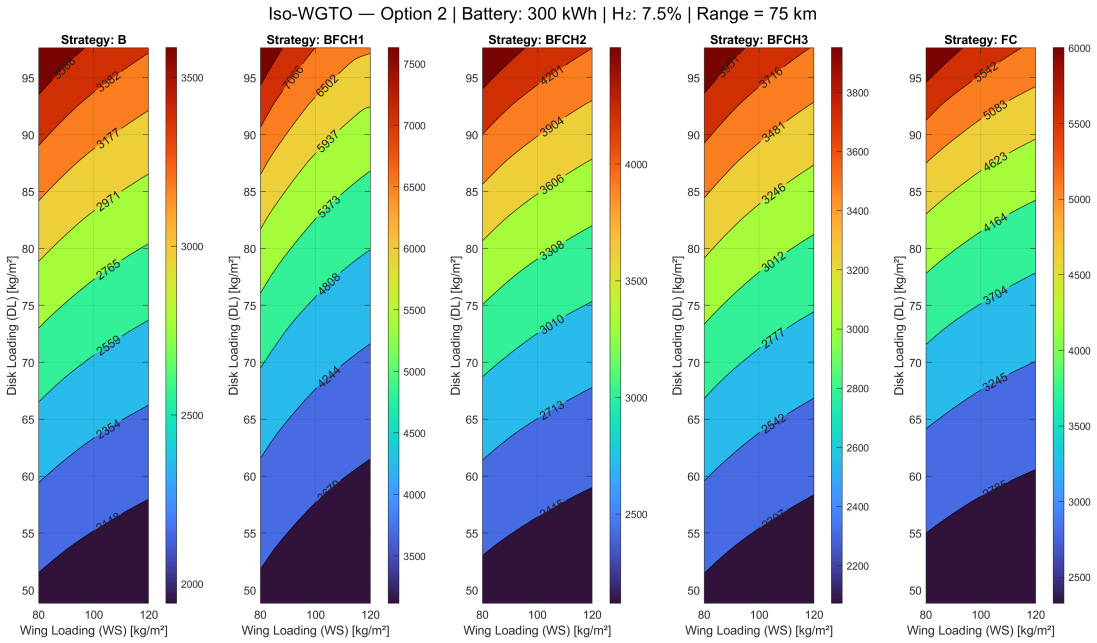


Figure 4.8: Disk and Wing loading effect on MTOW. Range = 75 km, Tech Level = 2

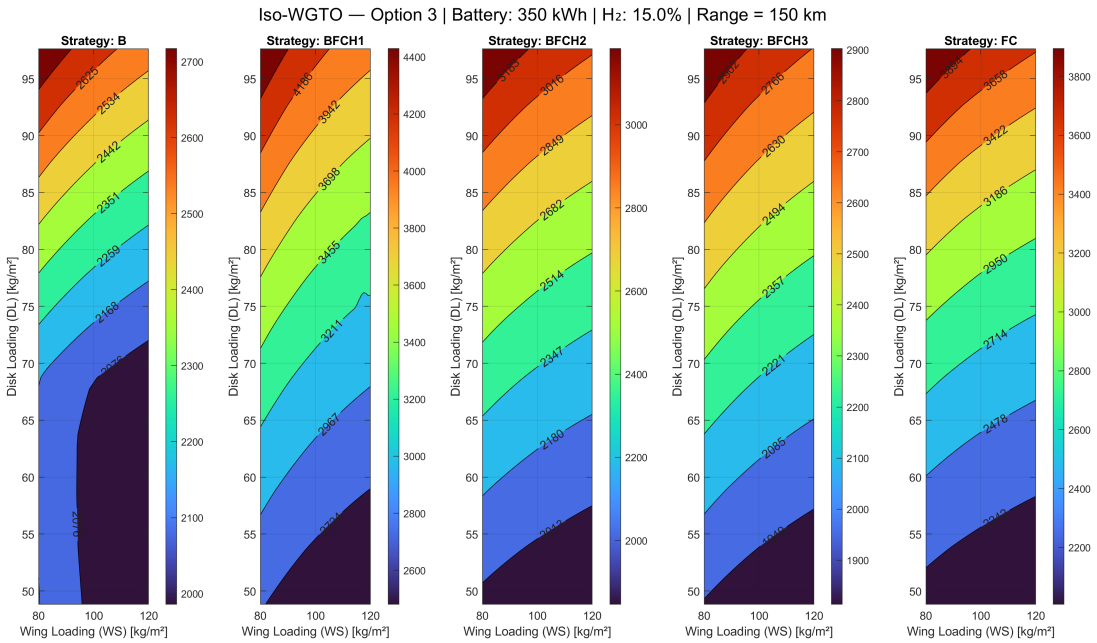


Figure 4.9: Disk and Wing loading effect on MTOW. Range = 150 km, Tech Level = 3

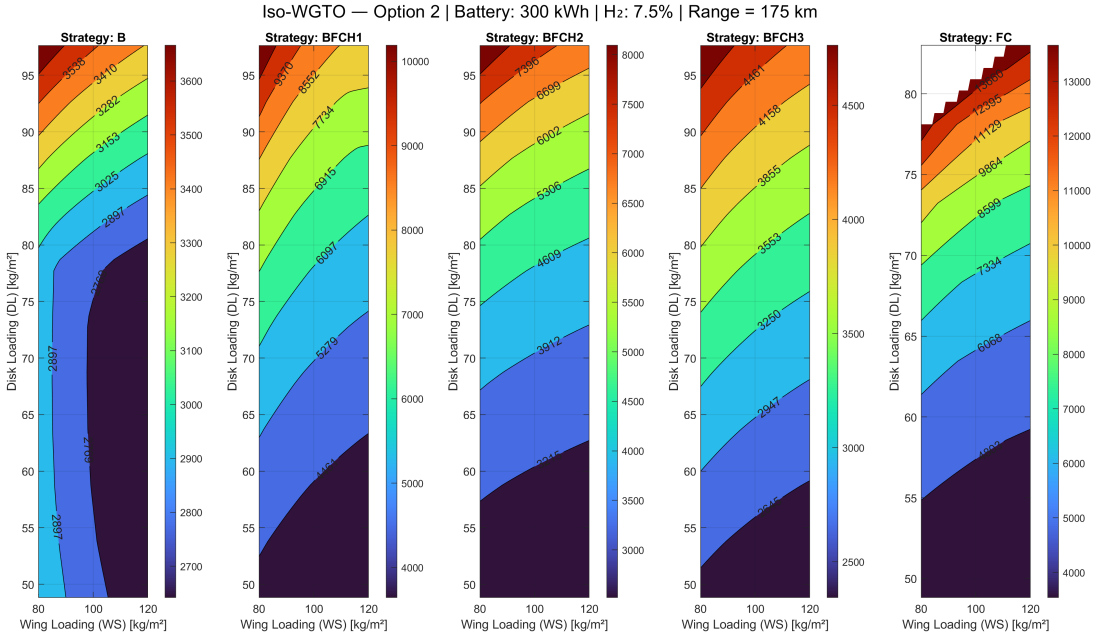


Figure 4.10: Disk and Wing loading effect on MTOW. Range = 175 km, Tech Level = 2

In accordance to the result presented in the previous section, aircraft with

BFCH3 configurations, result in being lighter than Battery-only configurations. It is important to consider how only "accepted configurations" (MTOW $< 14000$ kg) are considered in the iso-contour plot definition, this is the reason why some plots have white areas on the top side, due to the absence of data, meaning that those configurations characterized by high WL and DL values reach a MTOW greater then the imposed limit.

## 4.4 Weights distribution

In the following images, subsystems and different components weights are analysed. In this case, only technology level and range have been kept constant, while disk loading, wing loading and powerplant configuration have not been filtered, aiming at assessing their general behaviour across a variety of conditions.

As it can be seen, weight distributions, tend to increase with range; on the other hand, improved characteristics of the powerplant make them lighter.

### Effect of Range

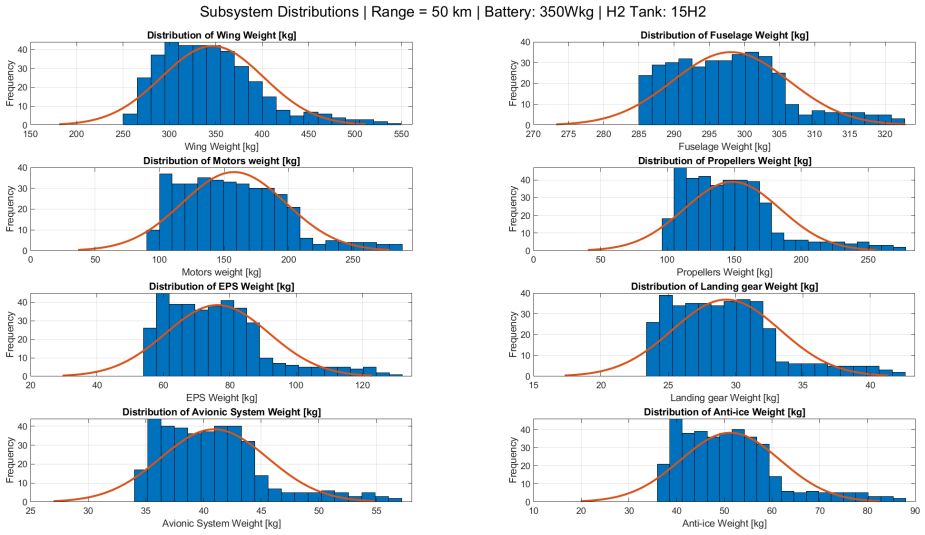


Figure 4.11: Subsystem Distribution. Range = 50 km, Tech Level = 3.

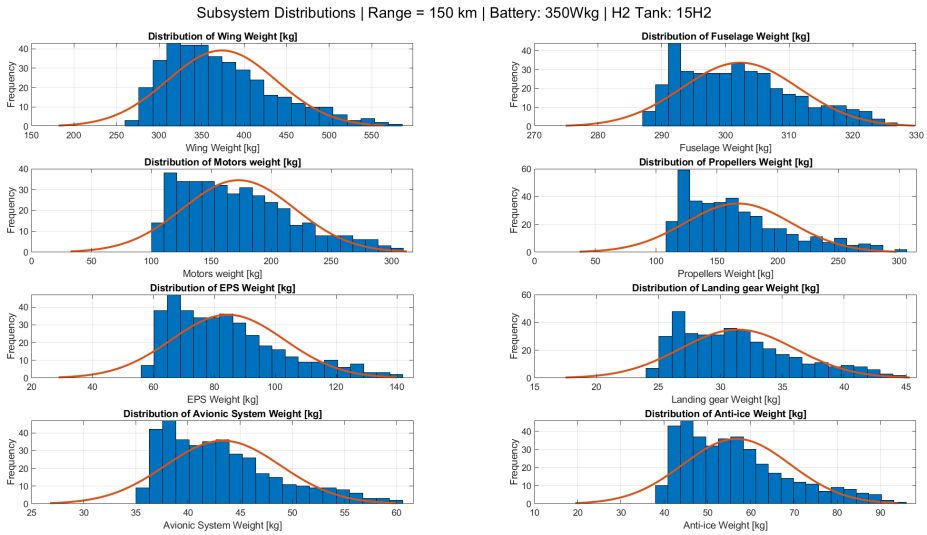


Figure 4.12: Subsystem Distribution. Range = 150 km, Tech Level = 3.

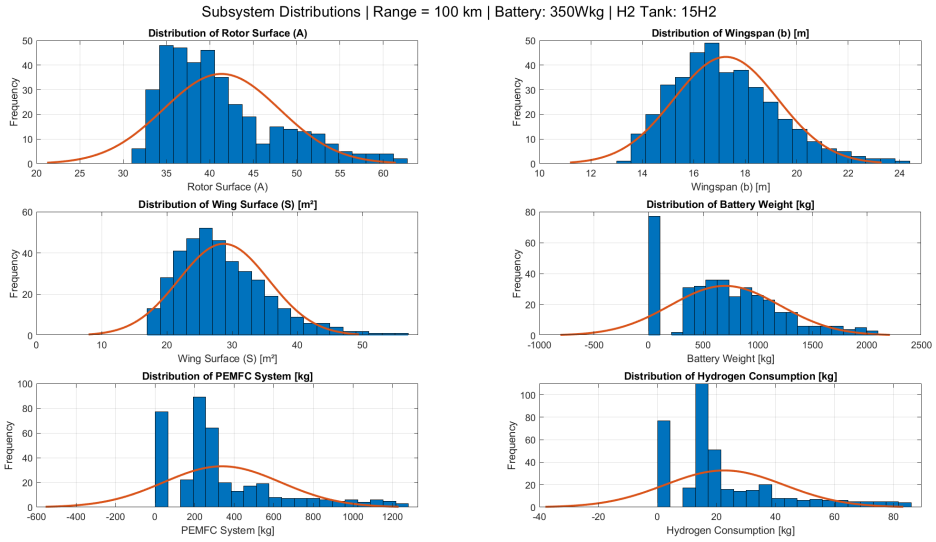


Figure 4.13: Other elements Distribution. Range = 100 km, Tech Level = 3.

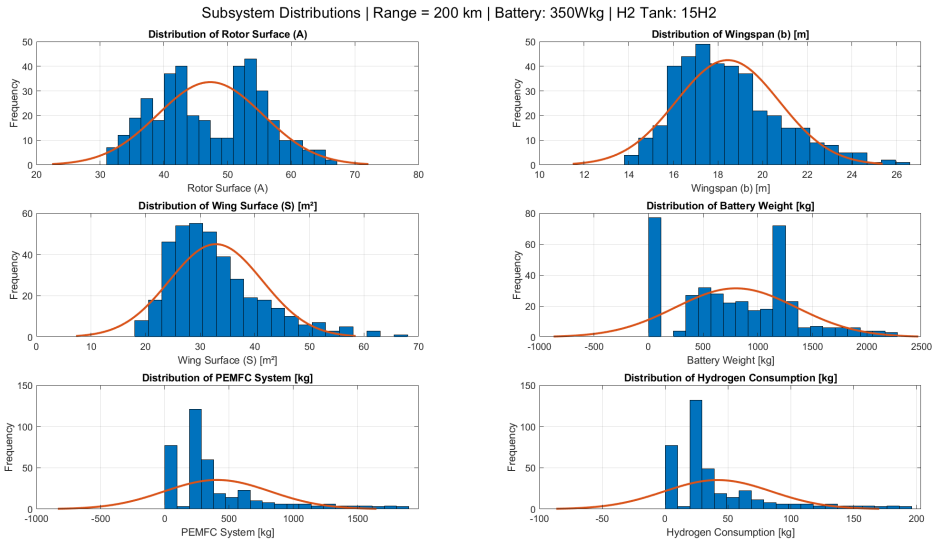


Figure 4.14: Other elements Distribution. Range = 200 km, Tech Level = 3.

## Effect of Tech Level

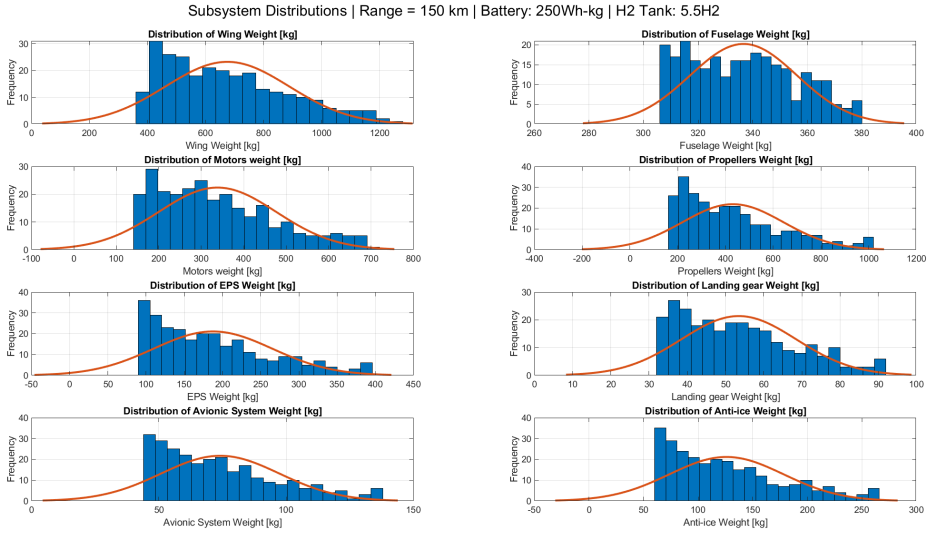


Figure 4.15: Subsystem Distribution. Range = 150 km, Tech Level = 1.

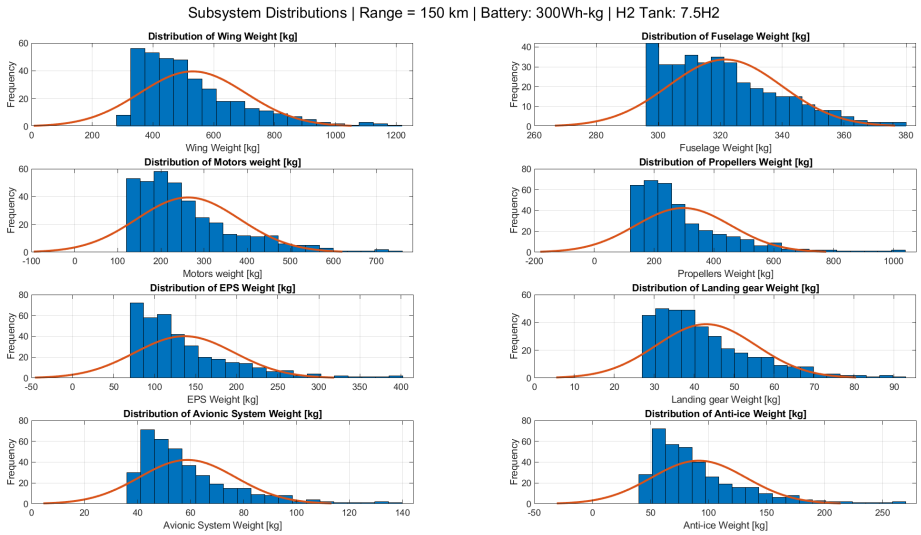


Figure 4.16: Subsystem Distribution. Range = 150 km, Tech Level = 2.

The avionic system is one of the least affected by range and even by technological level, due to the fact that most elements of this subsystem are independent of aircraft weight. For this subsystem, as with others, even though a classical approach was used for its estimation, it must be taken into account that eVTOLs will require robust and complex avionics in order to manage highly integrated electronics capable of allowing the pilot to manoeuvre a vehicle that behaves both as a helicopter and as a fixed-wing aircraft. Therefore, in practice, this value tends to increase. The major effects of range can be seen in the structural elements of the aircraft, particularly in the weight of the wings and fuselage. The wingspan distribution aligns with current trends observed in existing prototypes: it typically reaches about half the value of conventional commercial aircraft (ICAO-C constraint for wingspan below 36 m). On average, hydrogen consumption for a 100 km range is four times the full-tank capacity of a Fuel Cell Electric Vehicle (FCEV), which typically achieves a 600 km range. This implies that the eVTOL consumes approximately **24 times** more hydrogen per kilometer than the car. The Robinson R44, one of the few helicopters still employing piston engines, enables a maximum

range of 300 miles (482 km) with a maximum capacity of 46 gallons (about 175 liters), while cars—depending on fuel efficiency and flight conditions—can cover a similar range, at lower speeds, with about one-third of that capacity. Therefore, for the same passenger capacity, the eVTOL would be more fuel-consuming than an FCEV, with a significantly larger margin compared to conventional helicopters and fossil-fuel-based cars. However, beyond the higher costs associated with its much greater fuel consumption, both eVTOL aircraft powered by a fuel-cell battery hybrid system and FCEVs would have a net-zero environmental impact on urban air quality. Batteries, on average—including both battery-only and hybrid configurations—are heavier than those used in cars offering longer ranges (e.g., the Nissan Leaf has a 360 kg battery for 226 miles [363 km], and the Chevrolet Bolt EV has a 435 kg battery for 259 miles [416 km]).

# 5. Selected eVTOL configurations

Following the design space exploration of the previous chapter, in the following section, several configurations are proposed and evaluated using different figures of merit for various urban operational scenarios.

## 5.1 Figures of merit

In order to assess and compare several configurations, figures of merit are typically introduced in the conceptual design phase. FoMs enable deeper analysis, drawing additional information from the configurations calculated, that might regard economic or environmental aspects. In the final results discussion, some configurations will be presented throughout the following metrics: Maximum Take-off Weight, Cruise Lift-to-Drag ratio, Environmental and Acoustic Impact, Operating Cost.

### 5.1.1 Environmental Impact

As discussed in chapter 5, eVTOL aircraft are intended to enter the urban transportation sector, aiming to address traffic congestion problems and enabling reduced travelling times for several scenarios, with net-zero emissions, since in both cases, batteries and fuel cells, they do not emit pollutants during operation. eVTOL aircraft, therefore, will not worsen air quality of cities and urban areas. On the other hand, it is not possible to consider eVTOL completely free from any possible climate impact. A full and complete Life Cycle Assessment (LCA) for eVTOL aircraft, lies beyond the scope of this thesis. However, in order to assess the environmental impact of each aircraft configuration, a decision was made to evaluate the $CO_2$ emissions by analysing both the climate impact of the electricity generation for battery recharging and the emissions associated with hydrogen production methods. First of all, the greenhouse gas emission intensity

of electricity generation in Europe, has been extensively studied. The European Union, has experienced, and continues to experience, a decreasing trend in the $CO_2$ emissions from electricity production over the last two decades, in line with its decarbonization objectives aimed at achieving carbon neutrality by 2050. The most recent available data (2023), show that the average GHG intensity in Europe is 210 $gCO_2e/kWh$, as depicted in the figure below. Italy is slightly above the average, with a value of 225 $gCO_2e/kWh$. The environmental impact of hydrogen

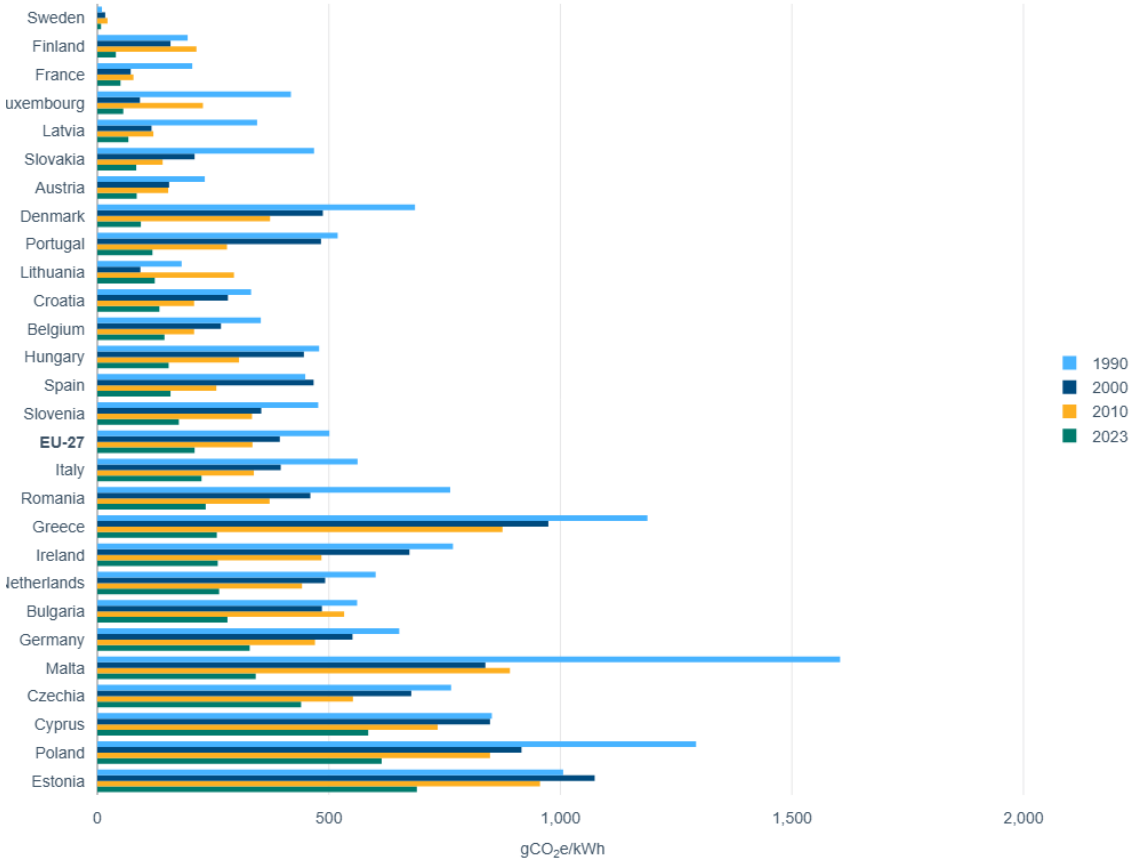


Figure 5.1: $gCO_2e/kWh$ per Nation.[30]

production depends significantly on the production method employed. As presented in 2, approximately 95% of global hydrogen production currently involves the use of fossil fuels, leading unavoidably to $CO_2$ emissions. However, some production processes have a greater environmental impact than others. Consequently, hydrogen has been categorized by "colour labels" according to the pro-

duction method and associated environmental impact, as outlined below: Patel et al.[31], conducted a life cycle assessment (LCA) of hydrogen production, taking into account variations in natural gas supply. The study differentiates between the use of pipelines and LNG (Liquefied Natural Gas), which involve additional regasification processes and infrastructure.

| Hydrogen Colour | Method/Note | $gC0_2/gH_2$ |
|---|---|---|
| Grey Hydrogen | SMR, LNG route | 13.9 |
| Grey Hydrogen | SMR, Pipeline route | 12.3 |
| Blue Hydrogen | SMR with Carbon capture technology. LNG route. | 9.3 |
| Blue Hydrogen | SMR with Carbon capture technology. Pipeline route. | 7.6 |
| Turquoise Hydrogen | Pyrolysis. LNG route. | 8.3 |
| Turquoise Hydrogen | Pyrolysis. Pipeline route. | 6.1 |
| Green Hydrogen | Solar energy. | 2.5 |
| Green Hydrogen. | Wind energy. | 0.6 |

Table 5.1: GHG emissions depending on hydrogen production method. [31]

Beyond the hydrogen produced via renewable sources, all other processes involve a significant environmental impact in terms of $CO_2$ emitted. Unfortunately, as can be observed in the cost analysis, the most environmentally friendly options, tend to be more expensive, deeply affecting the overall cost of the hydrogen used in eVTOL operations

In order to define a figure of merit, since the most significant amount of Hydrogen produced in Europe, is made through SMR methods, already discussed in 2, a choice was made to consider a value of 12.3 $gC0_2/gH_2$.

The final figure of merit implemented, is therefore presented:

$$(GHG)_{gCO_2} = 210 \cdot E_{BAT,\ kWh} + 12.3 \cdot m_{H_{2,g}}$$

### 5.1.2 Acoustic Impact

When designing an eVTOL aircraft, whose operations are intended to happen within an urban environment, acoustic impact and therefore noise is a leading requirement. Public acceptance of noise, which is very difficult to quantify, would be critical in order for eVTOL aircraft to fully operate within the urban context. **ICAO's Annex 16 (Environmental Protection)** through its four volumes, deals with the environmental impact of aircraft. The document, in fact, represents a comprehensive document providing a set of standards and recommended practices (SARPs) aimed at minimizing the environmental impact of aviation. The first three volumes deal respectively with: noise, engine emissions and $CO_2$ metric-value. In particular, the 13th chapter in the first volume addresses tilt-rotors noise emissions. The presented set of standards and recommended practices (SARPs) highlighted in the document, in order for certificating authorities to demonstrate compliance with the standards, are then accompanied by an additional document, which is the **Environmental Technical Manual**, which defines the procedures for the Noise Certification. In the context of Urban Air Mobility, in July 2024, EASA published the "Environmental Protection Technical Specification" for VTOL-capable aircraft with tilting rotors. The document is divided into several parts; in subpart B, noise evaluation metrics are defined, in particular, as for helicopters and aircraft, the noise evaluation metric is the **Effective Perceived Noise Level (EPNL)**, measured in EPNdB, an integrated measure over time, regarding different flight conditions, among which there are: take-off, overflight and approach. Acoustic impact could represent an issue not only for the communities overflown by eVTOL aircraft but even for passengers on board, therefore, some companies' concepts require passengers to wear protective headphones, as it happens in helicopters. Helicopters' acoustic impact is due to several subsystems and components, among which, we find: the main rotor and tail rotor, mechanical elements for the transmission of the motion and the propulsive systems. Although the adoption of electric motors, which are significantly quieter than gas turbines, allow eVTOL operations to be

quieter, the aeroacoustic behaviour of rotors, would remain a central source of noise. An eVTOL could be subjected to several acoustic components, similarly to helicopters, travelling along different directions and through different planes, among which we find: **thickness noise**, due to the thickness of the aerodynamic profile of the blades, **loading noise**, due to the pressure fluctuations along the stream tube passing through the rotors, **blade-vortex interaction**, caused by the impact of blade tip vortices and the following rotating blade encountering and the **broadband noise**, due to turbulence mechanisms. Helicopters are usually also described by an additional contribution, which is the one of High Speed Impulsive Noise, due to transonic regime effects, that should not affect eVTOL aircraft. It is also important to highlight how international regulations for noise emissions refer to single-event noise, overlooking effects of cumulative noise emission caused by contemporary and continuous operations throughout the entire day, from this point of view, local community legislation might impose noise budgeting, limiting the number of eVTOL operations. In[1], an equation is proposed to estimate the A-weighted PWL of eVTOL vehicles, that can be very useful in the preliminary design stage. Before presenting the equation, that has been used in the conceptual design process to label each configuration, bringing an additional discussion element to facilitate comparison among configurations, it is important to highlight the definition of PWL. PWL is in fact the Sound Power Level, given by the following formula:

$$PWL = 10 \cdot \log_{10} \frac{W}{W_0} \text{ in dB, } W_0 = 1pW$$

PWL, in fact, differently from other quantities, such as SPL, does not depend on the distance, enabling therefore the characterization of aircraft acoustic properties without any knowledge of the surrounding environment. The reference values for SPL and PWL, $20Pa$ and $1pW$, in a perfect free field, at a distance where the propagation area is $1m^2$, lead to the same value for both quantities in dB[33]. In

[1] Sen Wang, Lourenço Tércio Lima Pereira, and Daniele Ragni. "Design exploration of UAM vehicles". English. In: *Aerospace Science and Technology* 160 (2025). ISSN: 1270-9638. DOI: 10.1016/j.ast.2025.110058.

addition, since human response to noise deeply depends on the frequency of the source, weighting techniques are frequently introduced to correlate measurements to human response. A-weighting is usually the most adopted one. The proposed formula is hereafter presented:

$$(PWL)_{dBA} = k_P \log_{10} P_s + k_D \log_{10} D + k_M \log_{10} M_t + k_B B + 10 \log_{10} N_{prop} + C$$

| Term | Take-off | Cruise |
|---|---|---|
| $k_P$ | 3.2 | 0 |
| $k_D$ | -20.3 | 14.1 |
| $k_M$ | 60 | 60 |
| $k_B$ | -2.9 | 0.5 |
| C | 124.1 | 102.2 |

Table 5.2: Equation parameters for two different flight phases: take-off and cruise.

Where, in the formula:

- $P_s = \frac{P}{FM}$, Shaft Power, an increase in the amount of shaft power required, leads to a greater noise
- $D$, rotors diameter, the negative sign in the formulation, suggests how greater diameters, lower the noise level. Similarly, fewer propellers, decrease the noise level.
- $M_t$, tip Mach number, it has a significant effect on the noise level given by its high coefficient value
- $B$, number of blades

In the configurations discussion, the acoustic impact as a figure of merit has been considered only for the take-off phase, which resulted to be the most impacting one.

### 5.1.3 Operating Cost

In order to introduce a higher degree of evaluation within the design exploration space, Operating Cost, are fundamental key figures of merit. For eVTOL aircraft, standardized cost models are not yet established, since the significant variability of the new technologies the new concept involve. The existing cost models found in literature, are derived from conventional aviation and rely on several assumptions for each cost component. To assign a cost estimate to each aircraft configuration, a cost model has been implemented in the sizing process, based on two references: Sclifò's[34] thesis and Xu's[35] thesis. The first source enabled the estimation of aircraft production cost, which could be particularly relevant from an operator's perspective. The second was fundamental in addressing cost components related to aspects such as infrastructures and others. Additional assumptions, particularly those regarding fuel costs for configurations using fuel cells, will be detailed in the following description. Development costs have not been included in the analysis, as they are considered non-recurring expenses and therefore typically excluded from operational or pre-flight cost assessments. In operational analysis, it is common to focus on recurring costs such as maintenance, energy, crew and infrastructure, since they reflect the economic performance during operation. These assumptions are very common when discussing route feasibility and mobility studies or cost-per-passenger evaluations.

#### Fixed Direct Operating Cost

In the MATLAB function implemented, the aircraft production cost is calculated based on aircraft parameters such as weights and power. Assuming an electric motors life of 5000 hours, the numbers of flights is evaluated in the following way:

$$n_{flights} = \frac{5000}{Range} \cdot \frac{Speed}{3600}$$

Therefore, aircraft depreciation is calculated in the following way:

$$C_{ACD} = \frac{C_{AC}}{n_{flights}}$$

Battery depreciation's assessment has been conducted similarly. Battery life-cycle has been assumed to be 2000 cycles, the opportunity for batteries to be recharged by the hydrogen stores, has not been considered in the present analysis. To estimate the insurance cost of the aircraft, the following equation has been introduced:

$$C_{ins} = 500 + 0.015 \cdot \tau_{AC}$$

where $\tau_{AC}$, is the aircraft production cost.

### Variable Direct Operating Cost

To include variable direct operating cost, the average electricity price in the European Union was considered. In addition to the maintenance model proposed by[2], an if condition was introduced: for configurations involving fuel cells, an additional 40% maintenance cost is added to account for the initial additional challenges associated with the emerging technologies. Pilot salary and miscellaneous costs have been included as found in the reference. Eventually, in addition to the model used, hydrogen fuel cost has been included, considering an average hydrogen price of 2.75$/ kg. The value aligns with the assumptions made in the environmental impact assessment, where grey hydrogen was assumed for GHG emissions estimation.

### Indirect Operating Cost

As it is typical in aviation cost models, indirect operating costs (IOC) account for 40% of the total. As pointed in [35], under this category, "Sales, Reservation and Administrative Costs" are included. These items encompass the expenses associated with the commercial, customer service and management functions, that support the operation of the service, even though they are directly proportional to the physical operations of the aircraft. Finally, even though it is difficult at this

[2]Xiaolong Wu. "Performance Evaluation of UAM Configurations: Cost Estimation for the eVTOLs". Thesis or dissertation. SATM Department: Cranfield University, Aug. 2021.

stage of the eVTOL market development to state with certainty, it can be possible to include costs associated with infrastructure and facilities; in the future, it is likely that companies would pay fees to the vertiports rather than building and owning them. Together with infrastructural cost, costs related to the regulatory and market operation aspects have been included. As discussed in the reference, the regulation cost is not easy to define, therefore the price associated to a single engine helicopter has been taken into consideration.

Finally, is it important to clarify that all DOC values are expressed in USD per passenger per nautical mile (USD/pax/nm).

## 5.2 City Pairs

### 5.2.1 Range within 100 km

#### London City - Cambridge City

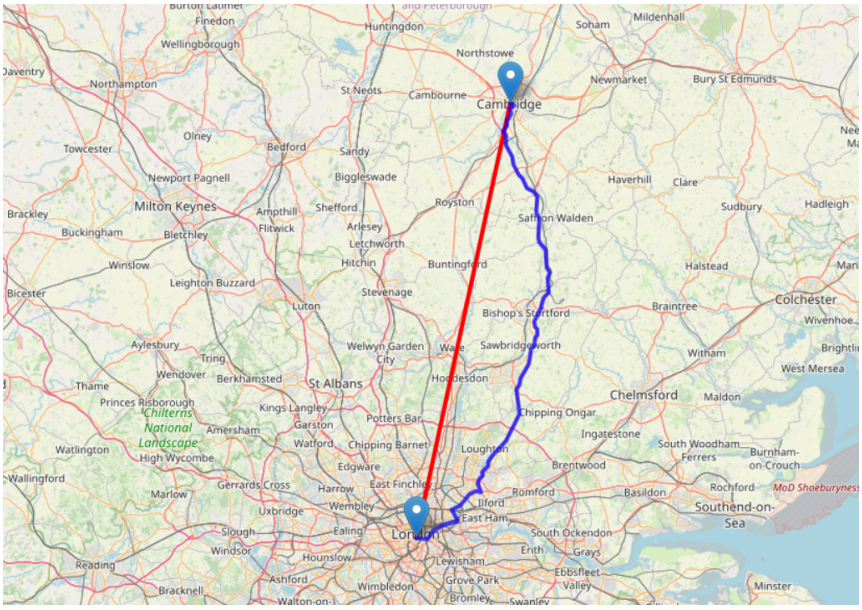


Figure 5.2: London city - Cambridge city

| Ground distance [km] | Beeline [km] | Road Journey Duration | eVTOL Duration |
|---|---|---|---|
| 98 | 78 | 1 h 20 min | 20 min |

The London-Cambridge route would enable a fast connection between the London's multiple international airports and Cambridge's advanced business and technology hubs. This connection might be particularly interesting for investors, researchers and business travellers travelling between the two cities for industrial and economic reasons. The two cities are not connected by domestic flights.

### 5.2.2 Range between 100 km and 200 km

#### Turin (TRN)-Milan (MXP)

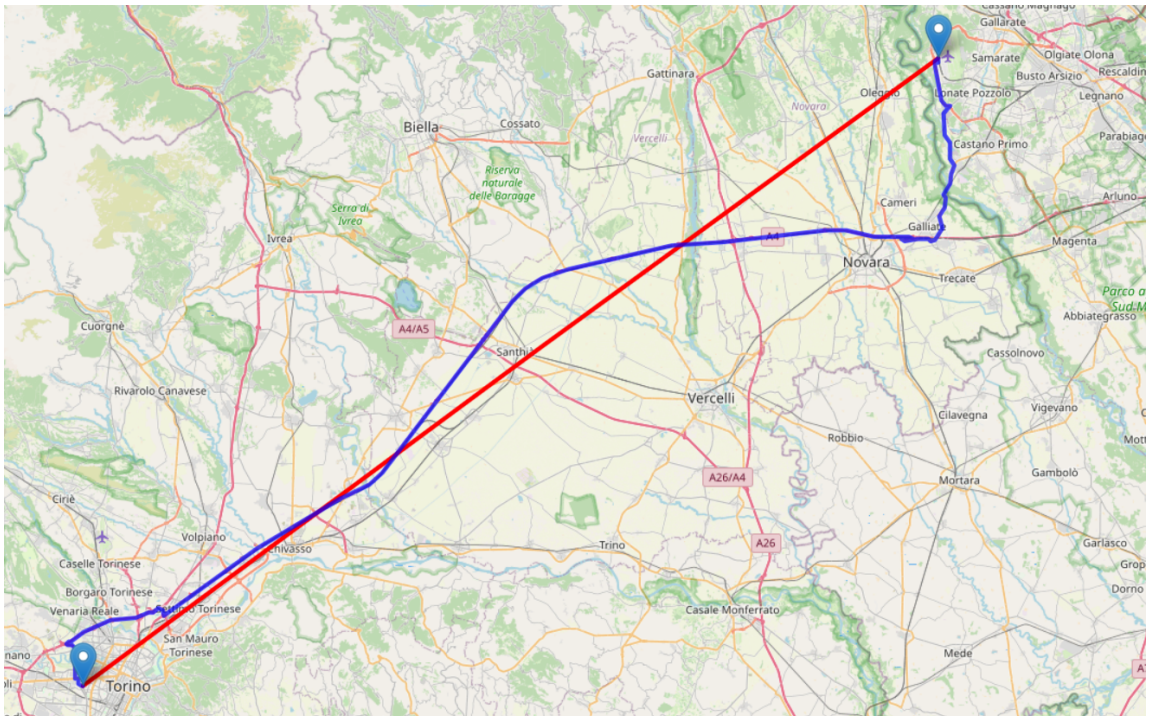


Figure 5.3: Turin (TRN) - Milan (MXP)

| Ground distance [km] | Beeline [km] | Road Journey Duration | eVTOL Duration |
|---|---|---|---|
| 132 | 105 | 1 h 50 min | 25 min |

The Turin TRN – Milan MXP would provide a direct connection between two of Northern Italy's most influential airports, serving regions known for their industrial, manufacturing and economic importance; although these cities are connected by high-speed rail, the considerable distance between the central stations and the airports increases overall travel time. An eVTOL connection could significantly improve efficiency for business travellers flying into or our of either hub.

### Rome FCO - Naples NAP

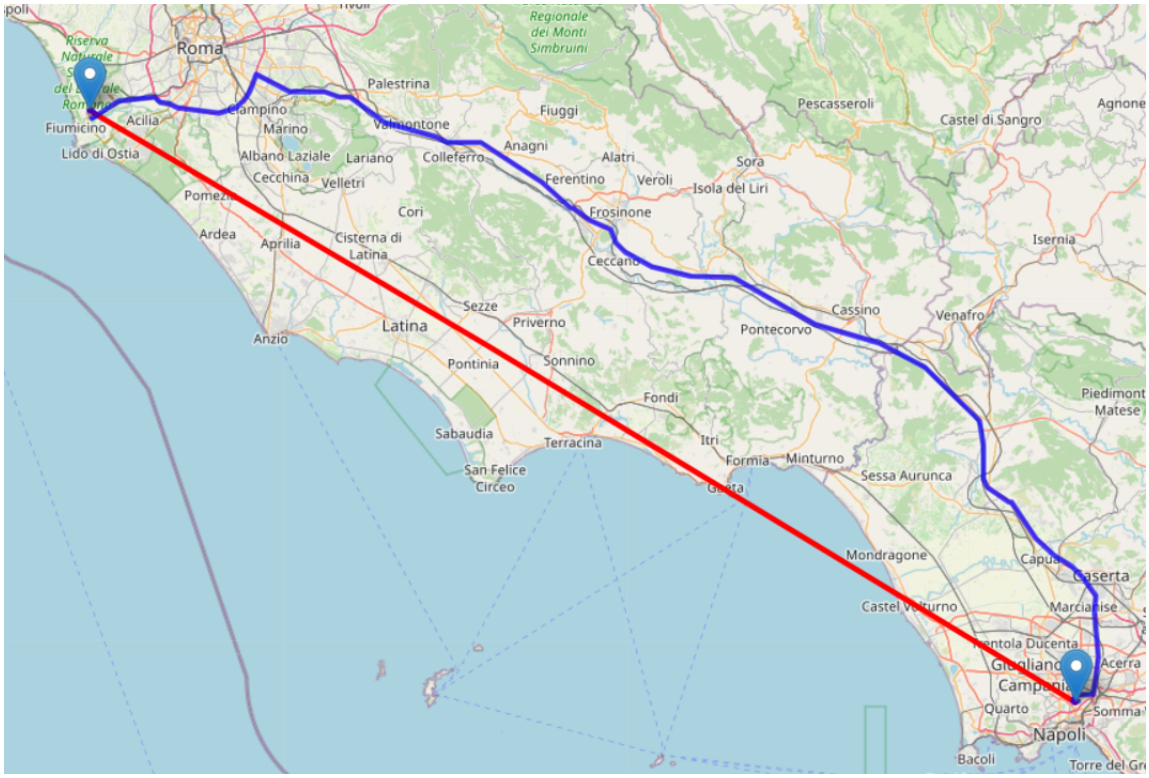


Figure 5.4: Rome (FCO) - Naples (NAP)

| Ground distance [km] | Beeline [km] | Road Journey Duration | eVTOL Duration |
|---|---|---|---|
| 240 | 197 | 3 h 20 min | 50 min |

The Rome FCO – Naples NAP route would provide rapid transfers between two of Italy's most influential cities, serving governmental, touristic and economic needs;

For this route, high-speed trains only depart from Rome's central stations, which are far from the international airport. Domestic flights do exist for this route with an average 50 min flight duration. This makes it an ideal opportunity for eVTOL services, especially for passengers arriving directly at FCO or NAP, offering a fast connection without the need of long ground transfer.

### 5.2.3 Range beyond 200 km

**Milan, Italy - Venice, Italy**

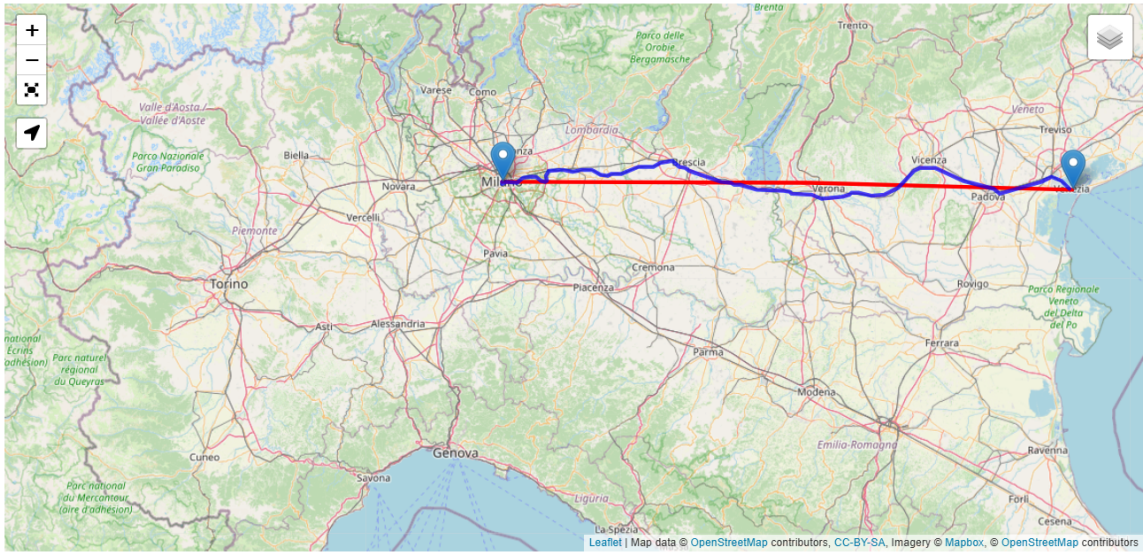


Figure 5.5: Milan, Italy - Venice, Italy

| Ground distance [km] | Beeline [km] | Road Journey Duration | eVTOL Duration |
|---|---|---|---|
| 268 | 245 | 2 h 50 min | 1 h |

The Milan–Venice connection already exists via high-speed rail, with an estimated travel time ranging from 2 to 3 hours. This corridor connects two major cities in Northern Italy, both of which are internationally renowned for tourism. Although the sizing process indicates that configurations with efficient hybrid powerplants could support this route, the range would begin to fall within the scope of RAM (Regional Air Mobility), as part of the broader concept of Innovative Air Mobility.

## 5.3 Selected Configurations

### 5.3.1 Range within 100 km

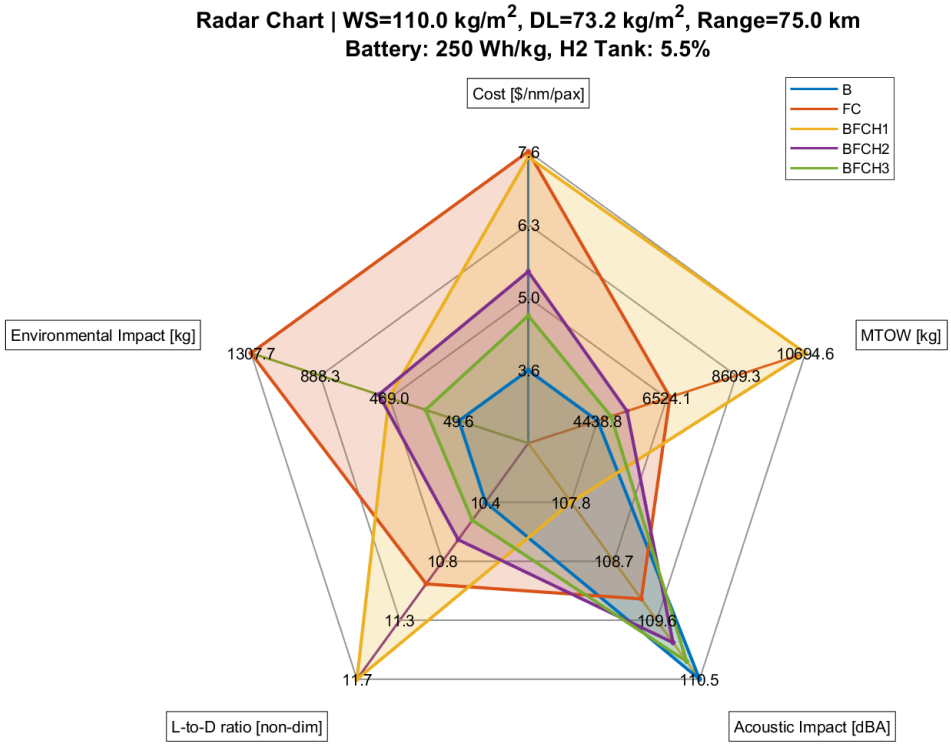


Figure 5.6: Radar Chart (All powerplant configurations)

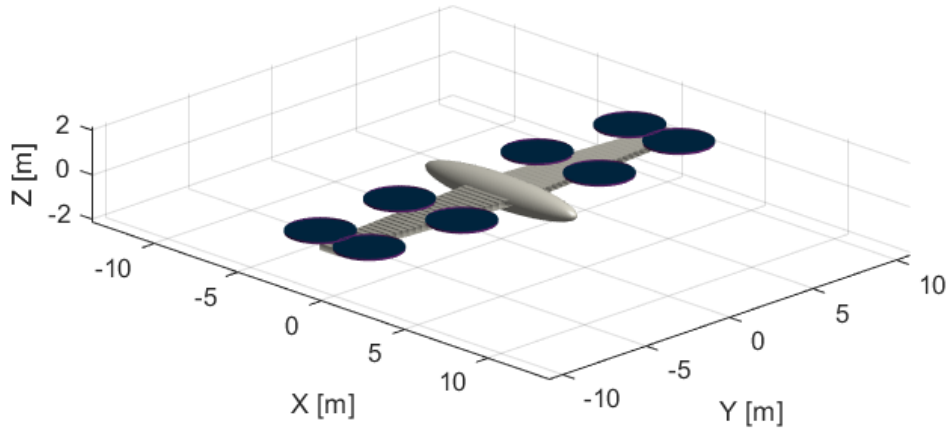


Figure 5.7: Aircraft representation (Battery only)

| | |
|---|---|
| **Wing Surface** $[m^2]$ | 40.35 |
| **Wingspan** $[m]$ | 20.58 |
| **Disk Area** $[m^2]$ | 60.61 |
| $\#\ rotors$ | 8 |
| **Rotors radius** $[m]$ | 1.550 |
| **MTOW** [kg] | 4438 |

Table 5.3: Aircraft Geometry (Battery Only)

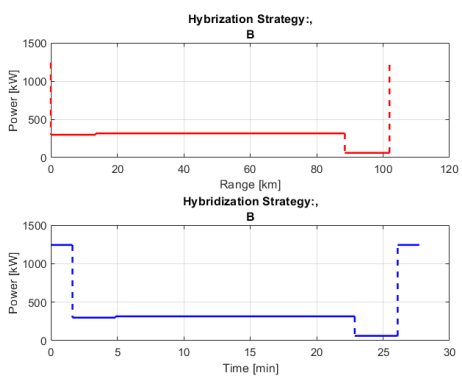


(a) Power demand (Battery only)

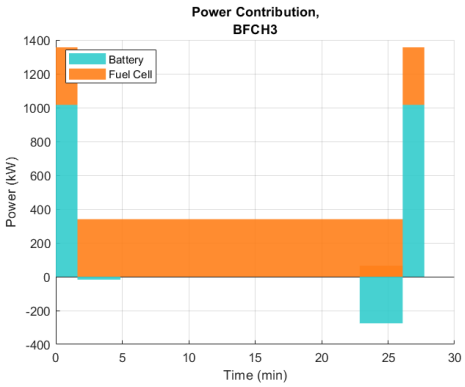


(b) Power sharing (BFCH3)

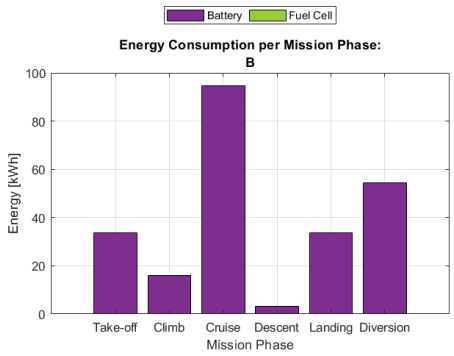


(a) Energy demand (Battery only)

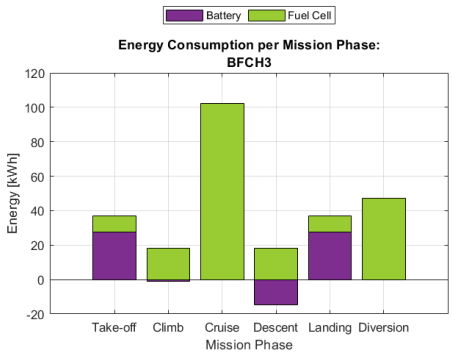


(b) Energy Demand (BFCH3)

Figure 5.9: WS = 110 $kg/m^2$, DL = 15 $lb/ft^2$, Range = 75 $km$, Tech Level = 1

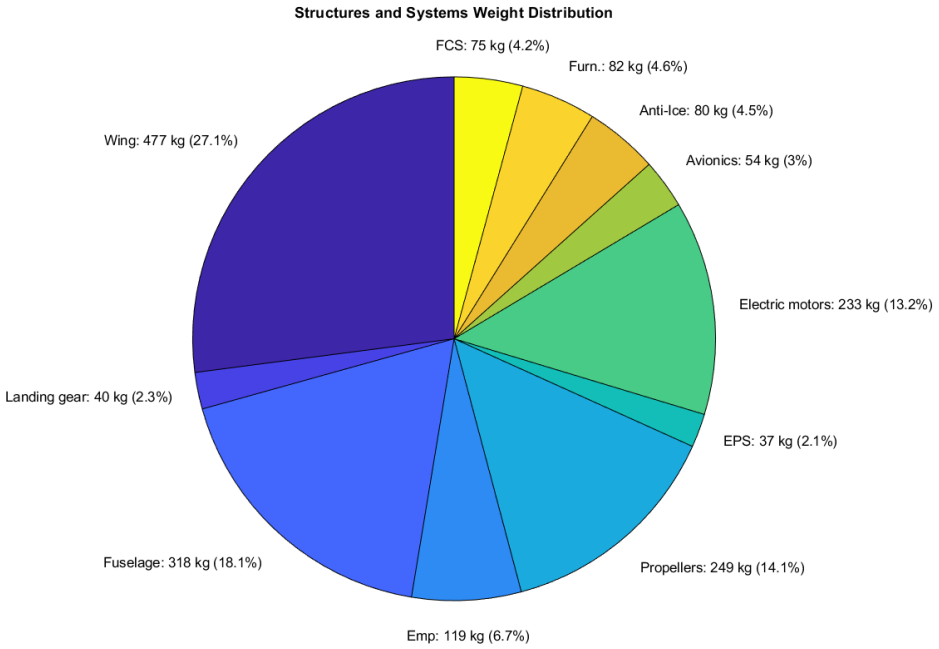


Figure 5.10: Structures and Subsystems Weight contribution (Battery only)

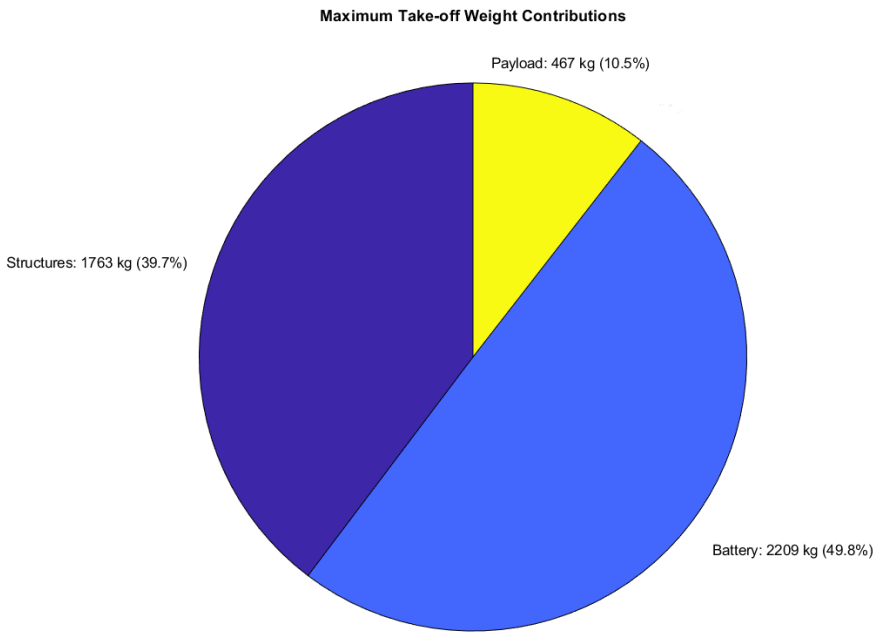


Figure 5.11: Maximum Take-off Weight Contributions (Battery only)

Although the TLARs specified in Chapter 3 refer to a range twice as the one discussed in this section, it is still useful to compare several configurations for a 75 km range ($\approx 40nm$).This is the typical range which characterizes eVTOL aircraft designed for intra-city missions. As expected for this range, the battery-only configuration represents the lightest one, followed by the BFCH3 one (+9.17%). This configuration also results in lower costs and emissions; in fact, hybrid solutions can reach up ten-times the emission of the battery-only case. However, it is important to note that these configurations are analysed assuming a basic technological level (Tech Level = 1), with a lower battery energy density and highly inefficient hydrogen tanks, compared to improved levels included in the design process. Due to the low power density of fuel cells, the fuel cell-only configuration easily accumulates weight, exceeding 10000 kg. All the proposed configurations, result in higher weights compared to existing eVTOL prototypes summarized in table in section 3.2 – which are generally under 3175 kg. The BFCH3 configuration leads to a 30% higher cost than the battery-only option, due to the integration of fuel cells, and shows a 8.28% increase in energy demand. As discussed in the previous chapter, the given range does not make hybrid solutions competitive with battery-only configurations. It is also noteworthy that batteries contribute the highest share of weight, accounting for approximately 50% of the total. Regarding the on-board systems, the structural elements include the wing, the fuselage, and the empennage. For the empennage, given the lack of data in these early stages of the design process, the sizing has been based on a generic configuration, even though many eVTOL concepts adopt a V-tail. The Flight Control System (FCS) includes actuators, sensors, and flight computers, necessary to enable eVTOL manoeuvring. The Electric Power System (EPS) includes power distribution units, DC/DC converters, and cabling. The low weight is due to the exclusion of electric motors and batteries from this subsystem, as well as the relatively small scale of the system itself. The landing gear refers to a fixed skid without retraction mechanisms, which may include shock absorbers.

### 5.3.2 Range between 100 km and 200 km

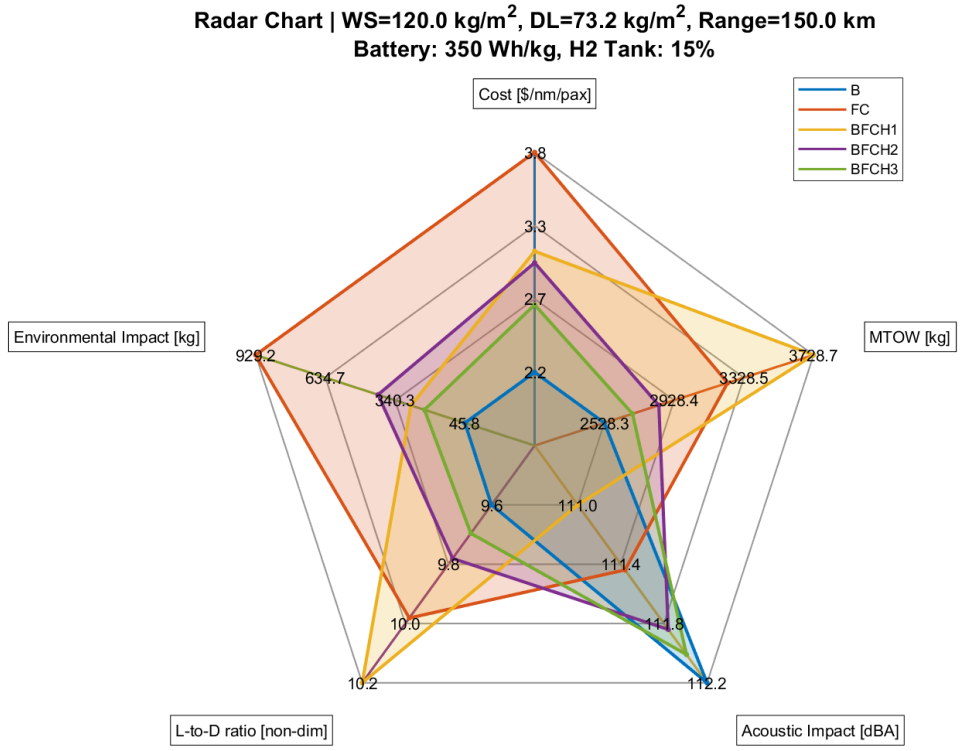


Figure 5.12: Radar Chart (All powerplant configurations)

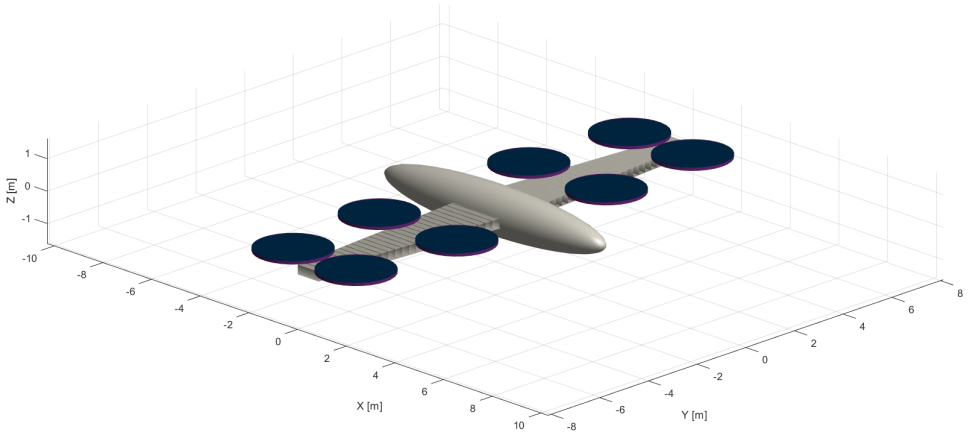


Figure 5.13: Aircraft representation (BFCH3)

| | |
|---|---|
| **Wing Surface** $[m^2]$ | 22.41 |
| **Wingspan** $[m]$ | 15.34 |
| **Disk Area** $[m^2]$ | 36.73 |
| $\#\ rotors$ | 8 |
| **Rotors radius** $[m]$ | 1.209 |
| **MTOW** [kg] | 2689 |

Table 5.4: Aircraft Geometry (BFCH3)

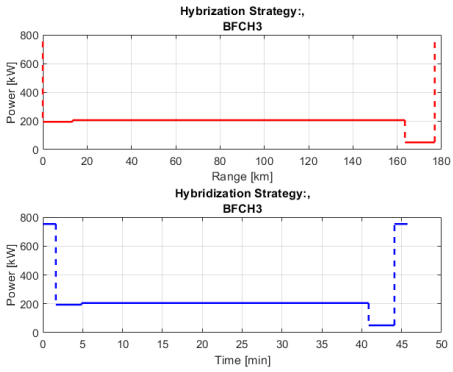


(a) Power demand (BFCH3)

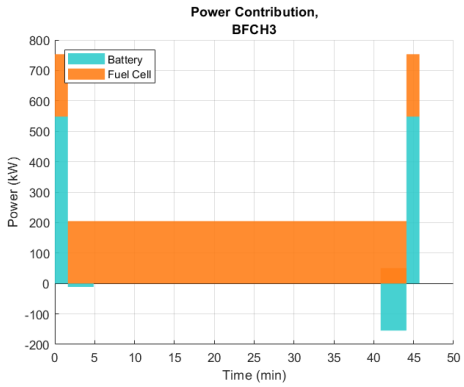


(b) Power sharing (BFCH3)

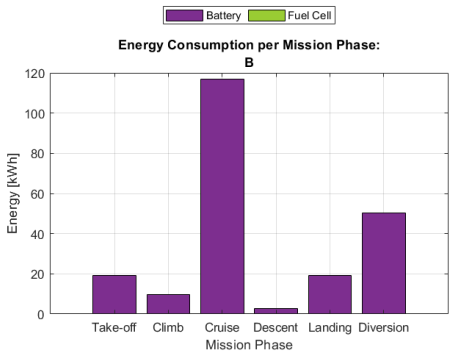


(a) Energy demand (Battery only)

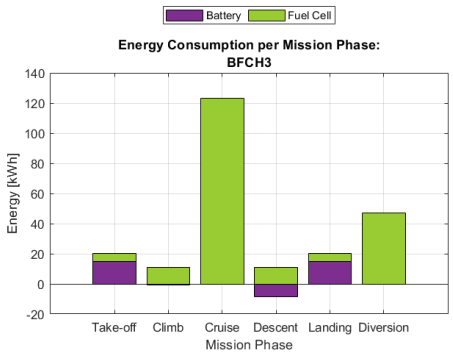


(b) Energy Demand (BFCH3)

Figure 5.15: WS = 120 $kg/m^2$, DL = 15 $lb/ft^2$, Range = 150 $km$, Tech Level = 3

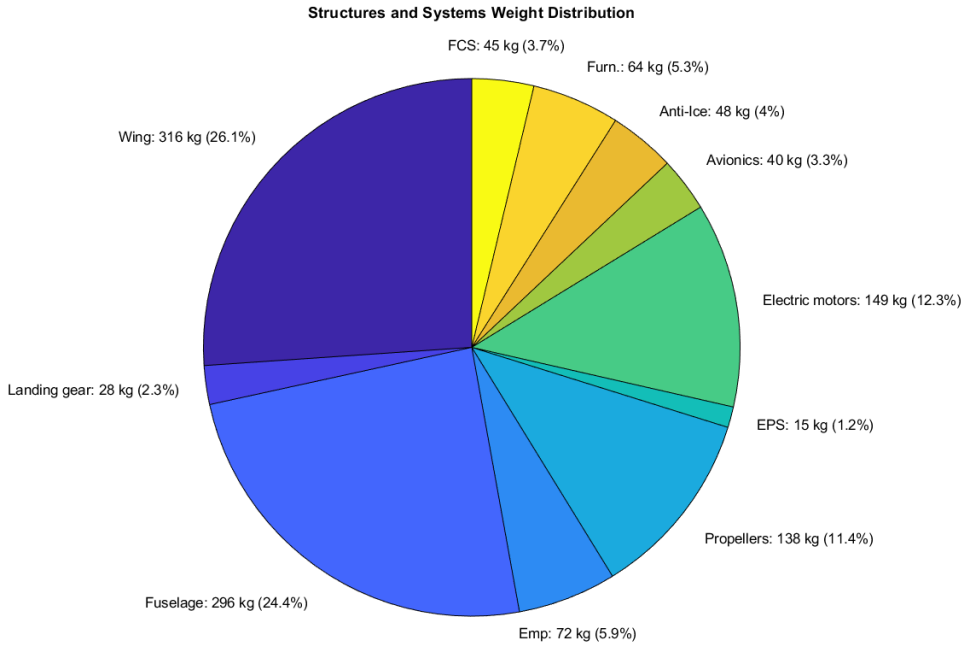


Figure 5.16: Structures and Subsystems Weight contribution (BFCH3)

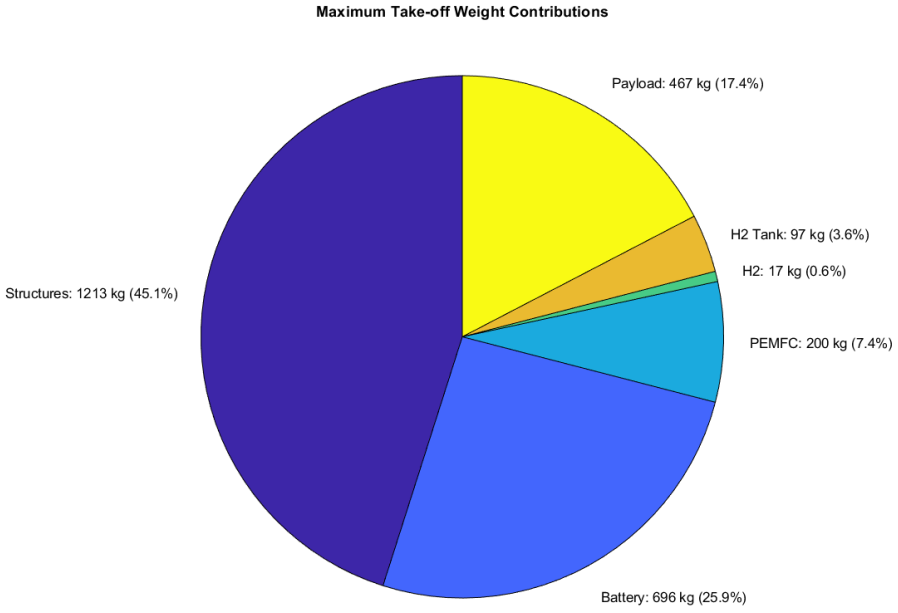


Figure 5.17: Maximum Take-off Weight Contributions (BFCH3)

The 150 km range fully satisfies the top-level requirement established in Chapter 3. As discussed in the previous section, by fixing certain parameters (Disk Loading, Wing Loading, and Technology Level), it is possible to identify the Break-Even

Point (BEP) where hybrid configurations become competitive with battery-only ones. For this specific range, battery-only configurations still lead to lighter solutions; however, the weight margin is significantly reduced compared to the 75 km case. In fact, the BFCH3 configuration is only 7.8% heavier than the battery-only one. Moreover, both configurations benefit from the improved technology level, resulting in an overall lower weight. The hybrid BFCH3 configuration shows a higher environmental impact due to the assumed hydrogen production through conventional fossil-fuel-based methods, leading to emissions approximately five times greater. Further analysis, involving more sustainable hydrogen production (e.g. electrolysis with renewable energy) could reduce emissions, although this would increase costs. In terms of operational costs, the hybrid solution (BFCH3) is about 22% more expensive than the battery-only configuration, although improved tank characteristics also reduce costs in the fuel-cell-only case. Unlike the previous range, the energy demand of the hybrid solution is only 5.29% higher than that of the battery-only configuration. In general, the reduced performance gap between battery-only and hybrid solutions at this range raises important questions regarding optimal design choices. These may include operational aspects not accounted in the sizing process, such as the faster refuelling time of hydrogen compared to battery recharging. As shown, the improved characteristics of the power system allow for a significantly smaller battery mass, even while incorporating the PEMFC system; this results in a combined power system weight of approximately 37.5% of the total take-off mass, compared to the 50% observed in the previous battery-only configuration. Structural components – including both the airframe and onboard systems – continue to account for roughly 40% of the total weight, a value consistent with the earlier configuration. Notably, the relative share of the payload increases, reflecting a more efficient distribution of mass enabled by the hybrid solution.

### 5.3.3 Range beyond 200 km

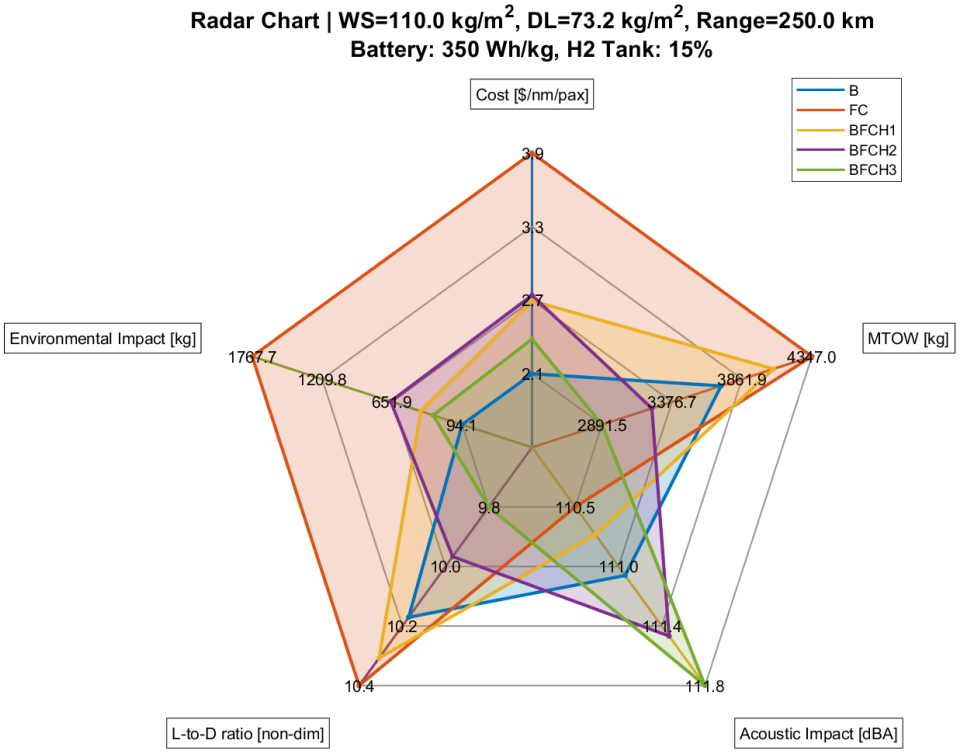


Figure 5.18: Radar Chart (All powerplant configurations)

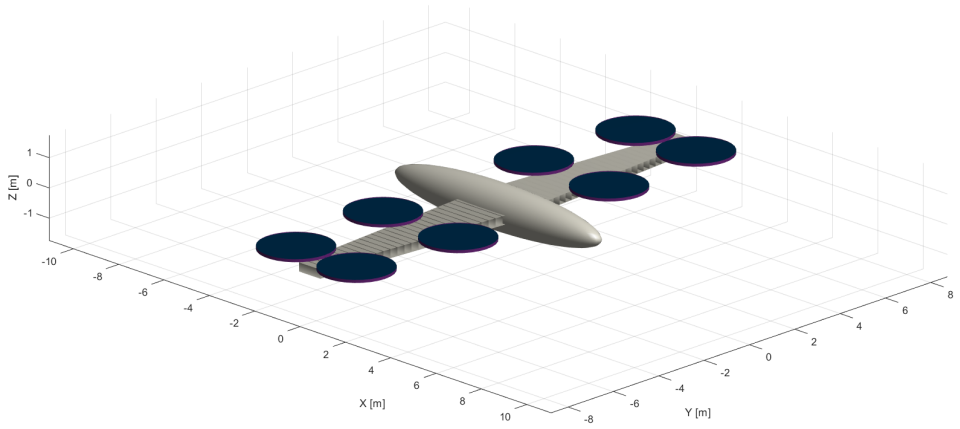


Figure 5.19: Aircraft representation (BFCH3)

| | |
|---|---|
| **Wing Surface** $[m^2]$ | 26.28 |
| **Wingspan** $[m]$ | 16.61 |
| **Disk Area** $[m^2]$ | 39.48 |
| $\#\ rotors$ | 8 |
| **Rotors radius** $[m]$ | 1.25 |
| **MTOW** [kg] | 2891 |

Table 5.5: Aircraft Geometry (BFCH3)

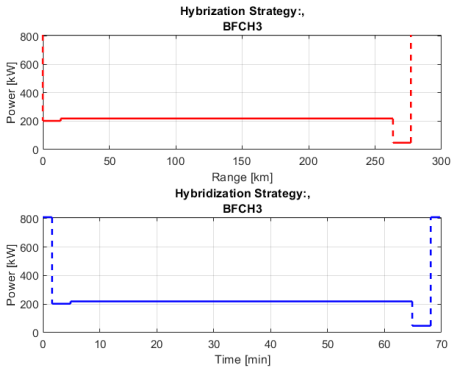


(a) Power demand (BFCH3)

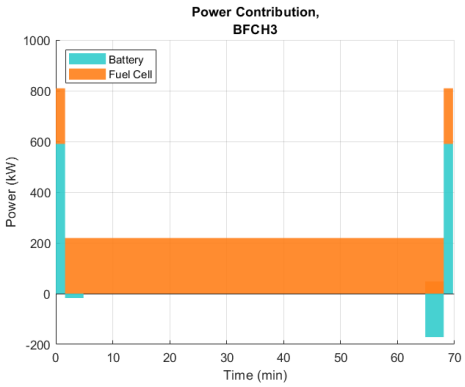


(b) Power sharing (BFCH3)

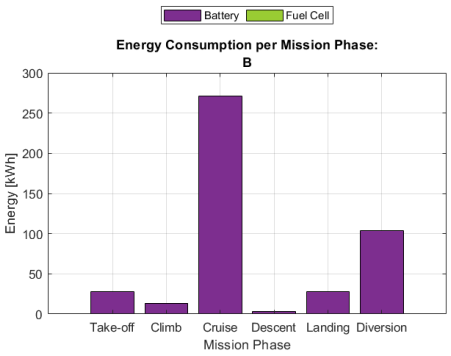


(a) Energy demand (Battery only)

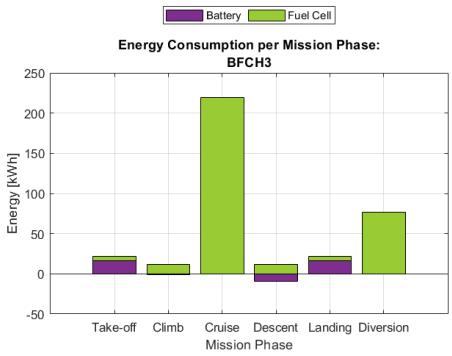


(b) Energy Demand (BFCH3)

Figure 5.21: WS = 110 $kg/m^2$, DL = 15 $lb/ft^2$, Range = 250 $km$, Tech Level = 3

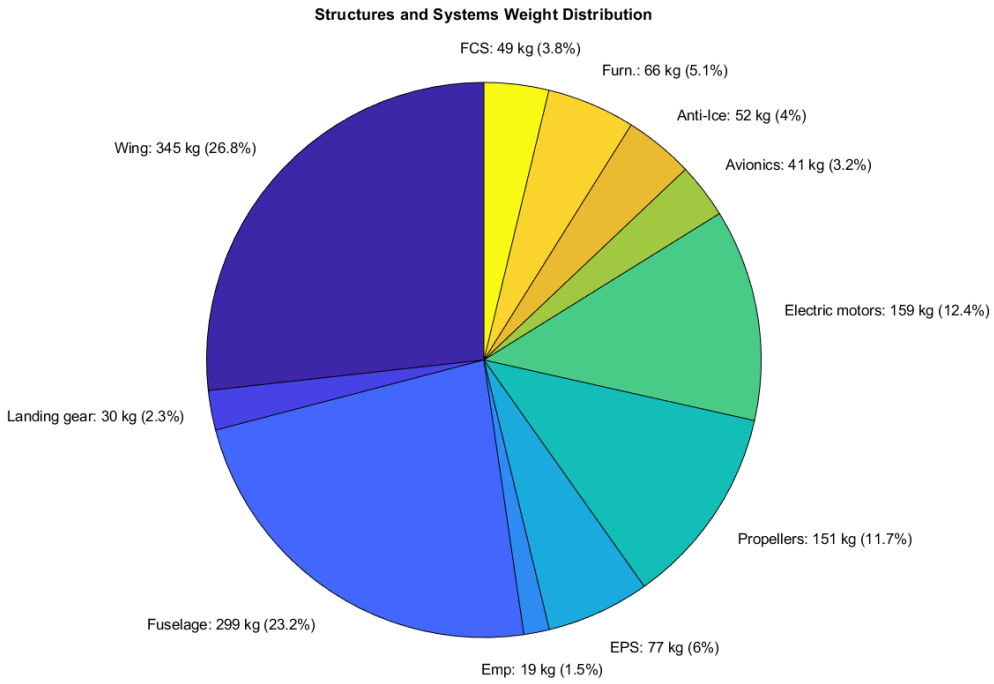


Figure 5.22: Structures and Subsystems Weight contribution (BFCH3)

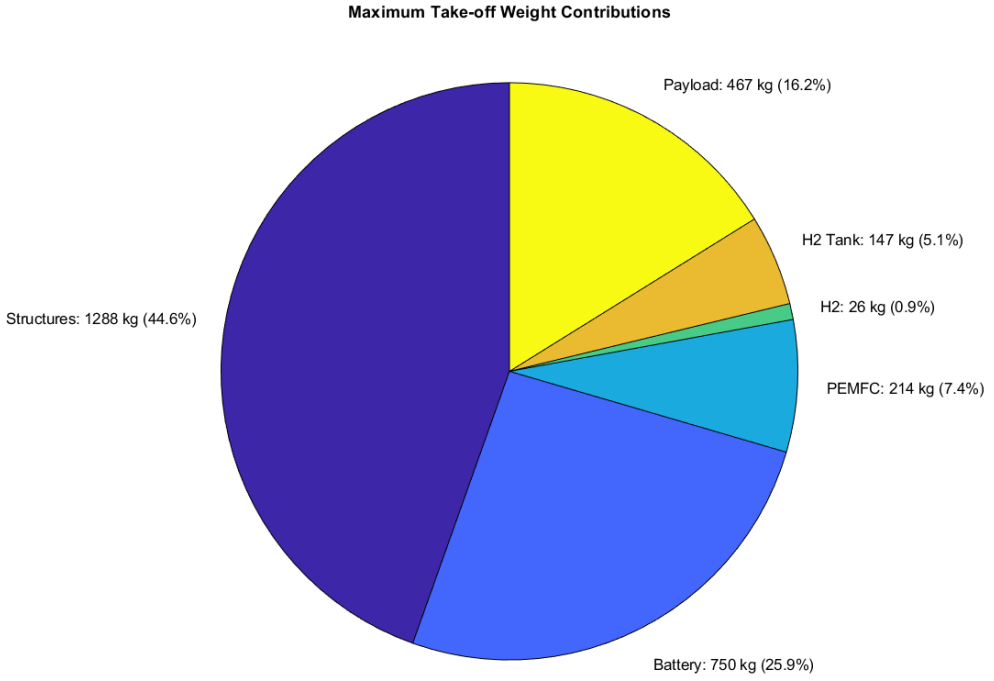


Figure 5.23: Maximum Take-off Weight Contributions (BFCH3)

As observed, at longer ranges, batteries tend to accumulate weight due to a self-reinforcing "weight-calling-weight" phenomenon: as the aircraft becomes heavier, it requires more energy, which in turn demands a larger and heavier power system. This feedback loop significantly penalizes the battery-only configuration. In contrast, the hybrid solution proves more efficient in this context, resulting in a configuration that is approximately 22% lighter than the battery-only counterpart. Among the considered architectures, the BFCH3 configuration consistently shows the best performance. However, the BFCH2 configuration also results in a lighter aircraft than the battery-only option. Additionally, the hybrid solutions lead to a 20% reduction in energy demand compared to the battery-based configuration. Despite these advantages, hybrid configurations still incur higher costs, with the BFCH3 configuration being around 18% more expensive than the battery-only solution – though this represents a smaller increase compared to the previous (shorter range) case. From an environmental perspective, the hybrid solution continues to have a higher impact than the battery-only configuration. However, this impact is significantly reduced compared to the 150 km case, now amounting to only 3.45 times the emissions of the battery-only solution. Regarding this aspect, the BFCH2 configuration – although closer in hybridization strategy to the BFCH3 one– results in twice the environmental impact of BFCH3 one, likely due to different operating profiles or power-split strategies. The weight distribution trends remain consistent with the previous findings: structural components represent about 45% of the total weight, the battery accounts for approximately 25%, and the PEMFC system contributes around 13.4%. As widely discussed in literature, fuel cell-only configurations still lack competitiveness with a battery-only or hybrid solutions, primarily due to their low power density. However, advances in fuel cell technology could significantly shift this balance in the near future.

# Conclusions

This thesis set out to investigate a possible methodology for the conceptual design of an eVTOL aircraft powered by different powerplant architectures, including battery-only, fuel cell-only, and hybrid solutions combining both. Hybrid powerplants and related power-sharing strategies were tailored to meet aircraft requirements in terms of power and energy demands throughout all flight phases. The initial literature review was essential to establish the motivations for Urban Air Mobility and to identify the specific needs this emerging transportation mode is intended to address, thus justifying the relevance of the study. This analysis was supported by a discussion of the EASA Special Condition, which guided several design requirements, and by the EASA report on public acceptance of UAM, which helped identify additional expectations from future users and citizens interacting with eVTOL aircraft. The technical literature review on electrical power generation technologies was necessary to identify current limitations, gather numerical data for the sizing process, and understand how these technologies behave under varying environmental conditions—an essential consideration in aeronautical applications. The investigation into the future European hydrogen infrastructure further reinforced the study's foundation, given its potential to supply hydrogen to eVTOL-dedicated facilities (vertiports) alongside the parallel development of hydrogen distribution systems and eVTOL aircraft manufacturing. A well-defined mission profile was fundamental to support the sizing process. Further investigation into this aspect could enhance the "Concept of Operations" enabling the definition of more refined environmental requirements and operational modes—crucial for the correct sizing of on-board systems. One key finding was the unique behavior of the matching chart, a fundamental tool in conceptual aircraft design. For this type of aircraft, it does not clearly reflect the impact of wing loading on power demand, due to the dominant power contribution during take-off being independent of wing loading. Nevertheless, the influence of disk

loading was particularly insightful across the project, affecting power requirements, weight distribution, and even considerations beyond conceptual design, such as downwash and outwash effects, which are critically relevant in urban environments. The conventional methodologies applied to size these new aircraft concepts still yielded results consistent with existing prototypes, confirming their robustness. However, certain components—particularly structural elements like the landing gear and empennage—warrant deeper analysis and dedicated formulation. The PEMFC system, a central element in this thesis, was sized using one of the few available formulations in the literature. Here again, future research could contribute to the development of dedicated tools to integrate this subsystem more seamlessly into the conceptual design process. All powerplant architectures were essential to assess the overall feasibility of the proposed concept. Although configurations with specific powerplants (battery-only, fuel cell-only, BFCH3) proved more competitive than others (BFCH2, BFCH1), all were retained within the design framework to illustrate the progression from the most intuitive (BFCH1) to the best-performing solutions (BFCH3). The hybrid configuration, as outlined in the powerplant schematics, presents a promising area for future work, particularly through the use of higher-fidelity tools capable of simulating the powertrain in greater detail. The performance analysis led to several key findings. First, the power distribution across flight phases was characterized for this unique aircraft category, which combines features of both helicopters and fixed-wing aircraft. Interestingly, despite additional drag-inducing elements, eVTOL aircraft still demonstrated favorable lift-to-drag ratios, superior to those of rotorcraft. Second, it was found that within operational ranges relevant to some UAM missions, hybrid configurations often yield better performance than battery-only systems—though the exact crossover point depends strongly on design parameters and technology level. Third, and as expected, both range and technological maturity significantly influence subsystem weights: greater ranges increase weight, while higher technology levels reduce it. The role of technology maturity is thus central to the discussion and the sizing outcomes, establishing realistic expectations for im-

provements in both battery and fuel cell systems. Beyond the conclusions already drawn in Chapter 5, it can be stated that for longer ranges—such as inter-city travel, island connections, or airport shuttle applications—hybrid configurations offer substantial advantages over battery-only systems. This applies particularly to distances greater than 150 km, where domestic flights are absent and rail alternatives are unavailable. For shorter ranges, battery-only configurations appear more favorable, although this does not account for operational aspects such as hydrogen refueling or battery recharging. Moreover, fuel cells generally offer a longer service life than batteries, whose capacity degrades over time. The thesis has validated several initial objectives regarding the advantages of hybrid powerplant architectures, though such conclusions must be framed within specific range and technology-level assumptions. This work lays the foundation for further research, particularly into the role of hybrid propulsion in light of future technology advancements and its potential for regional air mobility. The comparison between configurations could be enhanced through refined implementation of the figures of merit, incorporating, for instance, improved definitions of maintenance costs for hybrid systems or the impact of different hydrogen types on cost and environmental footprint. Lastly, future research could delve into detailed design of on-board systems, ensuring compliance with safety and redundancy requirements, especially given space constraints, and defining maneuvering strategies using both rotors and control surfaces.

# Bibliography


[1] Hannah Ritchie, Veronika Samborska, and Max Roser. "Urbanization". In: *Our World in Data* (2024). https://ourworldindata.org/urbanization.

[2] Eurostat. *Main place of work and commuting time - statistics*. Accessed: 2025-04. 2020. URL: https://ec.europa.eu/eurostat/statistics-explained/index.php?title=Main_place_of_work_and_commuting_time_-_statistics.

[3] L. Han, C. Peng, and Z. Xu. "The Effect of Commuting Time on Quality of Life: Evidence from China". In: *International Journal of Environmental Research and Public Health* 20.1 (2022). Accessed: 2025-04, p. 573. DOI: 10.3390/ijerph20010573. URL: https://doi.org/10.3390/ijerph20010573.

[4] European Environment Agency. *Greenhouse gas emissions from transport in Europe*. Accessed: 2025-04. 2024. URL: https://www.eea.europa.eu/en/analysis/indicators/greenhouse-gas-emissions-from-transport?activeAccordion=ecdb3bcf-bbe9-4978-b5cf-0b136399d9f8.

[5] Hannah Ritchie. "Sector by sector: where do global greenhouse gas emissions come from?" In: *Our World in Data* (2020). https://ourworldindata.org/ghg-emissions-by-sector.

[6] European Union Aviation Safety Agency. *Drones & Air Mobility Basics explained*. Accessed: 2025-04. 2024. URL: https://www.easa.europa.eu/en/domains/drones-air-mobility/drones-air-mobility-landscape/basics-explained.

[7] Osita Ugwueze et al. "An Efficient and Robust Sizing Method for eVTOL Aircraft Configurations in Conceptual Design". In: *Aerospace* 10 (Mar. 2023), p. 311. DOI: 10.3390/aerospace10030311.

[8] European Union Aviation Safety Agency. *Special Condition for VTOL and Means of Compliance*. Accessed: 2025-04. 2024. URL: https://www.easa.

europa.eu/en/document-library/product-certification-consultations/special-condition-vtol.

[9] European Union Aviation Safety Agency. *Study on the Societal Acceptance of Urban Air Mobility in Europe*. Tech. rep. Accessed: 2025-04. European Union Aviation Safety Agency, 2021. URL: https://www.easa.europa.eu/en/full-report-study-societal-acceptance-urban-air-mobility-europe.

[10] Wikipedia contributors. *Hydrogen*. Accessed: 2025-04. 2025. URL: https://en.wikipedia.org/wiki/Hydrogen.

[11] Wikipedia contributors. *Steam reforming*. Accessed: 2025-04. 2025. URL: https://en.wikipedia.org/wiki/Steam_reforming.

[12] Leonardo Vidas, Rui Castro, and Armando Pires. "A Review of the Impact of Hydrogen Integration in Natural Gas Distribution Networks and Electric Smart Grids". In: *Energies* 15.9 (2022). ISSN: 1996-1073. DOI: 10.3390/en15093160. URL: https://www.mdpi.com/1996-1073/15/9/3160.

[13] I. Pilatowsky et al. "Thermodynamics of Fuel Cells". In: *Cogeneration Fuel Cell-Sorption Air Conditioning Systems*. London: Springer London, 2011, pp. 25–36. ISBN: 978-1-84996-028-1. DOI: 10.1007/978-1-84996-028-1_2. URL: https://doi.org/10.1007/978-1-84996-028-1_2.

[14] Wikipedia contributors. *Pila a combustibile con membrana a scambio protonico*. 2025. URL: https://it.wikipedia.org/wiki/Pila_a_combustibile_con_membrana_a_scambio_protonico.

[15] Anubhav Datta. *PEM Fuel Cell Model for Conceptual Design of Hydrogen eVTOL Aircraft*. Contractor Report NASA/CR—20210000284. Accessed: 2025-03. National Aeronautics and Space Administration (NASA), Ames Research Center, 2021. URL: https://ntrs.nasa.gov/citations/20210000284.

[16] Clean Hydrogen Partnership. *European Hydrogen Refuelling Station Availability System)*. https://h2-stations.eu/. 2025.

[17] European Hydrogen Observatory, Clean Hydrogen Partnership. *Hydrogen Production*. https://observatory.clean-hydrogen.europa.eu/hydrogen-landscape/production-trade-and-cost/hydrogen-production. 2025.

[18] ENTSOG, GIE, Eurogas, CEDEC, GD4S, GEODE). *Hydrogen Infrastructure Map*. https://www.h2inframap.eu/\#map. 2025.

[19] Electric VTOL News. *Wisk Aero Generation 6 (pre-production prototype)*. Accessed: 2025-03. 2022. URL: https://evtol.news/wisk-aero-generation-6.

[20] Electric VTOL News. *Archer Aviation Midnight (production aircraft)*. Accessed: 2025-03. 2020. URL: https://evtol.news/archer/.

[21] Electric VTOL News. *Lilium GmbH Lilium Jet (7-seater)*. Accessed: 2025-03. 2021. URL: https://evtol.news/lilium-gmbh-lilium-jet-7-seater.

[22] Electric VTOL News. *Joby Aviation S4 (production prototype)*. Accessed: 2025-03. 2023. URL: https://evtol.news/joby-aviation-s4-production-prototype.

[23] Electric VTOL News. *Vertical Aerospace VX-4 (production model)*. Accessed: 2025-03. 2020. URL: https://evtol.news/vertical-aerospace-VA-1X.

[24] Electric VTOL News. *Beta Technologies ALIA-250*. Accessed: 2025-03. 2020. URL: https://evtol.news/beta-technologies-alia/.

[25] Giorgio Guglieri, Massimiliano Porta, and Andrea Quinci. *Meccanica del volo dell'elicottero. Principi della meccanica e della dinamica del volo*. Italian. 2nd ed. Esculapio, 2019, p. 256. ISBN: 9788893851633.

[26] Giuseppe Palaia et al. "A Conceptual Design Methodology for e-VTOL Aircraft for Urban Air Mobility". In: *Applied Sciences* 11.22 (2021). ISSN: 2076-3417. DOI: 10.3390/app112210815. URL: https://www.mdpi.com/2076-3417/11/22/10815.

[27] Jan Roskam. *Airplane design / Jan Roskam*. eng. Lawrence: The University of Kansas, 1985. ISBN: 9781884885112.

[28] Wanyi Ng and Anubhav Datta. "Hydrogen Fuel Cells and Batteries for Electric-Vertical Takeoff and Landing Aircraft". In: *Journal of Aircraft* 56.5 (2019), pp. 1765–1782. DOI: 10.2514/1.C035218. eprint: https://doi.org/10.2514/1.C035218. URL: https://doi.org/10.2514/1.C035218.

[29] Xiao-Guang Yang et al. "Challenges and key requirements of batteries for electric vertical takeoff and landing aircraft". In: *Joule* 5.7 (July 2021), pp. 1644–1659. ISSN: 2542-4785. DOI: 10.1016/j.joule.2021.05.001. URL: https://doi.org/10.1016/j.joule.2021.05.001.

[30] European Environment Agency. *Greenhouse gas emission intensity of electricity generation in Europe*. Accessed: 2025-05-25. 2024. URL: https://www.eea.europa.eu/en/analysis/indicators/greenhouse-gas-emission-intensity-of-1.

[31] Gulam Husain Patel et al. "Climate change performance of hydrogen production based on life cycle assessment". In: *Green Chem.* 26 (2 2024), pp. 992–1006. DOI: 10.1039/D3GC02410E. URL: http://dx.doi.org/10.1039/D3GC02410E.

[32] Sen Wang, Lourenço Tércio Lima Pereira, and Daniele Ragni. "Design exploration of UAM vehicles". English. In: *Aerospace Science and Technology* 160 (2025). ISSN: 1270-9638. DOI: 10.1016/j.ast.2025.110058.

[33] HBK. *Sound Power vs. Sound Pressure*. https://www.hbkworld.com/en/knowledge/resource-center/articles/sound-power-sound-pressure. n.d.

[34] Francesco Sclifo'. *Modello di stima dei costi per velivoli UAM = Cost estimation model for UAM aircraft*. Fioriti, Marco, 2023-07-24.

[35] Xiaolong Wu. "Performance Evaluation of UAM Configurations: Cost Estimation for the eVTOLs". Thesis or dissertation. SATM Department: Cranfield University, Aug. 2021.